

IDENTIFICATION AND QUANTIFICATION STUDIES ON STRUCTURES,  
DYNAMICS AND MECHANISM FOR THERMAL AND PHOTO-DEGRADATION  
PRODUCTS OF  $\beta$ -CAROTENE

Thesis

Submitted to

The College of Arts and Sciences of the

UNIVERSITY OF DAYTON

In Partial Fulfillment of the Requirements for

The Degree of

Master of Science in Chemistry

By

Yuan Zhao

UNIVERSITY OF DAYTON

Dayton, Ohio

December, 2011

IDENTIFICATION AND QUANTIFICATION STUDIES ON STRUCTURES,  
DYNAMICS AND MECHANISM FOR THERMAL AND PHOTO-DEGRADATION  
PRODUCTS OF  $\beta$ -CAROTENE

Name: Zhao, Yuan

APPROVED BY:

---

David W. Johnson, Ph.D.  
Committee Chairman  
Associate Professor

---

Mark B. Masthay, Ph.D.  
Committee Member  
Associate Professor

---

Dr. R. Gerald Keil, Ph.D.  
Committee Member  
Professor

© Copyright by

Yuan Zhao

All rights reserved

2011

## ABSTRACT

### IDENTIFICATION AND QUANTIFICATION STUDIES ON STRUCTURES, DYNAMICS AND MECHANISM FOR THERMAL AND PHOTO-DEGRADATION PRODUCTS OF $\beta$ -CAROTENE

Name: Zhao, Yuan

University of Dayton

Advisor: Dr. David Johnson, Dr. Mark Masthay

$\beta$ -carotene is comprised of isoprene units, and hence contain methyl-substituted polyene chromophores, which contains 11 highly unsaturated conjugated double bonds, nine of which are in a planar polyene chain and the other two of which are located in terminal  $\beta$ -ionylidene rings.

The first objective is to determine the kinetics of  $\beta$ -carotene ( $\beta$ C) thermal and photo-degradation rate and evaluate the correlation among content, bleaching time and temperature and solvent effects. The second objective is to figure out the chemical structure of unknown thermal and photo-degradation extents and products structures by instruments of UV-Vis spectrometry, NMR and GC-MS.

Solid  $\beta$ C was heated in sealed pyrex tubes to ensure isothermal heating and no oxygen impacts in open tubes with vents to detect oxygen impacts. Analysis of degradation kinetic data suggested a first-order reaction for the thermal-degradation of  $\beta$ C. The thermal-degradation of  $\beta$ -Carotene was studied at oven temperatures of 100, 150, 200, 250, 300, 350 °C for 30min, 60min, 90min, 120min, 4h, 8h, 24h, 72h separately. The kinetics parameters, rate constant  $k$ , activation energy  $E_a = 11.5763 \text{ kJ/mol}$ , and pre-exponential factor  $A (1.4041 \text{ h}^{-1})$  have been calculated based on the linear regression of concentration vs temperature (100-350°C).  $\beta$ -carotene is heat sensitive as expected and the degradation fate displayed a relative heat instability and temperature dependence. The higher the treatment temperature, the longer time exposure period, the faster the degradation rate. The degradation products, retinol,  $\beta$ -ionone etc are confirmed by GC-MS, most of other products are believed to be apocarotenals and epoxy compounds.

The kinetics from photochemical experiments using UV irradiation are compared with similar experiments conducted with two-photon laser irradiation. The kinetics of photochemical reactions of  $\beta$ -carotene was studied in hexane, carbon tetrachloride and percentages of carbon tetrachloride in hexane below 5%. At low percentages of carbon tetrachloride, the reaction is first order in both carbon tetrachloride and  $\beta$ -carotene. The activation energy of the reactions at temperatures around 25°C was found to be positive but very small. The

photochemical results are also compared with thermal-degradation experiments conducted at temperatures between 250 and 350°C.

In addition to the kinetic results, some products of the reaction have been identified by nuclear magnetic resonance spectroscopy. It is interesting to note that under thermal conditions, retinal and retinol with vinyl hydrogens are identified as products, while under UV irradiation, there are no identifiable products that contain double bonds.

## ACKNOWLEDGEMENTS

I would like to thank the University of Dayton Research Council, University of Dayton Graduate Summer Fellowship, University of Dayton Research Institute, The Dean of the University of Dayton College of Arts and Sciences for their support of this project.

My special thanks are for Dr. David W. Johnson, my research advisor, for guiding me through the research in his laboratory and offering me excellent source of ideas. Besides his tremendous help on my research work, I'm also grateful for his supplies on lab equipments, time and experience at all times. I also wish to express my deepest gratitude to my co-advisor, Dr. Mark. B Masthay for all his patience and encouragement on my photo-degradation analysis research. Without their great assistance and dedicated direct during the completion of this thesis it would never have been completed.

I would like to express my appreciation to everyone who has helped with my work in the chemistry department. This includes my committee members Dr. R. Gerald Keil. In addition, discussions between Dr. Masthay solved many of the problems we encountered during the course of this research. Everyone in the

chemistry department make me feel so warmed and appreciative in the two and half a year's study at University of Dayton. I also need to thank my family for their support and love under all circumstances during my time in the graduate program.



## TABLE OF CONTENTS

ABSTRACT .....	iii
ACKNOWLEDGEMENTS .....	vi
TABLE OF CONTENTS .....	viii
LIST OF FIGURES .....	x
LIST OF TABLES .....	xiii
CHAPTER I INTRODUCTION .....	1
CHAPTER II EXPERIMENTAL METHODS .....	10
MATERIALS & SUPPLIES .....	10
Experimental Method .....	10
Preparation of $\beta$ -Carotene Standard Solutions .....	10
The Thermal Treatment .....	11
Degradation Kinetics (Dynamics) Modeling on $\beta$ -Carotene Degradation .....	12
Photolysis and Analysis by UV-Lamp .....	12
Photo-degradation of $\beta$ -carotene by 532nm Laser .....	13
PHYSICAL METHODS .....	15
GC-MS .....	15
HPLC .....	15
UV-Visible Spectroscopy .....	16
Infrared Spectroscopy .....	16
CHAPTER III RESULTS AND DISCUSSION .....	17

QUALITATIVE ANALYSIS OF COMMERCIAL $\beta$ -CAROTENE .....	17
HPLC-VWD Determination.....	17
UV-Vis Spectroscopy .....	21
Ultraviolet Photochemistry of $\beta$ -carotene .....	26
Laser Photo-induced $\beta$ C Degradation.....	35
Quantitative Analysis of Commercial $\beta$ -carotene.....	39
Identification of Thermal-degradation Products of $\beta$ -Carotene by FT-IR.....	39
Identification of Products of the Thermal and Photo-degradation of $\beta$ -carotene Studies by GC-MS .....	42
A. Purification Effects Test on GC-MS.....	45
B. GC-MS Analysis of the Thermal-degradation Products .....	46
C. Identification of Thermal-degradation Products by Mass Spectroscopy .....	49
D. Identification of $\beta$ C Photo-degradation Using 532 nm Laser Radiation .....	56
E. Generation of the Proposed Thermal and Photo-degradation Intermediate and Final Products .....	71
CHAPTER IV CONCLUSIONS .....	76
UV Photo-degradation.....	77
Laser Light Irradiation .....	77
CHAPTER V FUTURE RESEARCH .....	79
BIBLIOGRAPHY .....	81
APPENDIX .....	87
APPENDIX I THERMAL-DEGRADATION OF CRYSTALLINE $\beta$ C RESULTS.....	88
APPENDIX II PHOTO-DEGRADATION OF $\beta$ —CAROTENE .....	102
APPENDIX III THE MASS SPECTRAL DATA OF SOME FRAGMENT IONS.....	109

## LIST OF FIGURES

Figure 1 Molecular Structure for $\beta$ -Carotene .....	2
Figure 2 The Photoemission Curve for UV Lamp (the purple curve).....	14
Figure 3 The Pictures of Srinivasan-Griffin Rayonet Photochemical Reactor and Its Lamp Holder with Fan in Operation(Southern NE Ultraviolet Co, MiddleTown, Connecticut), Lamp 3500A).....	14
Figure 4 RPLC Analysis of Std $\beta$ C, Mobile Phase (CH <sub>3</sub> CN: H <sub>2</sub> O=50:50).....	18
Figure 5 RPLC Analysis of Std $\beta$ C, Mobile Phase (CH <sub>3</sub> CN: H <sub>2</sub> O=70:30).....	19
Figure 6 RPLC Analysis of $\beta$ C Thermal Products, (CH <sub>3</sub> CN: H <sub>2</sub> O=70:30) .....	20
Figure 7 Relationship between A and Heating Time .....	23
Figure 8 Thermal-degradation of $\beta$ -carotene Rate Constant Determination .....	24
Figure 9 First Order Kinetic Plot for the Photo Degradation of $\beta$ -Carotene in Hexane Solution (15- 55°C) .....	28
Figure 10 Determination of Activation Energy of $\beta$ -carotene in Hexane Solvent .....	30
Figure 11 Rate of the Photo-degradation of $\beta$ -carotene Varied as the Percentage of Carbon Tetrachloride. ....	32
Figure 12 The Photo-degradation Rate of $\beta$ -Carotene in Hexane with Various Concentrations of Carbon Tetrachloride. ....	33
Figure 13. A Comparison of the Activation Energies for the Photo-degradation of $\beta$ -Carotene in Hexane with Various Concentrations of Carbon Tetrachloride.....	34
Figure 14. Dependence Effects of Irradiation Interval on $\beta$ -carotene in 1.00% CCl <sub>4</sub> /hexane Solvent Absorbance Drop (Test #1).....	36
Figure 15 $\beta$ -carotene in 1% CCl <sub>4</sub> +Hexane Irradiated by 0.115w Laser (25°C) .....	38

Figure 16 The FT-IR Spectra of $\beta$ C Thermal-degradation Products (Neat Liquid, KBr Plates) ....	41
Figure 17 Comparison of TIC Chromatogram for Purified and Unpurified $\beta$ -carotene Standard Aliquots. ....	45
Figure 18 The Mass Spectra of 2mg/mL $\beta$ -carotene After and Before Thermal Treatment at 200°C for 1 hour.....	47
Figure 19 Comparison of TIC Showing the Decreasing Response of $\beta$ -carotene after 17.5min Dependent on the Heating Temperatures.....	48
Figure 20 Proposed Mechanism of m/z 536 to 192, 180, 208, 218, 206 Thermal-degradation Products .....	50
Figure 21 Proposed Mechanism of m/z 180 to 192, 156 and Daughter Ions at m/z 137, 2-hydroxy-2,6,6-trimethyl-cyclohexaone .....	52
Figure 22. Scheme of Retro-Diels–Alder fragmentation and the Fragmental Pathways of $\alpha$ -Ionone and $\beta$ -Ionone .....	54
Figure 23 TIC Chromatogram for Laser-induced Reaction Products from 4mg/ mL $\beta$ C std Solution in the Presence of Air and Argon Separately.....	58
Figure 24 TIC of 0.2mg/ mL Retinal vs. 4mg/mL $\beta$ -carotene After Laser Degradation .....	59
Figure 25 The Main Peaks from TIC of Reaction Products for 4 mg/mL $\beta$ C Induced by 532 nm Laser with Full Intensity.....	60
Figure 26 The Extracted Mass Spectra for Retention Time at 12.469min for $\beta$ C in CCl <sub>4</sub> Solvent Laser Photo-degradation Products .....	61
Figure 27 The MS of Peak at m/z 273, 275, 277, 279 and the Possible M <sup>+</sup> Peak at m/z 290 .....	63
Figure 28 The Abundance of Each Ion with Descending Order of Intensity.....	65
Figure 29 The Possible Isomer Structures Based on MS Cleavage Products Formed by Addition of Chlorine to Double Bonds in $\beta$ -carotene.....	66
Figure 30 The Mass Spectra and the Proposed Structures by NIST Library between 10.096 and 14.586 min .....	68
Figure 31 Proposed Pathways of $\beta$ -carotene into <i>Trans</i> , 9- <i>cis</i> , and 11- <i>cis</i> Retinal Isomers and Retinols. ....	69

Figure 32 Generation of the Proposed Thermal and Photo-degradation Intermediate and Final Products .....	71
Figure 33 . The Scheme of Planar C+ at 5 and 8 Position to Form C-8 Diastereoisomers Products .....	73

## LIST OF TABLES

Table 1 Advantage and Disadvantage of Various Methods of Instrumental Analysis for $\beta$ -Carotene Cleavage Products .....	7
Table 2 RPLC Analysis of Std $\beta$ C, Mobile Phase (CH <sub>3</sub> CN: H <sub>2</sub> O=50:50).....	18
Table 3 RPLC Analysis of Std $\beta$ C, Mobile Phase (CH <sub>3</sub> CN: H <sub>2</sub> O=70:30).....	19
Table 4 RPLC Test Results of $\beta$ -carotene Thermal Products (CH <sub>3</sub> CN: H <sub>2</sub> O=70:30).....	20
Table 5 The UV Absorbance Reading for Different Thermal Treatment of $\beta$ -carotene Dependent on Time and Temperature and Its Relative R <sup>2</sup> Value for the Corresponding Reaction Orders .....	22
Table 6 The Summary of Rate Constant Varied with Temperature for Crystalline $\beta$ -carotene Thermal-degradation.....	25
Table 7 The Summary of Absorbance Reading on Degradation Results for $\beta$ C/heat Hexane Solution .....	27
Table 8 The Summary of Parameters Related with Rate Constant for $\beta$ C Dissolved in Neat Hexane (1st order) .....	29
Table 9 A Summary of the Rate of Photo-degradation of $\beta$ -Carotene with Variable Concentrations of Carbon Tetrachloride.....	31
Table 10 $\beta$ -carotene in 1% CCl <sub>4</sub> +Hexane Irradiated by 0.115w Laser (25°C).....	37
Table 11 Molecular Ion and Some Fragment Ions Observed in the Mass Spectra of Some Thermal-degradation Products. ....	49

## CHAPTER I

### INTRODUCTION

Carotenoids are the naturally-derived pigments which give the brilliant colors of red, yellow, orange etc to fruits and vegetables <sup>1</sup>. They have received the attention of researchers due to their intense colors and antioxidant properties. The most thoroughly studied member of the family is  $\beta$ -carotene which has important role in improving human health due to its conversion to vitamin A <sup>2</sup>. It is responsible for the prevention of the light-initiated oxidative damage to the human's retina, which results in age-related macular degeneration (AMD) and cataracts <sup>3</sup>.  $\beta$ -carotene is also considered a therapy preventing some cardiovascular diseases <sup>4</sup>.

The effectiveness of  $\beta$ -carotene as an antioxidant and anti-cancer activity is related to its ability to quench singlet oxygen because of the highly conjugated polyisoprene (diene polymers) structures.  $\beta$ -carotene can scavenge free peroxy radicals by resulting in cleavage or addition to double bonds <sup>5</sup>. The dietary deficiency in carotenoids is associated with the presence of free radicals. Free radicals can cause DNA damage <sup>6</sup>, impair immune system response.  $\beta$ -carotene prevents peroxidation of phospholipids associated with carcinogenic activity<sup>4</sup>. The  $\beta$ -carotene antioxidant mechanisms are generally in connection with radical

adduct formation, electron donation or hydrogen atom donation <sup>5</sup>. The application of those mechanisms are altered and relied upon the decay of radical species to more stable products <sup>7</sup>.

The essential carotenoids exhibiting superior vitamin A activity are  $\alpha$ -carotene,  $\beta$ -carotene,  $\gamma$ -carotene and  $\beta$ -cryptoxanthin. They are deposited in human tissues and circulating in the body's bloodstream but most come from dietary sources<sup>8</sup>. By far  $\beta$ -carotene is the more important precursor due to its unsubstituted double  $\beta$ -ionone ring skeleton at the terminals of a conjugated poly-isoprene (see Figure 1) as opposed to the single  $\beta$ -ionone ring present in the other above mentioned isomers or compounds.

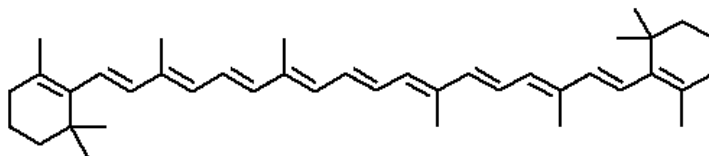


Figure 1 Molecular Structure for  $\beta$  –Carotene

The carotenoids absorb harmful UV light strongly and easily undergo oxidative degradation <sup>9</sup> leading to the rapid loss of total carotenoids contents <sup>10</sup>, thus yielding to structural variations during light, high temperature, acid and oxygen, sunburns, thermal disruption. Normally  $\beta$ -carotene in the food source has to go through the process due to commercial sterility requirements, such as extrusion cooking, industrial canning, air-dehydrating, cutting or disrupting and storage <sup>11</sup>. Significant reduction of  $\beta$ -carotene will lead to consequences not only in the food



acceptability caused by the loss of color, taste or texture, but also in its nutritional content <sup>12</sup>.

Most natural  $\beta$ -carotene occur in the all *trans*- form, since the *cis*-orientation for the polyenic chain of carotene has a higher steric hindrance causing free rotation to be hindered <sup>13</sup> than in the *trans*-configuration <sup>14</sup>. The *cis* configuration is less abundant and a less active substrate for the cleavage enzyme in vitamin A conversion <sup>15</sup>. Lee and Chen (2002) demonstrated in their research that *cis-trans* isomerization dominated in the first 9 hr in the relatively low temperature of 50°C thermal reaction of lycopene, in which occurred 2-3 times faster than the reverse reaction (*trans* to 9-*cis* and 13-*cis* isomers), however, degradation was favored afterward and proceed faster than the isomerization which dominated for at higher temperature such as 100 or 150°C while during illumination, the isomerization take controls <sup>16</sup>. In addition, the isomerization rate of  $\beta$ -carotene varies with the polarity of the solvents , the lower polarity of solvents, i.e, petroleum ether and toluene, give higher isomerization rates, and the more polarity of solvents such as tetrahydrofuran (THF), methanol and acetonitrile usually result in the lower isomerization rate <sup>17</sup>.

The investigation on the thermal oxidation of  $\beta$ -carotene in model systems has suggested that isomerization is not the only reaction involved. There are more reaction products that may not be isolated. As early as 1964, Mader found the volatile fraction from the thermal degradation of  $\beta$ -carotene containing toluene,

m-and p-xylene, 2,6-dimethylnaphthalene and ionene <sup>18</sup>. Years later until 1980, Ouyang et al identified the large fragments consist of  $\beta$ -13-apo-carotenone,  $\beta$ -15-apo-carotenal, and  $\beta$ -14-apo-carotenal by exhaustive TLC of the decomposition products of  $\beta$ -carotene found in palm oil <sup>19</sup>. Onyewu then discovered the formation of compound mass of 444 and 378 by heating  $\beta$ -carotene at 210 °C for 4 hr in 1982 <sup>10</sup>. In 1986, he isolated and identified six more compounds with molecular weights of 346, 274, 258, 210, 188 and 180 after extraction with ethyl acetate <sup>20</sup>. Before long, Evelyn applied strong free radical initiators to increase the oxidative stress to allow the cleavage products of  $\beta$ -carotene be detected. Those products were confirmed to be  $\beta$ -apo-8'/10'/12'/14'/15-carotenals ("/'" means or). The semi-  $\beta$ -carotenone and monohydroxy- $\beta$ -carotene-5,8-epoxide were found in the presence of atmospheric oxygen at ambient temperature in low-moisture and aqueous model systems <sup>21</sup>. Many of the oxidative breakdown products occur only in small quantities with similar polarities and closely related structure, are often present in complex biological matrices. Hence they are difficult to identify and have received little attention <sup>22</sup>.

The slow but spontaneous isomerization and autooxidation of  $\beta$ -carotene, and its subsequent fragmentation and decay and the complex decomposition yield a myriad of byproducts along with the initial, intermediate and final oxidant products. These products may arise during the activity of  $\beta$ -carotene due to its unstable chemical properties. Therefore, it is critical to monitor the low levels of compounds and evaluate the impact of heat and illumination , such as

temperature, exposed time, light source (UV, laser), light intensity and organic solvents type (photoreactive such as chloroalkanes or inert such as hexane) even oxygen concentration (saturated or depleted) in understanding its role in protection against radicals . More amenable analysis techniques are on demands to provide with rich spectral and chromatographic for the positive confirmation and acute assessment of the analytes that may crop up <sup>23</sup>.

Michel Carail tentatively tracked the appearance of the various reaction products and detected one of the intermediates. Final products, such as 5,6-Epoxides of  $\beta$ -apocarotenals were formed from either direct epoxidation of  $\beta$ -carotene and then be rearranged into 5,8-epoxy- $\beta$ -apo-carotenals, followed by subsequent cleavage <sup>24</sup>.

Current literature on the photobleaching of  $\beta$ -carotene is relatively scarce. Carbon tetrachloride ( $\text{CCl}_4$ ), is an active electron acceptor and an endogenous toxicant to be activated by cytochrom P-450 system generating radical  $\cdot\text{CCl}_3\text{OO}$  and  $\cdot\text{CCl}_3$  <sup>25</sup>.  $\text{CCl}_4$  bleaches photosensitized  $\beta$ -carotene with orders-of-magnitude faster than other solvents in pulse radiolysis experiment with a rate constant  $\approx 1.6 \times 10^9/\text{Msec}$ . This observation indicates the high reactivity of peroxy radical  $\cdot\text{CCl}_3\text{OO}$  or  $\cdot\text{CCl}_3$  <sup>26</sup>. However, the complete profile towards the structures formed between  $\beta$ -carotene and induced laser photo was not clearly proposed yet <sup>27</sup>. So far, only retinol was confirmed with HPLC by S. Adhikari et al. in 2000,

they recorded the transient absorption spectra of  $\beta$ -carotene reacting with  $\bullet\text{CCl}_3\text{OO}$  at 50  $\mu\text{s}$  with a considerable blue shift <sup>28</sup>.

Numerous methods for the analysis  $\beta$ -Carotene cleavage products are summarized as table 1. The methods serve the purposes: 1) to elucidate the mechanism for the reversible isomerization or irreversible cleavage into carbonyls, i.e, apo-carotenal <sup>29</sup> or epoxides <sup>30</sup>; 2) to investigate the effects from thermal treatment and photo Irradiation on these thermally-labile or photo-sensitizing compounds. The methods must provide a reliable chiral separation, mild analytical environment, rigorous determination, highly reproducible, reasonably short analysis time, unambiguous resolution of overlapping peaks, dependable quantification, and unequivocal confirmation. Take High-performance liquid chromatography (HPLC) analysis for an example, the long unsaturated alkene chain, provides the chromophore giving absorption maxima in the region of 400 to 550 nm <sup>31</sup>. However, in light of the unusual linearity and rigidity of  $\beta$ -carotene's structure, its capability to enter the pores stationary phase is greatly influenced. Development of column stationary phases from  $\text{C}_{18}$  to triacontyl ( $\text{C}_{30}$ ) polymeric column afford better interaction of  $\beta$ -carotene with the alkyl chains, enhancing HPLC's separation <sup>32</sup>. The column has huge selectivity and resolution towards isomer analysis of similar structures. However, as for the characterization of the chromatographic peaks,  $\text{C}_{30}$  reversed phase HPLC has a long analysis time.

Table 1 Advantage and Disadvantage of Various Methods of Instrumental Analysis for  $\beta$ -Carotene Cleavage Products

Instruments	Advantage	Disadvantage
GC-MS	Library available to search for degradation products structure;	May not be suitable for heat labile products
UV-Vis	Quantification of $\beta$ C at $\lambda_{max}$	Unable to identify reaction products
HPLC	Ideal for the quantification of thermally labile and nonvolatile compounds analysis	1) Only based on a fixed wavelength and retention time alone results in other compounds might be ignored; 2) No confirmation methods; 3) Need standards; 4) special requirements for capillary columns and high resolution;
FT-IR	1) Qualification of simple mixtures by fingerprint spectrums ; 2) Analytes can be in solution form	1) Inability to quantify almost all compounds; 2) analytes need to high-concentration
NMR	Qualification of purified single compound	1) Hardly to quantify mixtures; 2) the analytes need to be in high amount
LC-MS	1 )Separate, identification, quantification of mixtures. 2) prevent isomerization of $\beta$ -Carotene Full scan, MRM, MS <sup>n</sup> multi-modes	1) Expensive analysis costs and N/A in lab; 2) Less responsive to low-molecules than GC-MS; 3) No Mass Spectral Database to get unknown compounds mass information.

Mass spectrometric analysis, which provide molecular weight and characteristic fragmentation patterns, may then provide final confirmation of individual compounds when mass spectrometry in conjunction with HPLC. The combination of GC and MS allows GC to separate and introduce those analytes of interest into MS where the rich mass spectra information of each component will be deciphered and identified. Once the identity is established and confirmed, the

quantitative information obtained can be correctly interpreted without producing false positive results. There is a mass spectral library linked in a “fit & match index in GC-MS that can provide identification for molecular and fragment ions by comparison with even without authentic standards.

Despite of numerous reports on  $\beta$ -Carotene's biological effects at clinical levels, the reaction products have not been identified and the changes of solid  $\beta$ -carotene w/o matrix interference is not well understood <sup>33</sup>. Therefore, it is timely to develop rugged analytical methods particularly towards unknown complexes to elucidate structures during the thermal and photochemical reactions.

The objective of the project is to clarify the  $\beta$ -Carotene thermal and photo-degradation behavior and the nature of the products. These findings will help determine optimal processing conditions to minimize the degradation of  $\beta$ -Carotene in food source through a knowledge of studying its kinetics. The characterization of breakdown products will help us better understanding the cleavage pathways of  $\beta$ -carotene, underpinning the underlying  $\beta$ -carotene/radicals reactions and its protective mechanism.

Gas chromatography-mass spectrometry (GC-MS) will be applied (in concert with other instruments, HPLC, UV-VIS, IR, NMR) to analyze the influence of heat, UV and laser photo, solvent on the degradation of  $\beta$  -Carotene. The possible unknown compounds' structures and determine what chemical interactions and

degradation products are dominant in the mixture were investigated. Macroscopic batch-degradation experiments on stability were also performed to evaluate the impact of heat and illumination, such as temperature, exposed time, photo-type (UV, laser), light intensity, organic solvents type (photoreactive chloroalkane or inert hexane) and so forth on the degradation process. Detailed structural information for different reactions that constitute the process, the inspection and identification of nonvolatile products formed were studied. Increasing the temperature (heating & ambient) and prolonging the treatment time will accelerate the unstable  $\beta$ -carotene compound in a forward direction and in a very predictable manner.

## CHAPTER II

### EXPERIMENTAL METHODS

#### MATERIALS & SUPPLIES

All solvents are HPLC grade provided from Fisher Scientific. Benzene (99.0%) was purchased from Alfa Aesar (Melting point. 180-182 °C).

#### Experimental Method

##### Preparation of $\beta$ -Carotene Standard Solutions

All  $\beta$ -carotene(  $\beta$ C) was purchased from Sigma-Aldrich Chemical Company and was purified by flash chromatography under minimum light as described below before use. A 22 mm i.d. flash chromatography column was prepared by mixing a certain amount of silica gel (Silica Gel 60, 0.040-0.063 mm particle size, 230-400 mesh; EM Science) with benzene and stirred with a stir rod to make an evenly distributed mixture. The slurry was slowly poured into the column under a flow of argon gas sufficient pressure to allow a collection rate of  $\sim 1$ -2 drops  $\text{sec}^{-1}$ . The column was loaded with five 4 mL aliquots of a saturated solution of synthetic 95% all-trans  $\beta$ -carotene pre-dissolved in benzene. The polar dark



maroon band of impurities remained at the top of the flash column. The less-polar  $\beta$ -carotene fraction moved into the middle of the column with a distinct dark-orange colored wide heading and a vague pale-yellow colored tailing. The excess solvent was evaporated under a stream of  $N_2$  gas, leaving purified  $\beta$ C as dark red crystals judged by naked eyes on the bottom and side of the beaker. The purified  $\beta$ C powder was then carefully scraped by a scoopula from the vessel and stored in the dark in sealed vials under nitrogen at  $T \leq -20^\circ\text{C}$ . Concentrated solutions of  $\beta$ -carotene ( $4.0 - 5.0 \times 10^{-6}$  M, for which  $1.4 \leq A_{450} \leq 2.0$ ) were prepared by dissolving approximately 0.00625g  $\beta$ C into 250mL volumetric flask, and diluted with THF, mix well and fill to the mark of meniscus level, then pipet 10.00mL aliquot into a 100.00 mL volumetric flask, mix well by using THF solvent and fill to the mark.

### The Thermal Treatment

The thermal-degradation of  $\beta$ -Carotene was carried out at temperatures of 100, 150, 200, 250, 300, 350  $^\circ\text{C}$  for time periods of 30min, 60min, 90min, 120min and relatively fairly prolonged heating 4h, 8h, 24h, 72h separately using a Blue M Industrial Oven Chamber. Approximately 0.1g solid crystalline  $\beta$ -Carotene was heated and melted in a pyrex tube equipped with a teflon stopcock and side arm. After the reaction, the tube was cooled, and two portions of 4mL THF was added to the tube bottom to rinse the samples out into a target container. Each solution was diluted with THF to obtain an absorbance reading at  $\lambda_{\text{max}}$  between 0.4 and

2.2. A 2.00 mL aliquot of solution was saved for analysis by GC-MS. The thermal-degradation rate was obtained by measuring the decrease in  $A_{\lambda_{\max}}$ .

### Degradation Kinetics (Dynamics) Modeling on $\beta$ -Carotene Degradation

To evaluate the correlation among content, bleaching time and temperature, the parameters of degradation kinetics were identified by linear regressions on the logarithmic curves of experimental data. The induced degradation of  $\beta$ -carotene loss was calculated by using the standard equation for a nth-order reaction (the order number of reaction depends on the experimental data).

### Photolysis and Analysis by UV-Lamp

Samples for irradiation were dissolved in neat hexane or a mixture of hexane and the appropriate amount of carbon tetrachloride. The samples were placed in a water jacketed quartz reaction vessel. The water jacket was connected to a refrigerated circulating bath to insure constant temperature. The samples were irradiated in a Rayonet photoreactor using UV lamp of 3500 Å wavelength. The photoemission curve of the lamp shown by the purple curve illustrated in Fig 2. The pictures of Srinivasan-Griffin Rayonet Rayonet Photochemical Reactor and its lamp holder with fan in operation was shown in Fig 3.

A brown 250 mL volumetric flask was used to prepare the  $\beta$ -carotene in neat hexane solution. Aluminum foil was employed to wrap the volumetric flask, thus minimizing photo-degradation which might result from exposure to the short wavelength components of ambient light. Given by the comparatively poor solubility of  $\beta$ -carotene in hexane solvent, a magnetic stir bar was put in the volumetric flask to stir the solution at Barnstead Thermolyne Stir Plate at  $25\pm 1^\circ\text{C}$  for at least 1 hour until all solid  $\beta$ -carotene was dissolved, about 2mL aliquot was withdrawn by using a disposable dropper to assure that the maximum absorbance of initial solution was around 2.0.

During the irradiation, aliquots around 2mL were withdrawn at appropriate time intervals for immediate spectrophotometric analysis until the final color turned from the  $A_{450}\approx 2$  into almost colorless. The solvent was removed by vacuum evaporation and the products were re-dissolved in 2mL deuterated chloroform  $\text{CDCl}_3$  (Sigma Aldrich, MO).

#### Photo-degradation of $\beta$ -carotene by 532nm Laser

Approximately 4mg/mL of  $\beta$ -carotene solutions were prepared in neat hexane solvent and in the mixed solvents of hexane/  $\leq 5\%$   $\text{CCl}_4$  in which  $1.4\leq A_{450}\leq 2.0$ . The solutions were placed in 1 cm pathlength quartz cuvettes and immediately irradiated with 1.0-1.2 mJ pulses from a Quanta-Ray Model INDI-40 Pulsed Nd:YAG laser. During irradiation, samples were stirred with a magnetic Starna "Spinette" stirrer, and sample temperatures were maintained at  $22.5^\circ\pm 0.5^\circ\text{C}$  with

a Fisher Scientific Model 9500 constant temperature circulator. Spectra were measured with a Hewlett-Packard 8453 Photodiode Array Spectrophotometer interfaced to Agilent Chemstation.

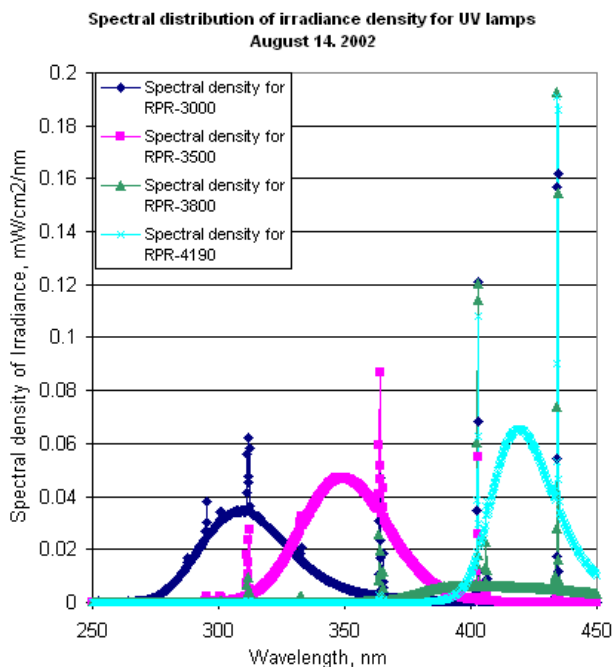


Figure 2 The Photoemission Curve for UV Lamp (the purple curve)<sup>35</sup>



Figure 3 The Pictures of Srinivasan-Griffin Rayonet Photochemical Reactor and Its Lamp Holder with Fan in Operation (Southern NE Ultraviolet Co, MiddleTown, Connecticut), Lamp 3500A)<sup>35</sup>

## PHYSICAL METHODS

### GC-MS

GC-MS analyses were conducted on a Varian Series 3800 GC interfaced with a 2000 mass-selective detector (CA, USA) using an VF-5MS capillary column (Varian, Inc., CA, cross-linked 5% phenyl-methylpolysiloxane, 30 m × 0.25 mm i.d., 0.25 µm film thickness) for thermal degraded and laser irradiated products in terms of their concentration. The injector port and transfer line were maintained at 320° and 280°C, respectively. Helium(99.999%) was used as the carrier gas at a flow-rate of 0.8mL/min. Splitless injection of a 2-µl extract solution was performed with the following oven temperatures. The initial temperature was 70°C, held for 2 min, and then programmed at 10°C/min up to 320°C with a final hold time of 7 min. The EI analysis was performed with ionization energy at 70 eV. Data were acquired in the full scan mode with a mass range of 40–650 (scan rate: 2 scans/s). The ion source temperature was 230°C. An aliquot of 1.0µL was evaporated for analysis by EI-MS afterwards. All the mass units in each mass spectra were labeled by 4-5% of plot for peak label threshold.

### HPLC

High performance liquid chromatographic experiments with a variable wavelength detector was used. 20 µL of isolated fraction was injected in a C30 YMC™ Carotenoid S-250n m × 2.0 mm 5 µm i.d. film thickness 3.20 x 250 mm column (YMC, made in USA) with an eluent composition of acetonitrile(Fisher,

USA)/H<sub>2</sub>O (50:50) (isocratic conditions) and a flow rate of 0.5mL/min. Subsequent analyses by GC-EI-MS were performed with each isolated compound. HPLC analyses were performed with a Waters 515 HPLC binary pump with 4441-4889 psi column pressure equipped with an Agilent1100 diode array detector and controlled with Agilent data acquisition station.

#### UV-Visible Spectroscopy

All the samples were placed in 1 cm pathlength quartz cuvettes and the absorption spectra were obtained by OCEAN – OPTICS Chem 2000 UV-Vis Spectrophotometer with USB2000 Miniature Fiber Optic Spectrometer Detector except for the laser induced photo-degradation products.

#### Infrared Spectroscopy

Infrared spectra of the reaction products analysis were obtained in transmission mode on a Perkin-Elmer Custom GX infrared spectrometer. Place a few small drops of the compound on one of the KBr plates and then place the second plate on top and make a quarter turn to obtain a nice even thin film by coating liquid samples on the two KBr disks to form a sandwiched plates in the spectrometer. Solid samples were prepared by mixing a very small amount of sampler with approximately 50mg of pure, dried KBr, grinding in an agate mortar and pestle, then compressing to form a solid, semi-transparent powder.

## CHAPTER III

### RESULTS AND DISCUSSION

#### QUALITATIVE ANALYSIS OF COMMERCIAL $\beta$ -CAROTENE

The commercially available  $\beta$ -carotene is listed as >95% purity. Before attempting to identify the minor reaction products, it is essential to know the nature of the impurities in the reactants. In order to know the contaminants in the  $\beta$ -carotene before reaction, the commercial material and the material purified by flash chromatography were examined by HPLC and GC-MS.

#### HPLC-VWD Determination

Samples of the purified  $\beta$ -carotene and the unpurified  $\beta$ -carotene were analyzed by high performance liquid chromatography. The quantities of  $\beta$ -carotene and impurities were estimated using the area normalization method. Samples were collected as components eluted from the column for further separation by thin layer chromatography, analysis by GC-MS, FTIR or NMR depending on each individual eluent. Three peaks, two minor peaks corresponding to impurities and one major peak corresponding to  $\beta$ -carotene, appeared on the chromatogram (Fig.4 and Table 2). The major peak due to  $\beta$ -carotene may have contained trans and cis-isomers which are not likely to be separated by the reversed-phase

HPLC. At a retention time of 9.974 min, the  $\beta$ -carotene eluted as the large peak (area 23312.4, 88%). The lower purity observed for the commercial  $\beta$ -carotene may be due to different response factors for the various ingredients or may be due to oxidation of the  $\beta$ -carotene during storage before use.

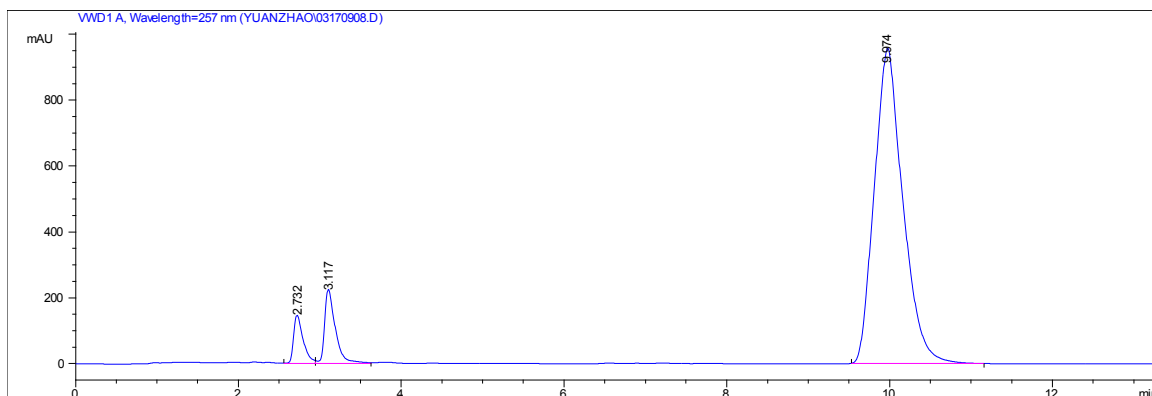


Figure 4 RPLC Analysis of Std  $\beta$ C, Mobile Phase (CH<sub>3</sub>CN: H<sub>2</sub>O=50:50)

Table 2 RPLC Analysis of Std  $\beta$ C, Mobile Phase (CH<sub>3</sub>CN: H<sub>2</sub>O=50:50)

#	Time	Area	Height	Width	Symmetry
1	2.732	1212.9	138.1	0.1374	0.682
2	3.117	2084.4	210.3	0.1506	0.622
3	9.974	23312.4	950.1	0.3678	0.792

The above red fonts are for the target peak  $\beta$ -carotene RT=9.974 min for std  $\beta$ -carotene solution (as seen in table 2). In order to look for other isomers, the mobile phase was changed from 50% acetonitrile to 30% acetonitrile. Two problems were observed when the mobile phase ratio was changed. 1), nitrogen purging was applied to degas the solvents which may lead to the evaporation of the more volatile solvent, thus affecting the mobile phase concentration (Fig. 5, Table 3) and causing baseline shift. Problem 2) , the percentage of  $\beta$ -carotene



calculated based on the same area normalization method for the sample standard sample gave a substantially lower percentage of  $\beta$ -carotene, 59.55% (70:30) vs. 87.61% (50:50), the 50:50 mixture seems much better to give better peak resolution, reduces baseline shift, and shows a purity more consistent with the provider's data.

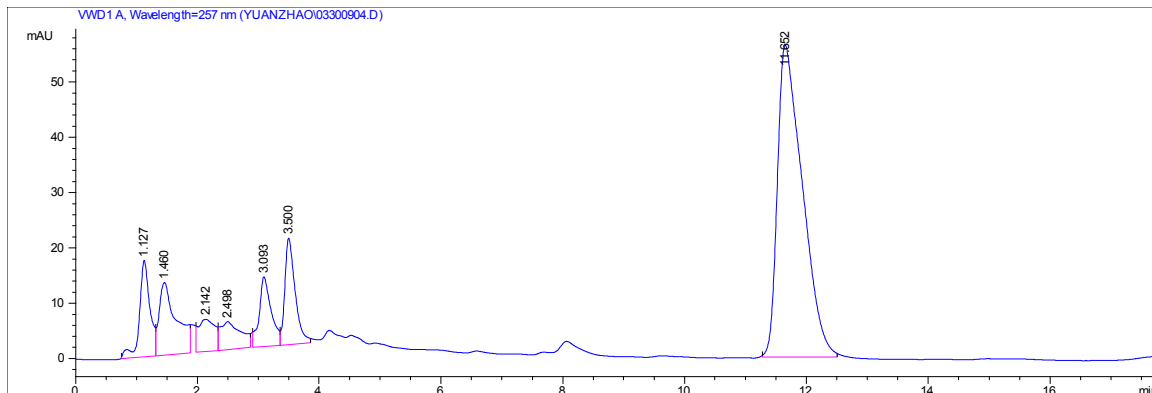


Figure 5 RPLC Analysis of Std  $\beta$ C, Mobile Phase ( $\text{CH}_3\text{CN}:\text{H}_2\text{O}=70:30$ )

Table 3 RPLC Analysis of Std  $\beta$ C, Mobile Phase ( $\text{CH}_3\text{CN}:\text{H}_2\text{O}=70:30$ )

#	Time	Area	Height	Width	Symmetry
1	1.127	208.3	17.4	0.1715	0.857
2	1.46	258	13.1	0.2722	0.404
3	2.142	108.5	5.8	0.2563	0.791
4	2.498	119.1	5.1	0.3047	0.526
5	3.093	172.3	12.6	0.1929	0.667
6	3.5	225.8	19.2	0.1736	0.584
7	11.652	1607.8	56.5	0.399	0.436

The above red fonts are for the target peak  $\beta$ -carotene RT=11.652 min.

The analysis of  $\beta$ -carotene using the auto-integration normalized area method did not always identify the peak near 8.10 min retention time. It was necessary to employ manual integration to identify this peak and make corrections for the shifting background.

The chromatogram below shows the results of one the thermal-degradation of a sample of  $\beta$ -carotene after heating at 150°C for 2 hour. (Fig. 6, Table 4) At least six new peaks are detectable indicating the of degradation of the  $\beta$ -Carotene.

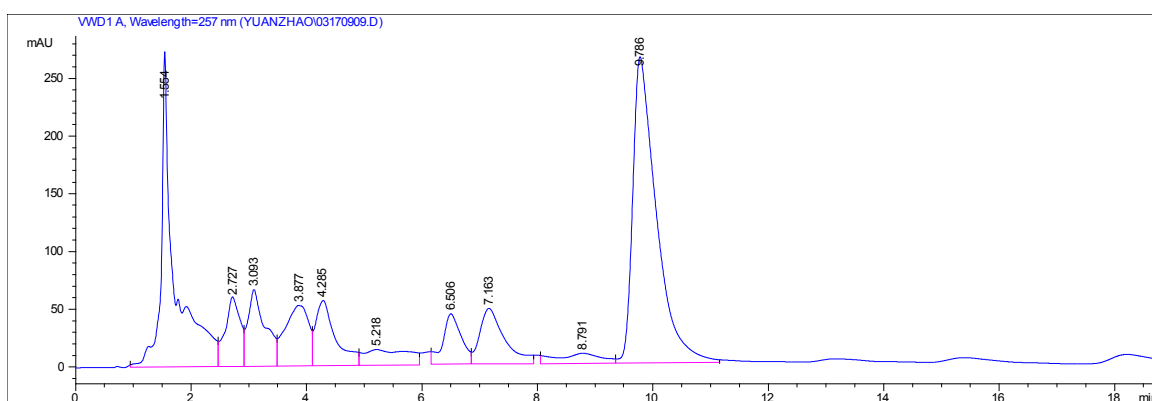


Figure 6 RPLC Analysis of  $\beta$ C Thermal Products, (CH<sub>3</sub>CN: H<sub>2</sub>O=70:30)

Table 4 RPLC Test Results of  $\beta$ -carotene Thermal Products (CH<sub>3</sub>CN: H<sub>2</sub>O=70:30)

#	Time	Area	Height	Width	Symmetry
1	1.554	4350.9	228.7	0.2453	0.345
2	2.727	1092	59.1	0.262	1.105
3	3.093	1399.4	65.9	0.2945	0.49
4	3.877	1470.9	52.4	0.4322	1.57
5	4.285	1355.4	56.2	0.3398	0.506
6	5.218	728.9	13.5	0.698	0.399
7	6.506	983.4	43.8	0.3318	0.821
8	7.163	1440.2	48.3	0.4413	0.552
9	8.791	471.7	8.8	0.731	1.455
10	9.786	7539.5	262.4	0.4284	0.44

RT=9.786 min for one of the thermal-degradation products samples, apply the ratio of 50:50 ratio mobile phase.

The peaks at 2.72 and 3.09 minutes are due to impurities found in the  $\beta$ -carotene prior to reaction. The peaks at 3.877, 4.285, 5.218, 6.506, 7.163 and 8.791 minutes are due to decomposition products. The  $\beta$ -carotene peak at 9.786 minutes while still present is at a much lower intensity than was present before heating.

#### UV-Vis Spectroscopy

Absorbance changes of  $\beta$ C after thermal treatment were determined by UV-Vis spectrophotometry in order to determine the degradation rate. For a given irradiation time, the higher the heating temperature, the greater the loss of  $\beta$ C. For heating at a given temperature, the longer the heating time, the greater the degradation of  $\beta$ C. The use of crystalline  $\beta$ C eliminates the impact of complex matrix such as would be found in food, drinks etc. The absorbance was obtained by averaging the 10 absorbance readings in the vicinity of the maximum ( $\pm 5$ nm). A blank of tetrahydrofuran was used to calibrate the instrument. A plot of the natural log of absorbance versus time, was found to be linear, The absorbance value for a freshly made 2.5  $\mu$ g/mL (equivalent to 4.664 $\mu$ M)  $\beta$ C std solution was measured as 1.4594 and converted to 2918.8 for 5000  $\mu$ g/mL  $\beta$ C.

The ultraviolet absorbance data, after correction for dilution and the initial mass of the solid  $\beta$ -carotene used in the thermal-degradation experiment was treated as a first order reaction to determine the rate constant. The first order treatment was chosen because it provided a better fit to the data ( $R^2$  0.97-0.99) than either the zero order or the second order models). The rate constant for each of the temperatures was calculated and is shown in Table 5 and Fig 7, 8.

Table 5 The UV Absorbance Reading for Different Thermal Treatment of  $\beta$ -carotene Dependent on Time and Temperature and Its Relative  $R^2$  Value for the Corresponding Reaction Orders

UV Absorbance (corrected for dilution and an initial mass of 5.00 $\mu\text{g/ml}$ $\beta$ -carotene)								
T( $^{\circ}\text{C}$ )	Time (hours)						Rate Constant	$R^2$ value
	1h	2h	4h	8h	24h	72h		
100	241.60	220.29	192.25	182.47	179.61	56.45	-0.0189	0.9535
150	224.86	172.00	167.86	157.58	108.78	35.20	-0.024	0.9831
200	40.452	32.944	21.656	21.156	13.092	2.632	-0.0351	0.9657
250	2.9688	2.3332	1.4460	1.3818	0.5460	0.0673	-0.0500	0.9746
300	1.0209	0.8006	0.6013	0.4298	0.1616	0.0101	-0.0624	0.9909
350	0.1558	0.1068	0.0747	0.0351	0.0101	0.0035	-0.0815	0.9754

Relationship between A and heating time

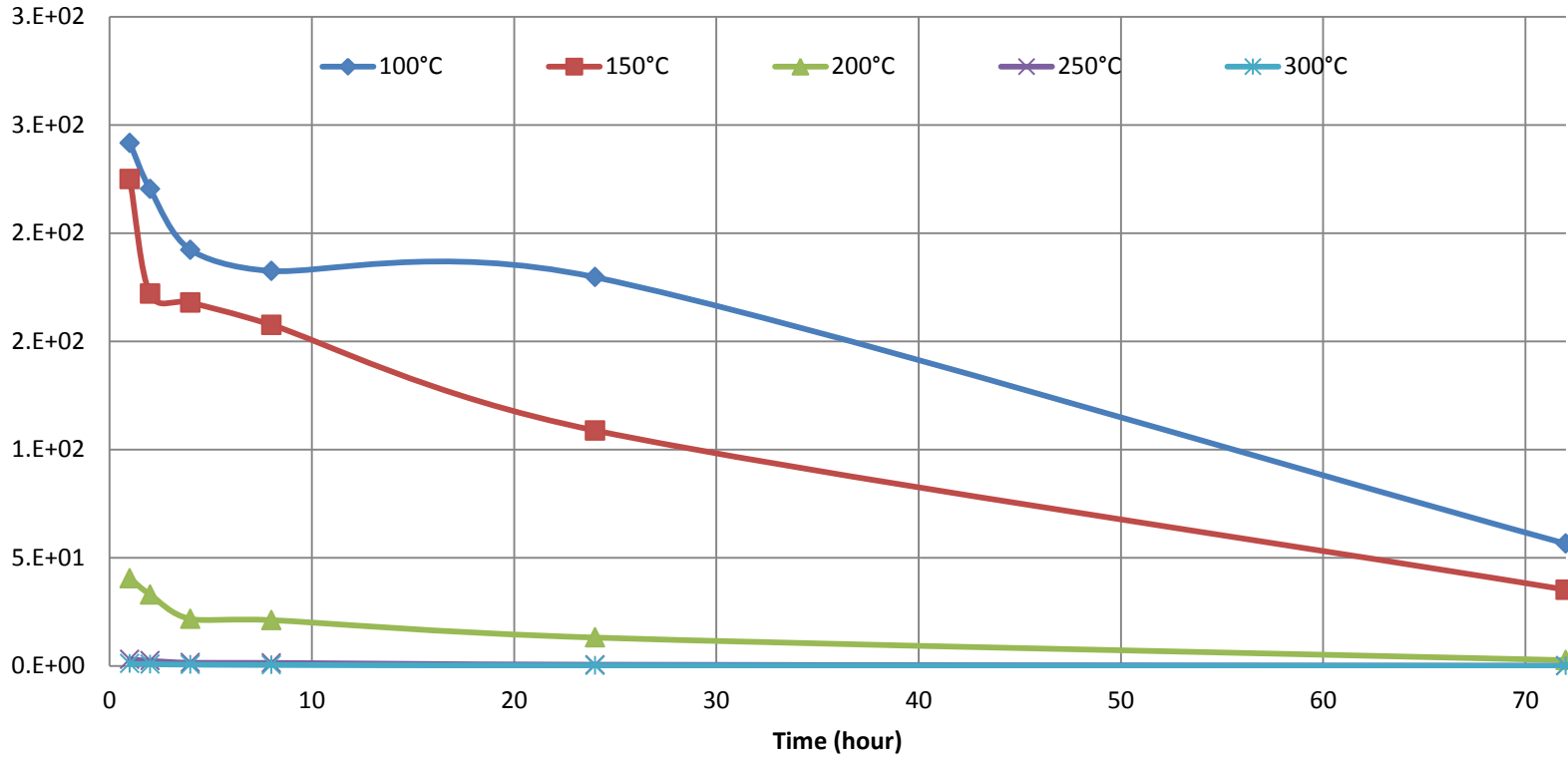


Figure 7 Relationship between A and Heating Time

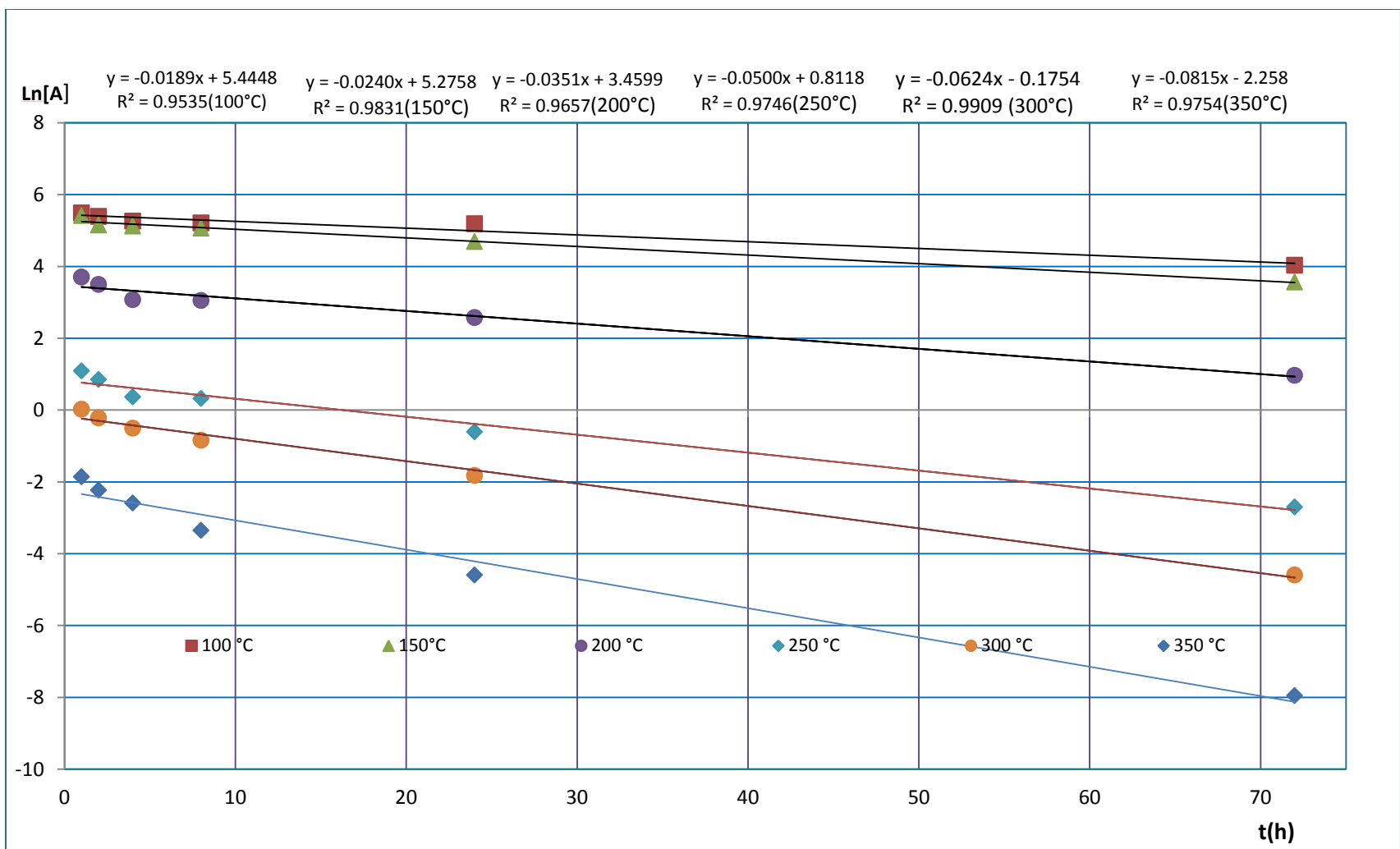


Figure 8 Thermal-degradation of  $\beta$ -carotene Rate Constant Determination

Table 6 The Summary of Rate Constant Varied with Temperature for Crystalline  $\beta$ -carotene Thermal-degradation

T (°C)	1/T (1/K)	1 <sup>st</sup> order		
		k	Slope(-k)	Ln(-k)
100	0.002680	0.0189	0.0189	-3.96859
150	0.002363	0.0240	0.0240	-3.7297
200	0.002113	0.0351	0.0351	-3.34955
250	0.001911	0.0500	0.0500	-2.99573
300	0.001745	0.0624	0.0624	-2.77419
350	0.001605	0.0815	0.0815	-2.50715

A summary of rate constant variation with temperature for crystalline  $\beta$ -carotene thermal-degradation are shown in table 6.

First order reaction,  $E_a = 1392.3 \times 8.3145 / 1000 = 11.5763 \text{ KJ/mol}$  ( $R^2 = 0.9815$ ,  $R = 0.9907$ ) between 100 to 350°C.  $E_a = 1599.4 \times 8.3145 / 1000 = 13.2982 \text{ KJ/mol}$  ( $R^2 = 0.9984$ ,  $R = 0.9992$ ) between 150 to 350°C.

It showed the result on the summary and comparison on the corresponding activation energy for different temperature groups and each individual temperature for first order reaction. These combinations were subjected to linear regression with respect to time as represented by Eq.  $\ln(c/c_0) = -kt$  and the coefficients were determined. Correlation coefficients and standard values were used as the basis to select the combination which best described the first order reaction for the entire temperature range.

## Ultraviolet Photochemistry of $\beta$ -carotene

To examine the photochemistry of  $\beta$ -carotene in solvents where it has limited solubility and under conditions where the photoproducts might be identified, the photochemistry of  $\beta$ -carotene was investigated using a *Rayonet* photo reactor. The reduction in  $\beta$ -carotene present was determined using UV-Visible spectrophotometry. An induction period of  $\geq 5$  min before the sample irradiation began to warm up the instrument. The UV absorbance readings began to decrease as the irradiation time increases. Preliminary experiments have shown that the rate of photo-degradation is significantly increased in good electron acceptor solvents such as carbon tetrachloride and chloroform compared with neat hexane<sup>36</sup>. This observation may be due to a direct photoinduced electron-transfer reaction from an excited singlet state of the  $\beta$ -carotene to the solvent in microsecond time scale to form an instantaneous ion-pair<sup>37</sup>.

The overlaid absorption spectra of  $\beta$ C in neat hexane after various irradiation times is shown in Appendix I. The decrease in absorbance induced by low intensity ultraviolet light ( $< 360\text{nm}$ ) from a 100 watt Hg lamp are presented in table 7.

In order to study the effect of electron acceptor solvents on the photo-degradation rate, the photo-degradation rate was determined in neat hexane and in dilute solutions of carbon tetrachloride in hexane. From the results, a plot of negative natural logarithm of the absorbance of versus time will result in a straight line with a slope equal to  $-k$ . All five plots and their corresponding rate



constants are completed on a single graph as below. Since the rate constant is temperature dependent from the table and graph's results (Table 7, Figure 9). Plot of the link on the ordinate and 1/T on the abscissa to determine the slope of the plot is -881.7692 Kelvin with a square regression coefficient value of 0.9960. The activation energy of the reaction fits the first order, and results in  $881.7692 \times 8.3145 / 1000 = 7.33147 \text{ KJ/mol}$ . The photosensitized activation energy is almost 1 times lower than for thermally activated reaction. The kinetic profile for the degradation of the starting parent single carotenoid ingredient of  $\beta$ -carotene is fitted well by a first-order equation model, i.e.

$$\ln[\beta\text{-carotene}]_t = -kt + \ln[\beta\text{-carotene}]_0$$

Table 7 The Summary of Absorbance Reading on Degradation Results for  $\beta\text{C}/\text{neat Hexane Solution}$

Time(min)	T(°C)				
	15	25	35	45	55
0	2.26	2.419	2.134	1.997	2.060
5	2.058	2.284	1.898	1.863	1.892
10	1.841	2.116	1.739	1.641	1.746
15	1.681	1.879	1.587	1.502	1.442
20	1.442	1.629	1.362	1.309	N/A
25	1.343	1.434	1.161	1.167	1.079
30	1.213	1.284	1.001	1.002	0.936
35	1.076	1.108	0.917	0.867	0.789
40	0.961	0.945	0.835	0.727	0.645
45	0.852	0.825	0.751	0.596	0.408
50	0.753	0.718	0.622	0.488	0.402
55	N/A	N/A	N/A	0.390	N/A

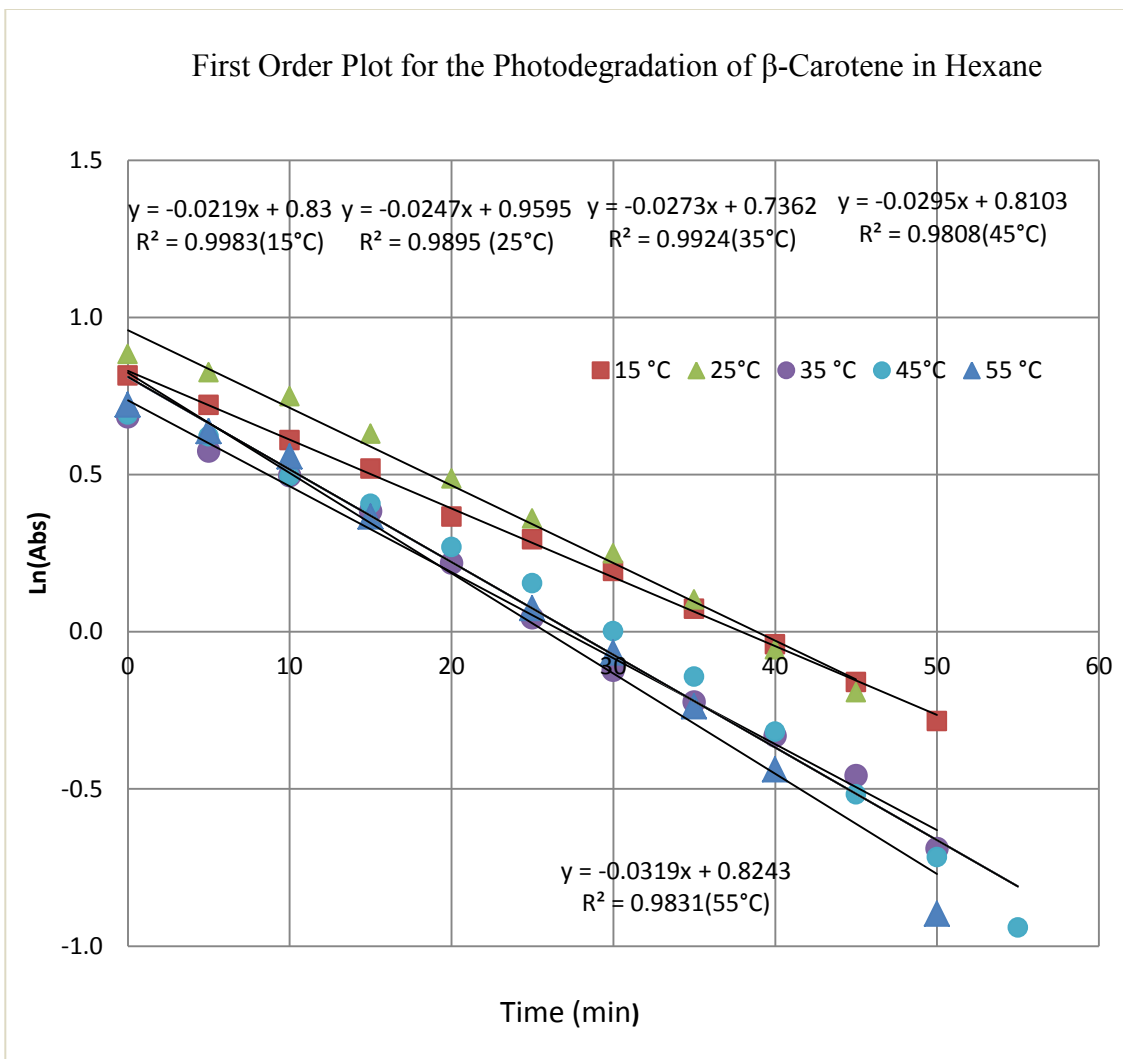


Figure 9 First Order Kinetic Plot for the Photo Degradation of  $\beta$ -Carotene in Hexane Solution (15-55°C)

In order to determine the activation energy in pure hexane, a plot of  $\ln(k)$  versus  $1/T$  was prepared. The slope of the line was determined to be  $-881.7692$  Kelvin with a  $R^2$  value of  $0.9960$ , the activation energy determined from this line is  $7.33$  kJ/mol as shown in Fig 10 based on the result of Table 8.

The photo-degradation rate of  $\beta$ -carotene in neat  $\text{CCl}_4$  solvent exceeds that of  $\beta$ -carotene in system (hexane+ $\text{CCl}_4$ ) replaced neat  $\text{CCl}_4$  solvent to better understand the mechanism on the significant enhancement of reaction rate. At 25°C, the five different ratios of carbon tetrachloride (0.05%, 0.20%, 1.00%, 2.00% and 4.00% )were added into 250 mL volumetric flask with hexane solvent. A direct linked relation between the ratio and photoreaction rate was found subjected to photooxidative conditions. The plot of volume percentage of  $\text{CCl}_4$  versus the rate constant of  $\beta$ -carotene without degassing was proved to be linear, the slope is 0.1282 with a high  $R^2$  value of 0.9995. At the same controlled temperature, the reaction rate for  $\beta$ -carotene in the hexane solvent without any  $\text{CCl}_4$  is  $0.0247 \text{ min}^{-1}$  with comparison to an enhancement of 0.40, 4.90, 9.60 to 20.30 folds by just adding 0.50mL, 2.50mL, 5.00mL and 10.00mL into a total volume of 250 mL solution. The more amount of  $\text{CCl}_4$  being added, the higher the reaction rate. As for 0.05% (0.5‰)  $\text{CCl}_4$ , its reaction rate was unaffected, which can be explainable that the amount is too miniscule to be mixed evenly to have a huge impact on the photo-degradation rate as other higher ratios.

Table 8 The Summary of Parameters Related with Rate Constant for  $\beta$ C

Dissolved in Neat Hexane (1st order)

T/°C	1/T(1/K)	k(rate, $\text{min}^{-1}$ )	Lnk	$R^2$	Time range(min)
15	0.003470	0.0219	-5.66348	0.9983	0-50
25	0.003354	0.0247	-5.69760	0.9877	0-50
35	0.003245	0.0273	-5.73059	0.9924	0-50
45	0.003143	0.0295	-5.76252	0.9871	0-55
55	0.003047	0.0319	-5.79347	0.9787	0-50

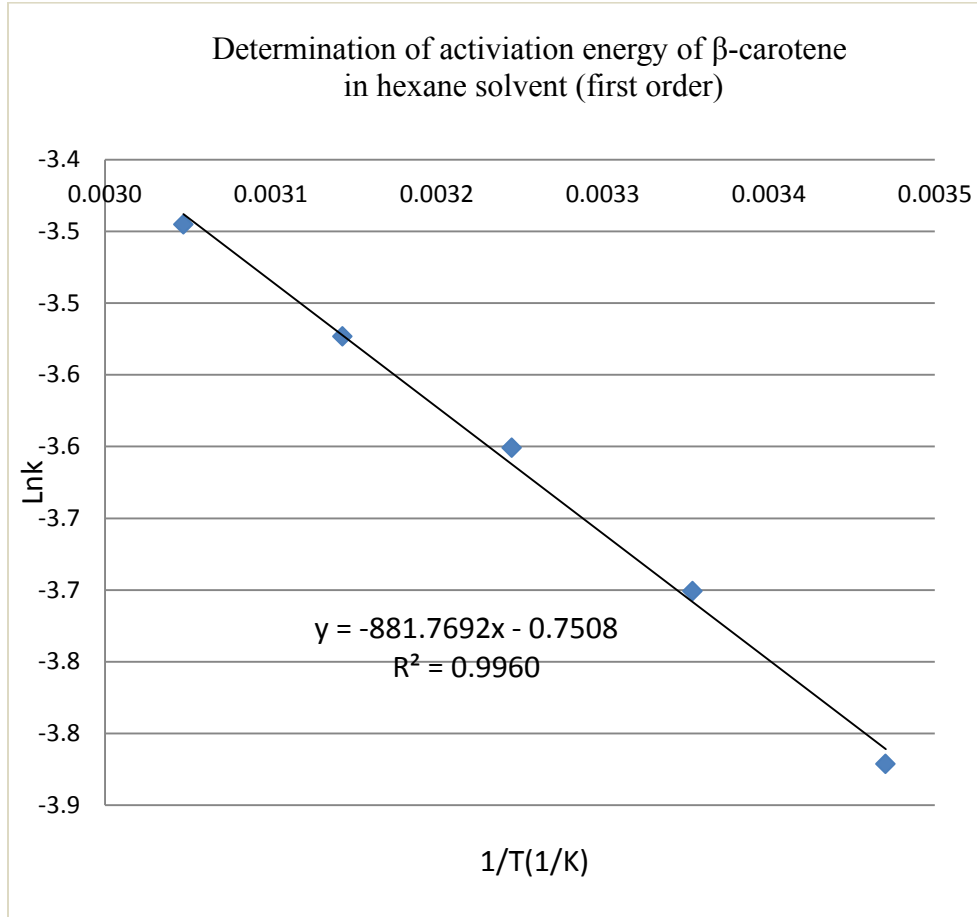


Figure 10 Determination of Activation Energy of  $\beta$ -carotene in Hexane Solvent

The photo-degradation rate of  $\beta$ -carotene in neat carbon tetrachloride is much greater than that of  $\beta$ -carotene in hexane. To better understand effect of solvent on the mechanism, experiments were conducted where small amounts of carbon tetrachloride was added to hexane and the photo-degradation of  $\beta$ -carotene in these mixed solvents was measured. The rate constants for solutions of  $\beta$ -carotene in hexane with a small amount of carbon tetrachloride are significantly greater than the rate constant in pure hexane. The reaction kinetics can still be

treated as being first order in  $\beta$ -carotene, the carbon tetrachloride concentration in even the most dilute solution is orders of magnitude greater than the  $\beta$ -carotene concentration. This set of conditions is typically considered as a pseudo-first order reaction.

The rate constants for the photo-degradation of  $\beta$ -carotene in the mixed solvent systems are observed to be by a factor of twenty as the carbon tetrachloride concentration is varied from 0.2% to 4 %. A plot of the photo-degradation rate constant versus carbon tetrachloride concentration is shown in Figure 11 and 12. The linear dependence of the rate on carbon tetrachloride concentration shows that the reaction is also first order in carbon tetrachloride. The activation energies for the reactions in the various concentrations of carbon tetrachloride are also contained in Table 9. A plot of the activation energy versus the concentration of carbon tetrachloride is shown in Figure 13.

Table 9 A Summary of the Rate of Photo-degradation of  $\beta$ -Carotene with Variable Concentrations of Carbon Tetrachloride.

% CCl <sub>4</sub> Mixed with hexane	Kinetic Data			E <sub>a</sub> (kJ/mol) 15- 55 °C	V <sub>% CCl<sub>4</sub></sub> /V <sub>hexane</sub> (Fold)
	k (min <sup>-1</sup> )	R <sup>2</sup>	R		
0.05	0.0185	0.9935	0.9967	N/A	
0.20	0.0345	0.9990	0.9995	6.215	1.40
1.00	0.1455	0.9962	0.9981	3.838	5.89
2.00	0.2613	0.9959	0.9979	2.689	10.58
4.00	0.5258	0.9949	0.9974	1.242	21.29

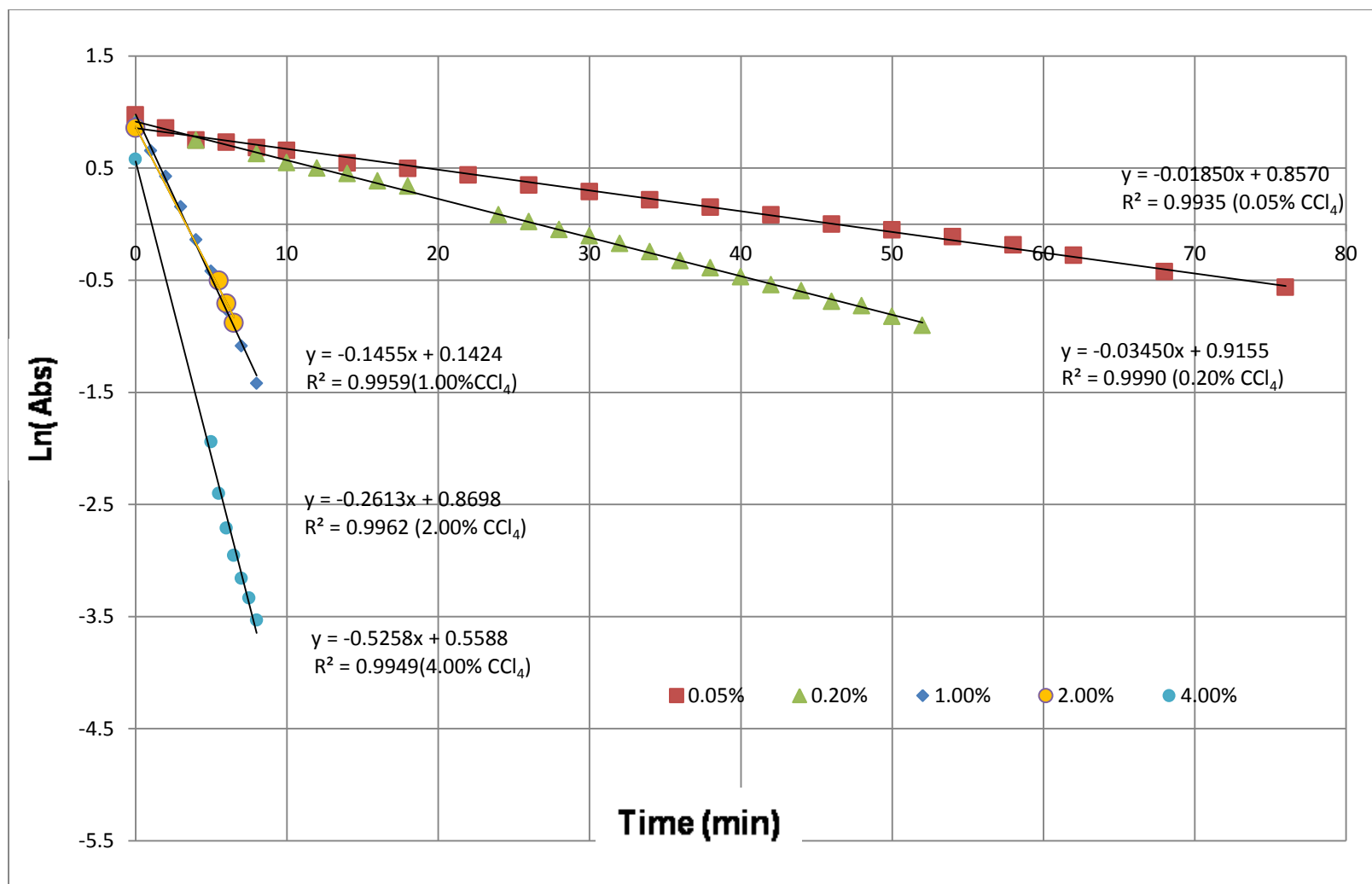


Figure 11 Rate of the Photo-degradation of  $\beta$ -carotene Varied as the Percentage of Carbon Tetrachloride.

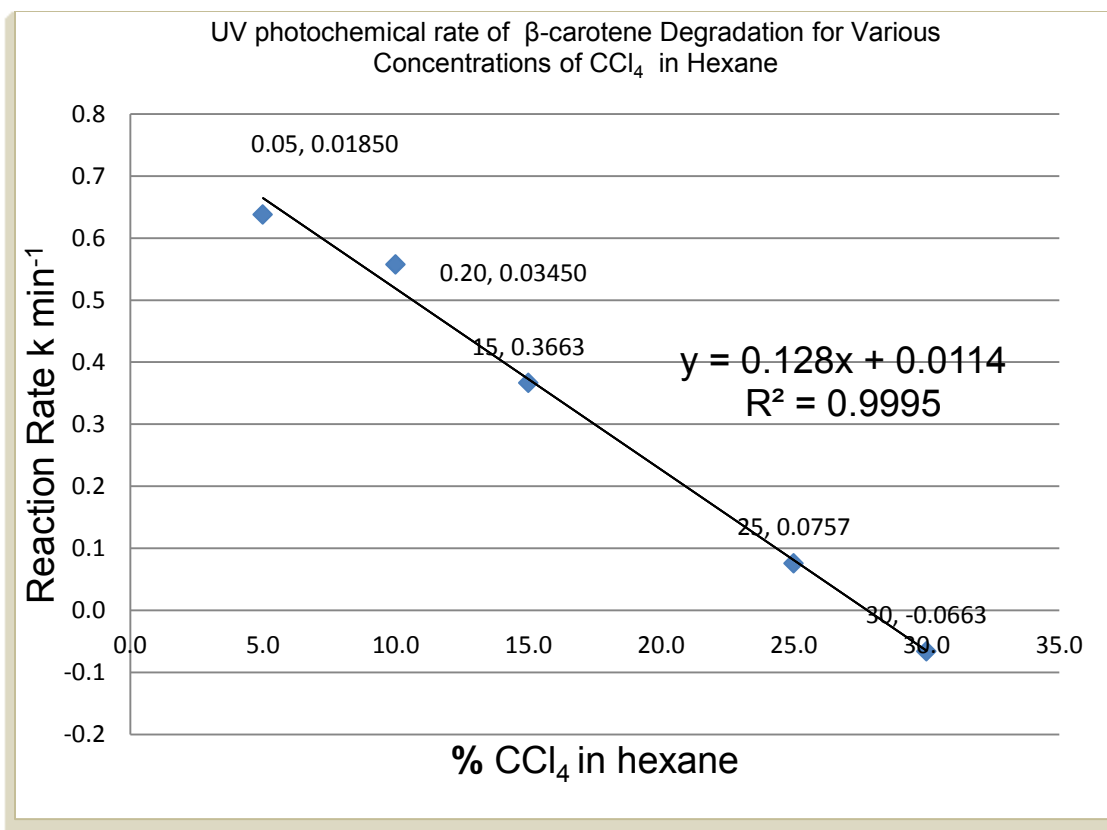


Figure 12 The Photo-degradation Rate of  $\beta$ -Carotene in Hexane with Various Concentrations of Carbon Tetrachloride.

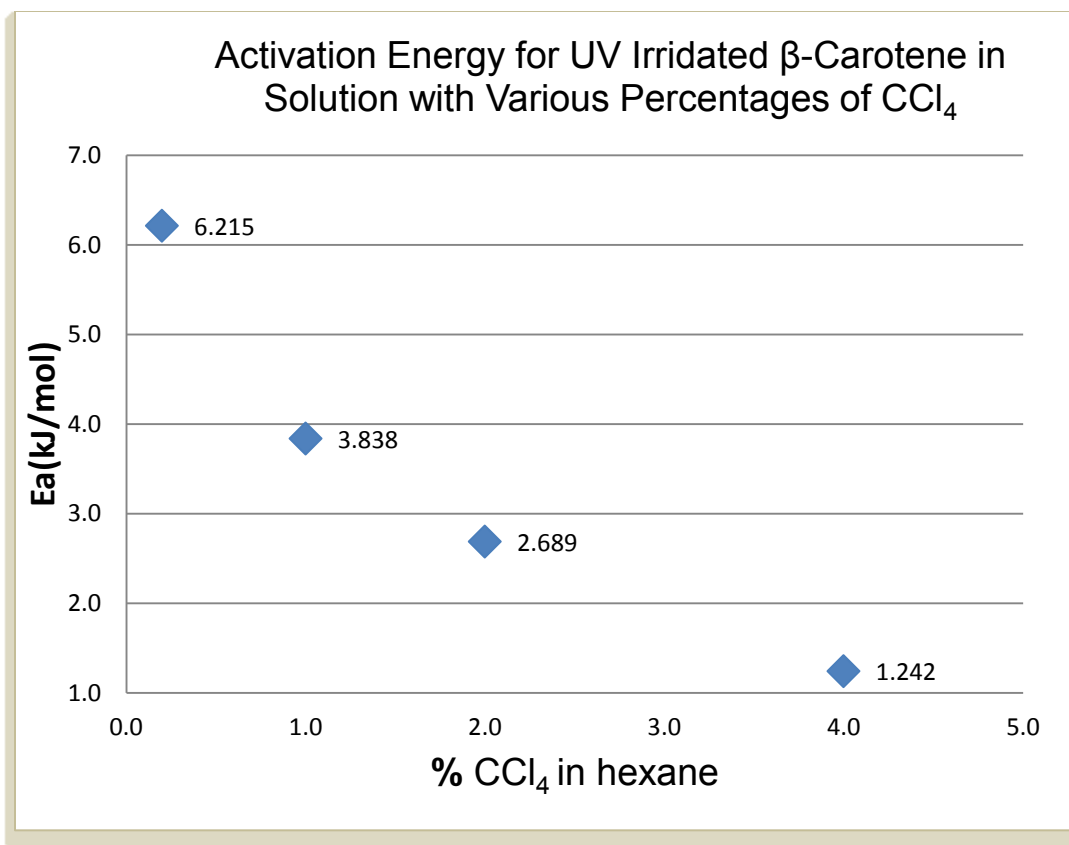


Figure 13. A Comparison of the Activation Energies for the Photo-degradation of  $\beta$ -Carotene in Hexane with Various Concentrations of Carbon Tetrachloride.



### Laser Photo-induced $\beta$ C Degradation

The laser photo-degradation of  $\beta$ -carotene in hexane and carbon tetrachloride was studied to determine the 2-photon reaction kinetics. Hexane solutions showed little change in what absorbance indicating that the laser photo-degradation rate in neat hexane is very slow. These extremely slow rates lead to very small changes in the degree of degradation induced by laser at a constant intensity, hence leading to the negligible variation to be further studied.

The photochemical reaction of  $\beta$ -carotene in 1.00%  $\text{CCl}_4$ /hexane solvent shows the absorbance of the solution drops as is shown in Fig. 14, Fig. 15 and Table 10. The three trials on rate constant are 0.1127, 0.1127 and 0.1113  $\text{min}^{-1}$ , respectively, the standard deviation of the three slopes is just 8.08E-04, which shows the results more reliable than a single determination. At the same temperature, the rate constant for  $\beta$ -carotene in 1%  $\text{CCl}_4$  mixed with hexane after UV light irradiation is 0.1455  $\text{min}^{-1}$ , which is comparable to laser induced photo-degradation at 0.115W pulse intensity.

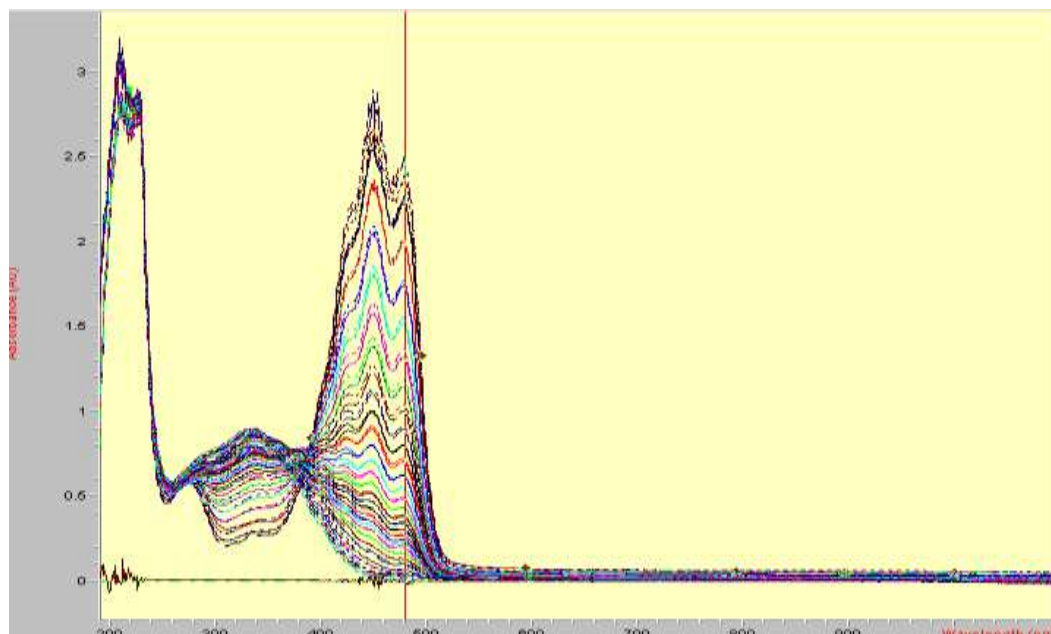


Figure 14. Dependence Effects of Irradiation Interval on  $\beta$ -carotene in 1.00% CCl<sub>4</sub>/hexane Solvent Absorbance Drop (Test #1)

Table 10  $\beta$ -carotene in 1% CCl<sub>4</sub>+Hexane Irradiated by 0.115w Laser (25°C)

Time(min)	Abs-1	LnA1	Abs-2	LnA2	Abs-3	LnA3	Avg	STDEV
0	2.4965	0.91489	2.5596	0.939851	2.49390	0.913848	0.922863	0.014721
1	2.2924	0.82960	2.2914	0.829163	2.27080	0.820132	0.826298	0.005344
2	2.0641	0.72469	2.0325	0.709267	2.02060	0.703394	0.712452	0.011001
3	1.8518	0.61616	1.7833	0.578466	1.77720	0.575039	0.589888	0.022815
4	1.6513	0.50156	1.5653	0.448077	1.55280	0.44006	0.463233	0.033436
5	1.4490	0.37087	1.3744	0.318017	1.36450	0.310788	0.333226	0.032803
6	1.2887	0.25363	1.2158	0.195402	1.19640	0.179317	0.209451	0.0391
7	1.1436	0.13418	1.0917	0.087736	1.02900	0.028587	0.083502	0.052924
8	1.0290	0.02859	0.98366	-0.01647	0.92317	-0.07994	-0.02261	0.054524
9	0.9199	-0.08349	0.90037	-0.10495	0.81656	-0.20265	-0.13036	0.063518
10	0.8187	-0.20005	0.78941	-0.23647	0.72582	-0.32045	-0.25232	0.061748
11	0.7443	-0.29526	0.69591	-0.36253	0.65030	-0.43032	-0.3627	0.067532
12	0.6652	-0.40764	0.62390	-0.47177	0.57937	-0.54581	-0.47507	0.069148
13	0.5858	-0.53474	0.56137	-0.57738	0.52029	-0.65337	-0.5885	0.06009
14	0.5215	-0.65112	0.49911	-0.69493	0.48666	-0.72019	-0.68875	0.034946
15	0.4650	-0.76583	0.45526	-0.78689	0.45913	-0.77842	-0.77704	0.010598
16	0.4201	-0.86724	0.40735	-0.89808	0.43087	-0.84195	-0.86909	0.028113
17	0.3780	-0.97276	0.36632	-1.00425	0.37747	-0.97426	-0.98376	0.017763
18	0.3361	-1.09041	0.33466	-1.09464	0.34278	-1.07067	-1.08524	0.012795
19	0.3038	-1.19148	0.30918	-1.17383	0.30767	-1.17873	-1.18135	0.009113

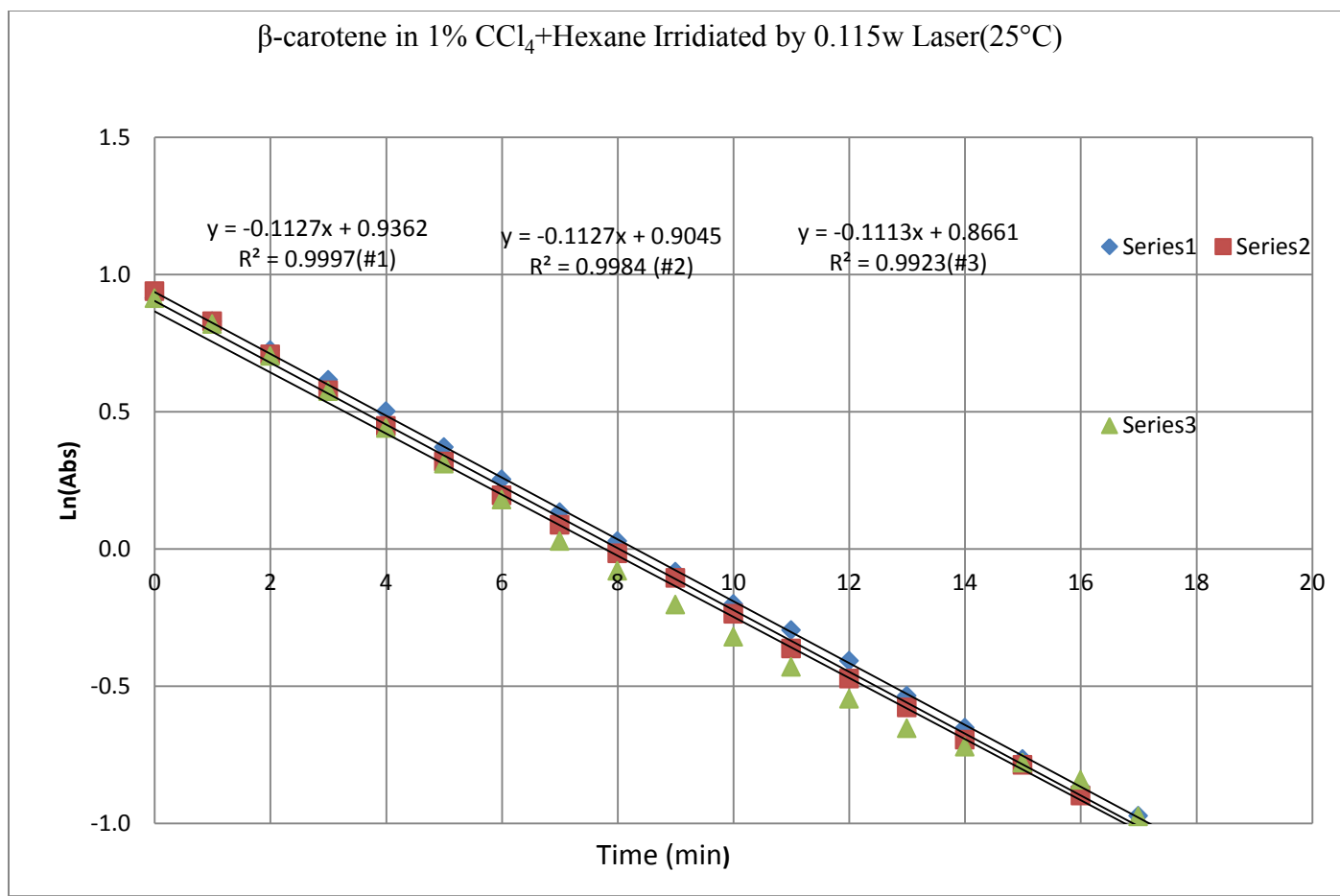


Figure 15  $\beta$ -carotene in 1%  $\text{CCl}_4$ +Hexane Irradiated by 0.115w Laser (25°C)

## Quantitative Analysis of Commercial $\beta$ -carotene

The products of the thermal and photo-degradation of  $\beta$ -Carotene were examined using a number of physical techniques. The identification of the products is a key step in understanding the basic features of the reaction. In previous work, the products of the reaction have not been fully characterized.

### Identification of Thermal-degradation Products of $\beta$ -Carotene by FT-IR

The products isolated after the evaporation of the solvent were examined by FT-IR spectroscopy. On the basis of simplified correlation chart, the alkene peak C=C stretch occurs at  $1660\text{-}1600\text{cm}^{-1}$  as the single peak #1 shows, conjugation double bonds of carotene will increase the intensity. In contrast, the C=C stretch peaks turned very weakly for the thermal-degradation products at  $1660\text{-}1600\text{cm}^{-1}$ , which might testify that some loss of conjugated C=C and the 11 conjugated double bonds subjected to be cleaved into a shorter chain( Fig. 16).

The FT-IR spectrum of  $\beta$ -carotene shows a large peak between  $1600$  and  $1660\text{ cm}^{-1}$  which can be identified as the carbon-carbon double bonds stretching frequency. After irradiation, there is a marked decrease in the intensity of this peak, indicating the loss of some of the carbon-carbon double bonds and a reduction in the conjugation. There is a weak and broad peak at  $3200\text{-}3400\text{ cm}^{-1}$ . This band is usually appears in combination with the hydrogen-bonded O-H peak (may be due to moisture). A rough bending appears as a broad and weak at  $1440\text{-}1220\text{ cm}^{-1}$ , this is C-O-H stretch which was often obscured by the  $\text{CH}_3$

bending. A wide seemingly overlapped but extremely intense absorption peak was observed around  $1000\text{ cm}^{-1}$ , which might be from =C-H vinyl stretch. The peaks at  $1650\text{-}1400\text{ cm}^{-1}$  are too vague to confirm the C=O stretch while it is possible. Some other observations based on the infrared spectroscopy of the samples is documented in the list below:

1) C=O stretch, broad, occurs at  $1730\text{-}1700\text{ cm}^{-1}$ , conjugation moves the absorption to a lower frequency.

2) Sp<sup>3</sup> C-H absorption occurs at frequencies between  $3000\text{-}2840\text{ cm}^{-1}$ , which is shown at  $2929\text{ cm}^{-1}$  in the spectra;

3) Aliphatic aldehyde usually show a band for the carbonyl group( H-C=O stretch) that appears in the range of  $1740\text{-}1725\text{ cm}^{-1}$ , which is shown at  $1722\text{ cm}^{-1}$  in the spectra.

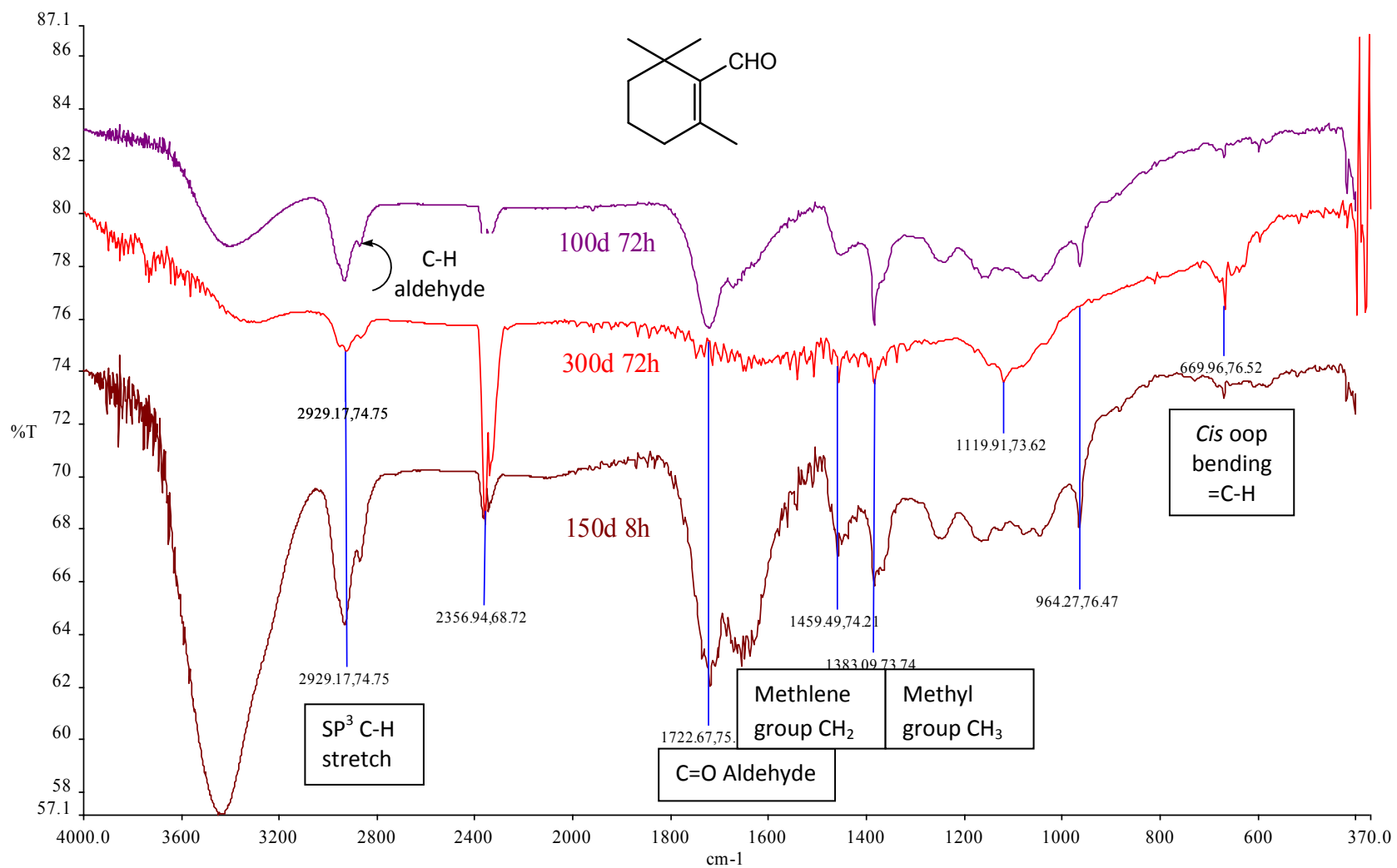


Figure 16 The FT-IR Spectra of  $\beta$ C Thermal-degradation Products (Neat Liquid, KBr Plates)

## Identification of Products of the Thermal and Photo-degradation of $\beta$ -carotene Studies by GC-MS

In order to understand the products found in the thermal and photochemical reaction of  $\beta$ -carotene, gas chromatography-mass spectrometry was used to separate compounds and identify them based on the mass of their parent ion and fragment ions. The total ion chromatogram for several  $\beta$ C samples are shown in Figure 17.

When  $\beta$ -carotene has been bombarded by 50-70eV electrons, not only it forms molecular ion containing an odd number of electrons, also called radical-cation, but also it will absorb some of extra energy to collide with the incident electrons to form some unstable intermediates with a short lifetime usually less than  $e^{-05}$  sec, then they might break apart into fragment ions before entering the ionization chamber of mass spectrometry. It is because not all fragment ions have the exact same lifetime, the mode of fragmentation is somewhat featured and even predictable involving group rearrangement, migration of groups and the formation of secondary fragment ions. The difference in mass unit of the fragment ion and the original ion involves a neutral loss. Overall, the golden rules generally lead to the formation of a more stable fragment ions over those less stable. It is noted of  $\beta$ -carotene's unique unsaturated structures, so it is worthwhile to dig in its unique fragment processes underlying to assist the judgment on the effects of thermal and photo treatment towards  $\beta$ -carotene by GC-MS. HPLC-ESI-MS as a soft ionization technique, usually cannot provide the fragment ions as rich as GC-MS



can afford when  $\beta$ -carotene, which might be an alternative analytical instrument over others in quantification. We tentatively gain some progress on the analysis of the thermally degraded products.

Light exposure and thermal processing are common in natural environmental circumstances that affect the  $\beta$ -carotene profile. Thermal and photo-degradation contribute to the presence of  $\beta$ -ionone and other reaction products, which initially involve epoxidation and furanoid rearrangement <sup>39</sup>. This will constitute a significant step in elucidating the hypothesis in the formation of norisoprenoids structures fragmental molecules from  $\beta$ -carotene <sup>40</sup>.

$\beta$ -carotene degradation was found to yield a range of  $\beta$ -apo-carotenals and  $\beta$ -apo-carotenones according to the previous reports <sup>41</sup>. Certainly, it is expected that the thermal reaction and the photochemical reaction in a solvent will give different products. The presence of different products is important in verifying possible mechanisms for the reaction. Any reaction mechanism must predict products consistent with those found in the experimental determinations.

$\beta$ -carotene, with its long conjugated chain, is prone to cleavage at points along the conjugated chain. This feature makes it very unstable both thermally and photochemically. Heat, light and oxidation are the three common impact factors that cause the degradation of  $\beta$ -carotene according to many authors. Those cleavage products are initially separated by GC and then identified by mass spectrometry. Norisoprenoids and sesquiterpenes are two classes of recognizable by GC-MS compounds upon thermal-degradation <sup>42</sup>.

It is also important to note that the purified sample of  $\beta$ -carotene and the commercial material do not appear to differ based on HPLC, TIC and UV-Vis spectrometry. For example, both purified sample and the commercial  $\beta$ -carotene have the same maximum absorbance wavelength at around 452 nm and shoulder peak appeared around 479nm. Based on those experimental results, it is possible that it fails to pass the purity tests, therefore, we decided to use the 95% labeled  $\beta$ -carotene as our main research materials.

Those products with short polyene structures resulting from cleavage of  $\beta$ -carotene appeared with a variety of retention times and molecular weights, but the mass spectra and polarity of these products were usually quite similar to one another due to the similar structures. The determination their chemical structures will provide some insight into the pathway and fate of  $\beta$ -carotene by stimulating natural environment.

Upon bombardment with 70 eV electrons, the parent ions have a tendency to readily break up into smaller fragments with the molecular ion hardly being detected unless a portion of the molecule can easily stabilize a positive charge. The use of fragmentation is difficult unless the compounds separate exceptionally well on the GC column. For instance,  $\beta$ -carotene, retinal, retinol,  $\beta$ -ionone, and cyclocitral – with molecular weights of 536, 284, 286, 218, and 152 g mole<sup>-1</sup>, respectively –all have similar fragmentation patterns for ions < 150 g/mol.

## A. Purification Effects Test on GC-MS

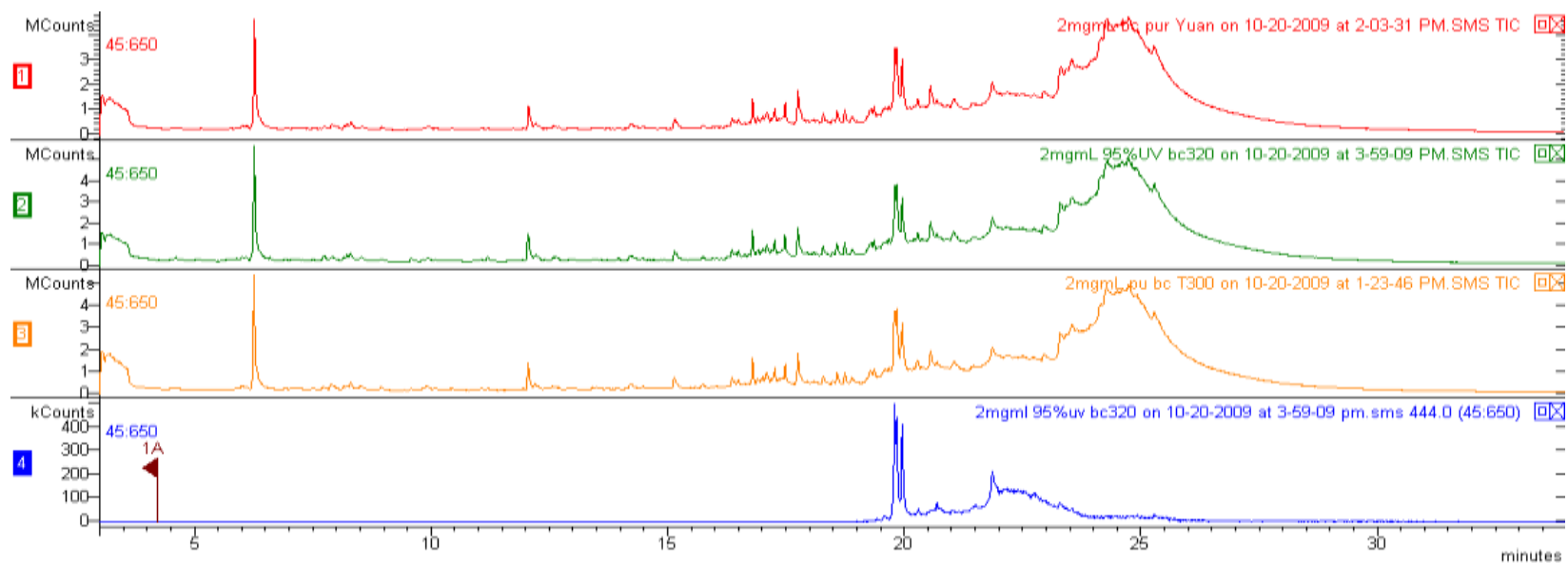


Figure 17 Comparison of TIC Chromatogram for Purified and Unpurified  $\beta$ -carotene Standard Aliquots.

- 1- Full scan acquisition resulting in the total ion current (TIC) plot for 2mg/mL purified  $\beta$ -carotene analyte;
- 2- Full scan acquisition resulting in the total ion current (TIC) plot for 95% UV passed commercialized  $\beta$ -carotene analyte;
- 3- Full scan acquisition resulting in the total ion current (TIC) plot for 2mg/mL purified  $\beta$ -carotene analyte by the third person;
- 4- Extracted ion chromatogram (444) from a GC-MS analysis of 2mg/mL 95% commercialized  $\beta$ -carotene.

## B. GC-MS Analysis of the Thermal-degradation Products

The mass spectra of 2mg/mL  $\beta$ -carotene after and before thermal-degradation treatment was shown on Fig. 18. The reaction products after thermal treatment at 200°C for 1 hour show the appearance of new peaks at retention times between 7 and 13 minutes ( $m/z$  156,192,248,180,208,218,206 etc). Comparison of total ion chromatogram show significant decrease in the response due to  $\beta$ -carotene at a retention time greater than 20 minutes. The decrease is dependent on the heating temperature (see Fig. 19 next page). The reaction of  $\beta$ -carotene is nearly complete after 6 hours at a temperature of 250°C.

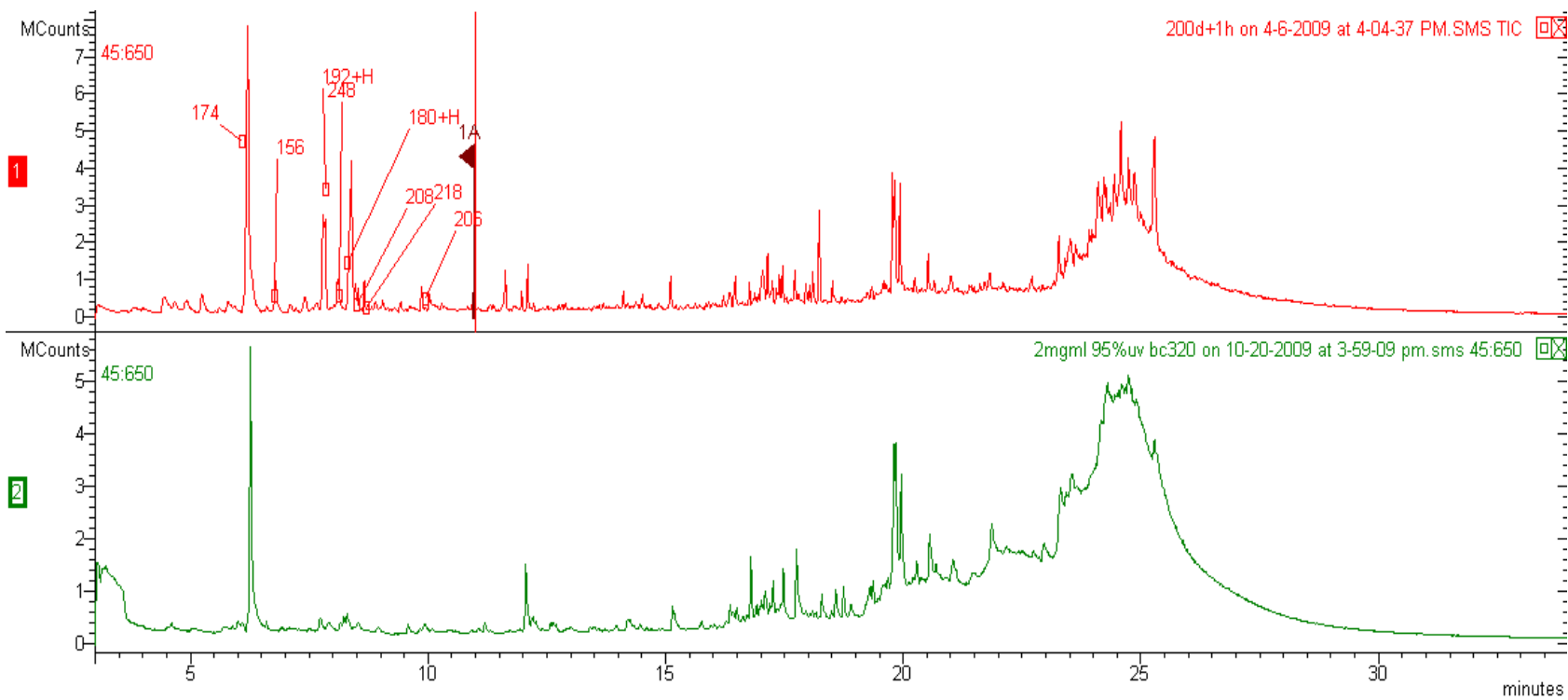


Figure 18 The Mass Spectra of 2mg/mL  $\beta$ -carotene After and Before Thermal Treatment at 200°C for 1 hour

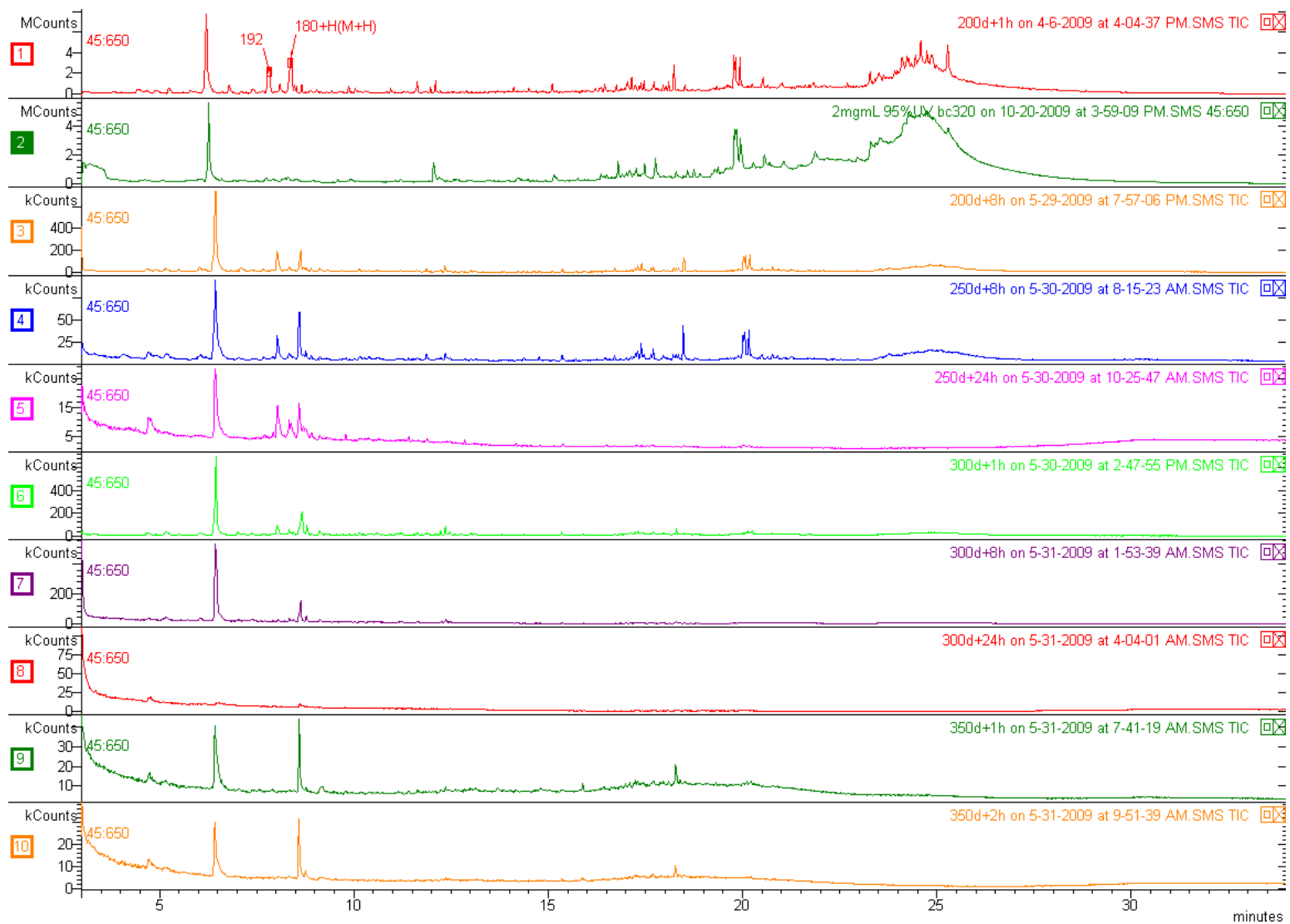


Figure 19 Comparison of TIC Showing the Decreasing Response of  $\beta$ -carotene after 17.5min Dependent on the Heating Temperatures

### C. Identification of Thermal-degradation Products by Mass Spectroscopy

As for (all-E)  $\beta$ -carotene ( $C_{40}H_{56}$ , with a molecular weight of 536), it presented the fragment ions of M-92, i.e., with a mass to charge ratio of 444(base peak) and M-137(m/e 399, secondary base peak). The identification and characterization was derived from the EI-MS profile with references of NIST library as shown in the following Table 11 and Fig 20.

Table 11 Molecular Ion and Some Fragment Ions Observed in the Mass Spectra of Some Thermal-degradation Products.

Product	Masses Detected
Ionene(TDN)	174(M+),159(100%), 144, 131, 115, 105, 91, 77
$\beta$ -cyclocitral	152(M+), 137, 123, 109(100%),95,81,67
Dihydroactinidiolide	180(M+), 165,152, 137, 123,111(100%), 95,81,67
4-oxo- $\beta$ -ionones	206(M+),191,163(100%),150,135,121,105,93,91

The products identified above are short chain byproducts that were identified by the NIST mass spectral library, the fit index of every of the identified compounds was above 700/1000. Because of the limitation of GC-MS, only the volatile compounds with low molecular weight (<650 amu) could be identified using the mass spectrometry. This won't influence the degradation pathway of  $\beta$ -carotene since most of the degradation products of the thermal reaction are expected to result from be breaking of the  $\beta$ -carotene in the conjugated polyene portion for the molecule. A few of the identifiable short chain products were observed

before the thermal-degradation experiments and upon investigation, all of them are plausible oxidation products of  $\beta$ -carotene.

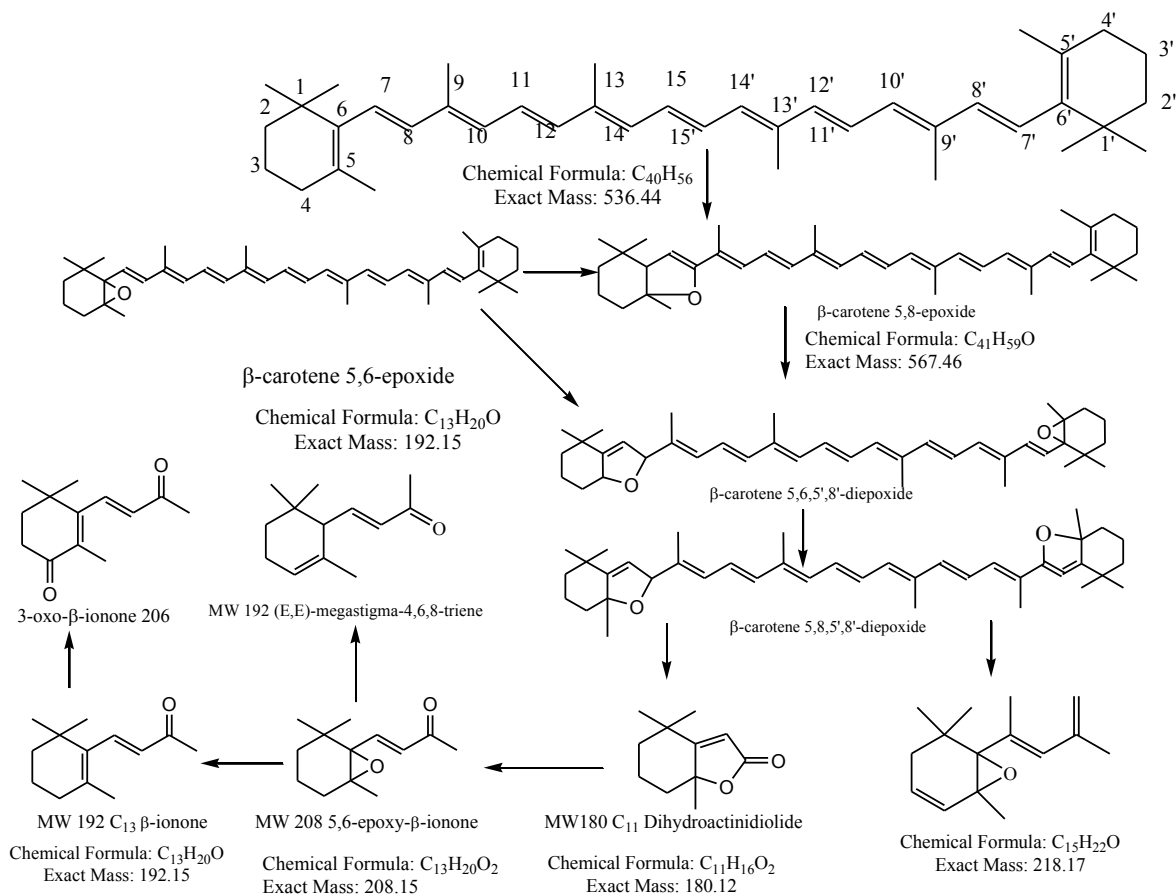


Figure 20 Proposed Mechanism of m/z 536 to 192, 180, 208, 218, 206 Thermal-degradation Products

Isomerization, epoxidation, oxidation and cleavage are well-known decomposition routes for  $\beta$ -carotene upon heating. Past and current research has focused on the presence of epoxidation and apocarotenal formation on thermal-degradation along with their geometric isomerization. Very few have tried to elucidate the final pathway of  $\beta$ -carotene decomposition upon heat treatment. The formation of a variety of monoepoxides and diepoxides were



reported to be as followings, 1)  $\beta$ -carotene-5,6-epoxide, 2)  $\beta$ -carotene-5,8-epoxide; 3)  $\beta$ -carotene-5,6,5',8'-diepoxide; 4) 5,8,5',8'-diepoxide<sup>43</sup>. Unreacted  $\beta$ -carotene could also be seen in the total ion chromatogram of the degradation products. Those compounds are very similar, the only differences are just the side chains located at the double bonds. The heat treatment of  $\beta$ -carotene has provided a detailed picture of its composition to yield apo-carotenals and apo-carotenones along with epoxides both in the presence of oxygen and absence of oxygen<sup>43</sup>. Under a specific condition, the identification on the authentic standard samples will arouse great interest in the better understanding of degradative pathways of  $\beta$ -carotene.  $\beta$ C was hypothesized to be the precursors of C-13 norisoprenoids aromatic compounds liberated from grapes and wines by Pasquale Crupi et al<sup>44</sup>. In 2005, Antonio et al. regarded the cyclization of polyolefins as the general reaction pathway in thermally induced reactions of carotenoids through his HPLC-ESI-MS results<sup>45</sup>.

With regard to the initial sample (2mg/mL  $\beta$ -carotene in THF solvent), as shown in Figure 18, the disappearance or relative decrease of peak intensity of the  $\beta$ -carotene not well-defined in the total ion chromatogram and the appearance of new five peaks, which were detected within the initial 5 min of the temperature program. The quantity of the decomposition products varied with the heating time and temperature.

The chromatographic peak at a retention time of 6.255 min has the mass

spectrum showing in Fig 18 and Appendix III( see mass spectra data for m/z 174). Based on compounds in the NIST library, the compound is identified as 1,6,8-trimethyl-1,2,3,4-tetrahydronaphthalene with the fragment ions with a mass of 174 amu.

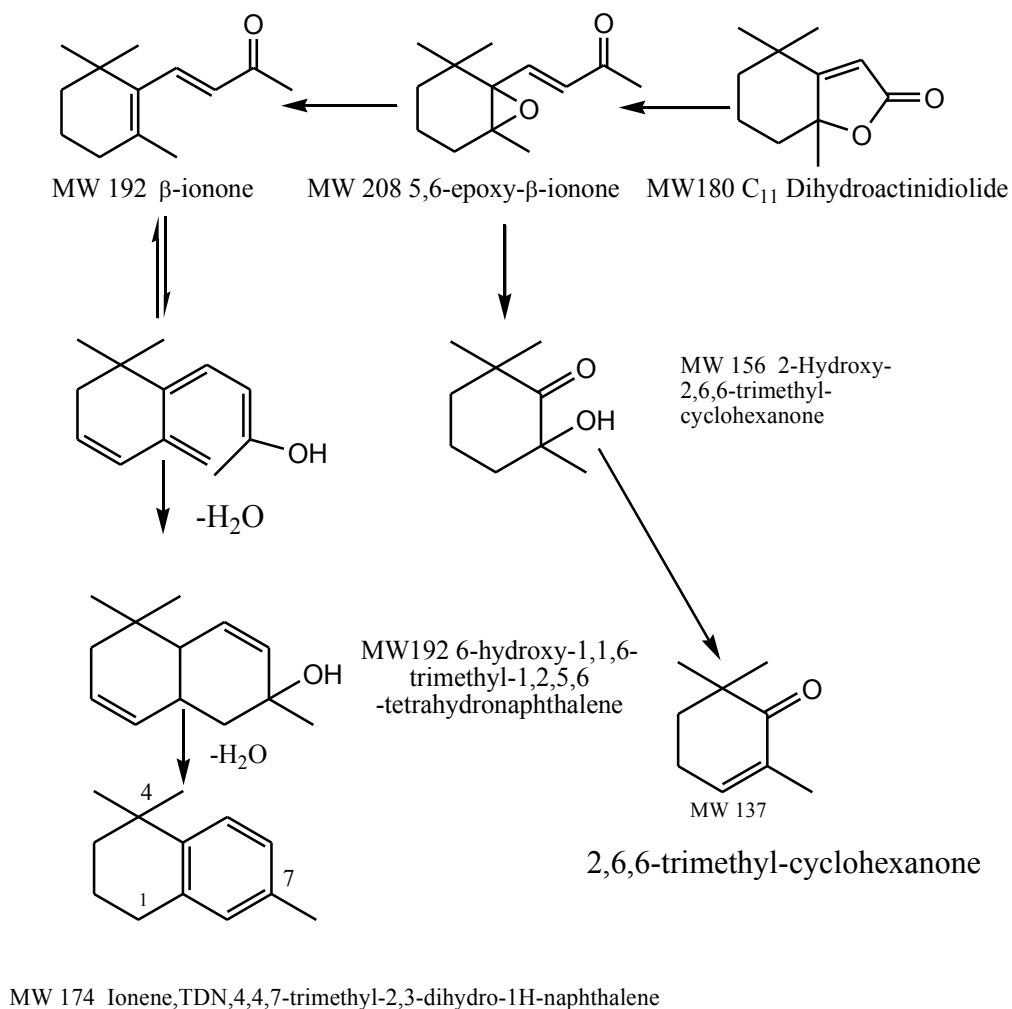


Figure 21 Proposed Mechanism of m/z 180 to 192, 156 and Daughter Ions at m/z 137, 2-hydroxy-2,6,6-trimethyl-cyclohexanone

This set of mechanisms, based on the GC-EI-MS identification of products initially forms from a cleavage of the  $\beta$ -carotene, followed by ring closure and aromatization to give tetra hydro naphthalenes as is shown in Figure 21. If  $\beta$ -ionone is oxidized, before ring closure, trimethyl cyclohexanone is the final product, observed in the total ion chromatogram. 5,6-epoxy- $\beta$ -ionone is a six-membered ring with an epoxide group, which is confirmed by the presence of the peak at  $m/z$  208 and rearranged into  $\beta$ -ionone with a generation of carbon-carbon double bond at 5,6-ortho position and a loss of epoxide moiety with a proton transfer.  $\beta$ -ionone (also called rose ketones) is extracted from rose essential oils. A ring closure of  $\beta$ -ionone and cyclization proceeds to generate TDN(4,4,7-trimethyl-2,3 dihydro-1H-naphthalene) following by an elimination of two water molecules proceeds where the double bond at position 7 is temporarily to form a carbocation which rearranges into an extended conjugated double bond systems <sup>44</sup>.

Decyclization and cyclization of the polyolefin segment may be a rational pathway to the rest of short in-chain products such as 2,6,6-Trimethyl-2-hydroxycyclohexanone (MW 156, also named by -hydroxy-2,6,6-trimethyl-cyclohexanone). However, considering the mixture of compounds observed in the thermal-degradation experiments, all of them share similar end-group-cyclohexanone segments with their parental compounds. The chair conformation of the cyclohexane ring was adopted, attached to a ketone to reduce torsional strain. This conformation is the most stable form and relatively lower energy

status to overcome the steric resistance. Due to the fact that  $\beta$ -carotene is a pretty potent antioxidant in vitro and in vivo like other carotenoids, it is reasonable to expect that the delocalization of the polyene  $\pi$ - $\pi$  electrons resists the attacks of photosensitizer and is resistant to high temperature. Epoxy- $\beta$ -carotene compounds were not identified in our EI-MS total ion chromatograms.

#### MS at $m/z$ 192+H

As often observed in mass spectrometry, seemingly small changes in ion structure isomers may cause significant difference in the mass spectra of the respective analytes. While  $\alpha$ -ionone significantly dissociates to yield the fragment ion at  $m/z$  136 upon isobutene loss via retro-Diels–Alder reaction. Unsaturated six-membered rings of cyclohexene derivatives can undergo a retro-Diels–Alder fragmentation to produce the radical cation of a diene and a neutral alkene—the hypothetical precursors as shown in Figure 22.

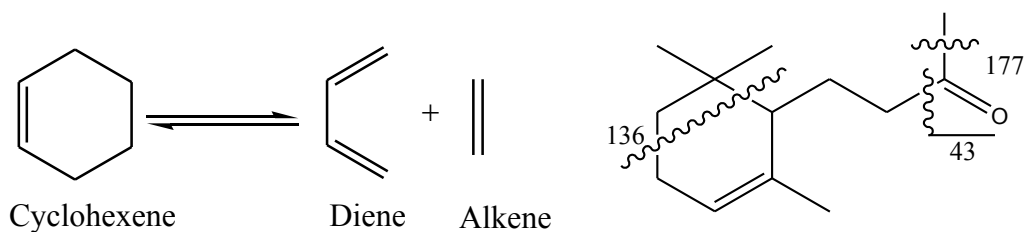


Figure 22. Scheme of Retro-Diels–Alder fragmentation and the Fragmental Pathways of  $\alpha$ -Ionone and  $\beta$ -Ionone<sup>38</sup>

The fragment ion at  $m/z$  177 should correspond to a  $\beta$ -ionone ion ( $C_{13}H_{20}O$ ) corresponding to a  $C_{12}H_{18}O$  elemental composition for the deprotonated ion. The molecular ion of 192 amu and loss of an unit of 15 amu were denoted in the

mass spectra of this set of compound as below, however, there is no loss of  $m/z$  136 fragments ions were observed which rules out  $\alpha$ -ionone. The isomer  $\beta$ -ionone mainly exhibits an intense  $[M-CH_3]^+$  signal, at  $m/z$  177 (192-15) which is due to the loss of a terminal methyl group from the allylic position to yield a thermodynamically favorable tertiary allyl cation<sup>38</sup>.

#### D. Identification of $\beta$ C Photo-degradation Using 532 nm Laser Radiation

Depending on the intensity and wavelength of the light source,  $\beta$ -carotene may undergo one or two photo-degradation process. The analysis of the photochemical behavior provides essential insights into the nature of the photoproducts generated in  $\text{CCl}_4$  and hexanes solvents.

The conventional one-photon process such as electron or proton transfer or bond cleavage through the UV light of 254, 313, and 365 nm. One-photon photo – reaction is described by a linear dependence of rate on intensity vs quadratic dependence on actinic intensity which would be typical of a two photon process. In contrast, the two-photon processes through the 532 nm pulsed laser light. The pulsed laser source offers intensities large enough that two photons-photon processes can occur to be absorbed and photohomolyzed by individual molecules within short-lived intermediate state.

Most current studies are focused on the characterization and identification of the transient intermediates, namely,  $\square\text{C}^+$  cation species or  $\text{C}\bullet$  neutral radical species. Those are usually generated immediately following the photoexcitation of  $\beta$ -carotene. While the studies of C-chloroalkane photoproducts is still rare, the fact that carbon tetrachloride is a good electron acceptor and will release the trichloromethyl radical  $\bullet\text{CCl}_3$  makes carbon tetrachloride a good candidate for study. The trichloromethyl radical can further react with oxygen to form the trichloromethylperoxyl radical  $\text{CCl}_3\text{O}_2\bullet$ <sup>46</sup>. The ability to form these two reactive

radicals obviously plays a role in the photoexcitation of  $\beta$ -carotene as indicated by the orders-of-magnitude faster rate of reaction of  $\beta$ -carotene in  $\text{CCl}_4$  solutions in comparison with  $\beta$ -carotene in-hexane solutions .

A 4mg/mL standard solution of  $\beta$ -carotene in  $\text{CCl}_4$  was prepared and placed in a cuvette, and degassed with argon gas for a total of 15 min. Significantly, the  $\beta$ -carotene in the chloromethane solvents loses its color within few seconds in a cuvette with intense 532 nm laser pulses from the pulsed Nd: YAG laser in a manner analogous to that observed with UV light (one photon) but appears to react more rapidly. This laser-induced photo-degradation has a quadratic dependence on the intensity of 532 nm laser pulses, which indicates that the process is a two-photon excitation process.

Based on the overlaid gas chromatography-mass spectrometry results there is no significant difference between  $\beta$ -carotene in carbon tetrachloride in the presence of saturated air and argon(Figure 23). Gretchen Laubacher observed the same trends on measuring the rate of degradation for  $\beta$ -carotene in carbon tetrachloride solutions irradiated with 254nm and 313 nm Hg lines. For both lines it was observed that the rate constants measured by UV-Vis spectrophotometry were, respectively,  $7.123 \times 10^{-3} \text{ sec}^{-1}$ (air saturated) vs.  $5.99 \times 10^{-3} \text{ sec}^{-1}$  (argon saturated) for 254 nm and  $1.68 \times 10^{-3} \text{ sec}^{-1}$  vs.  $2.54 \times 10^{-3} \text{ sec}^{-1}$  for 313 nm light. Despite that the rate of degradation for solutions for 313 nm Hg line when degassed with argon was approximately twice the rate of degradation

for solutions in the presence of air, it was concluded that the difference was not sufficient to adequately determine the effect of oxygen <sup>47</sup>.

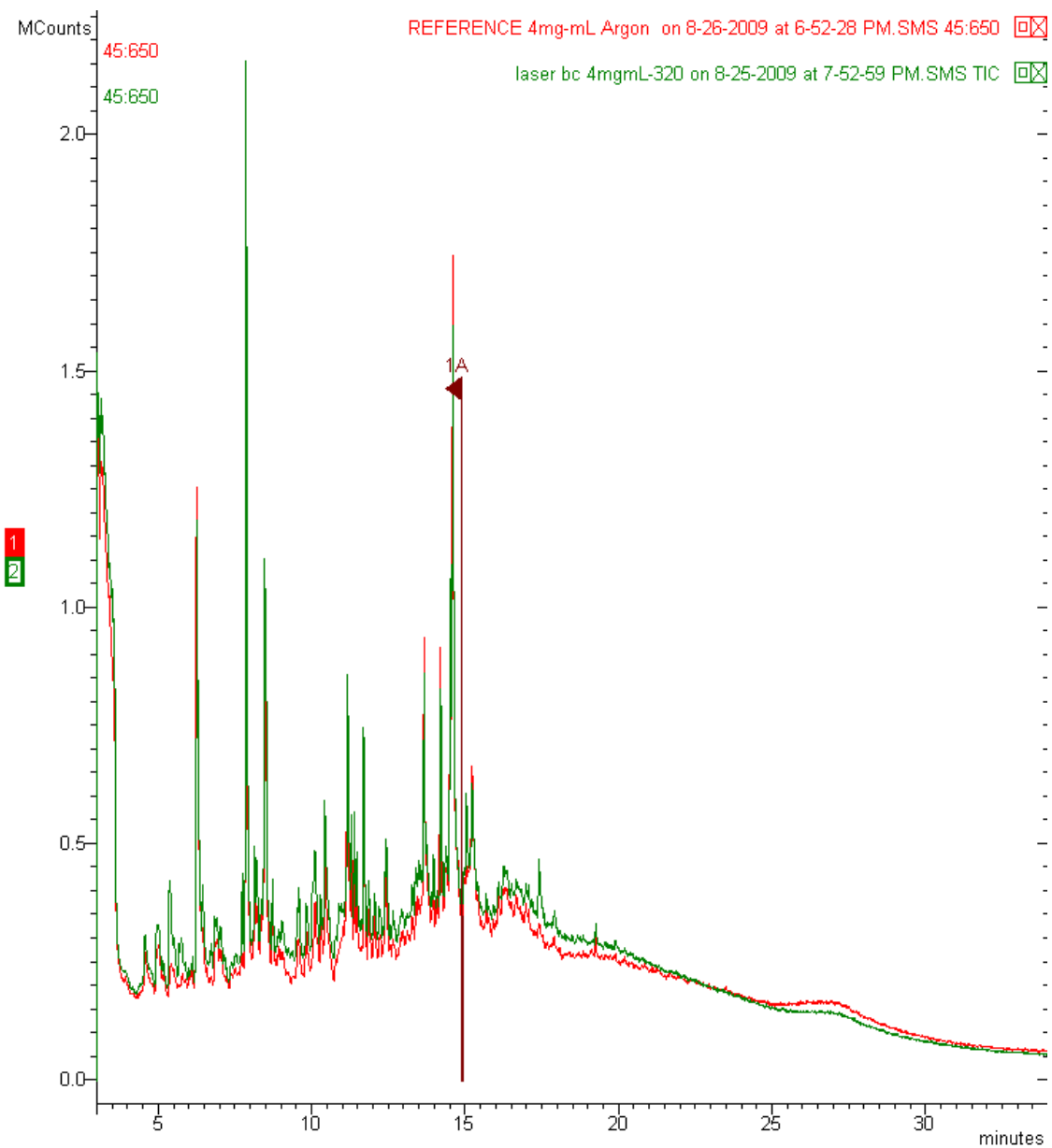


Figure 23 TIC Chromatogram for Laser-induced Reaction Products from 4mg/ mL  $\beta$ C std Solution in the Presence of Air and Argon Separately



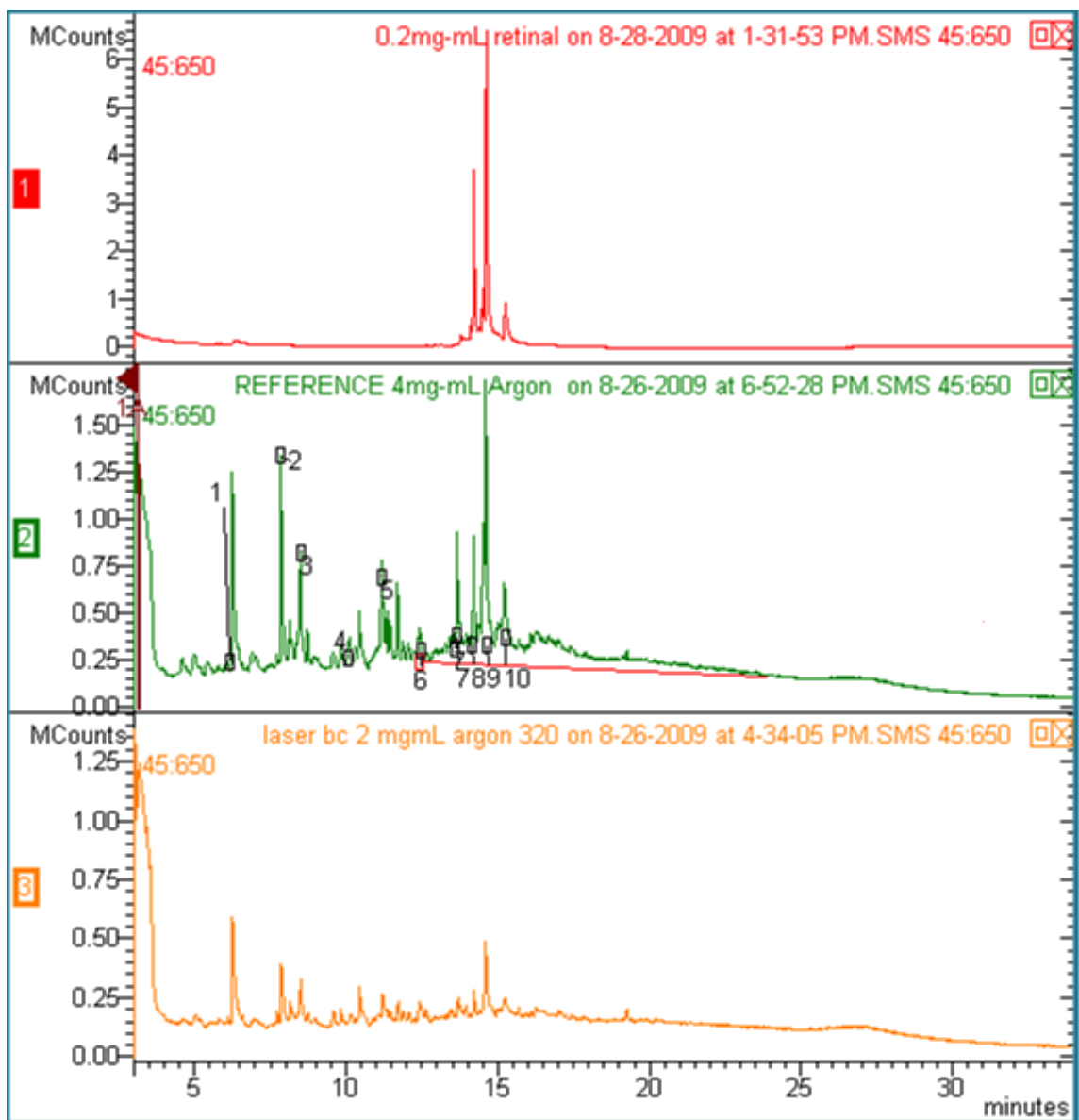


Figure 24 TIC of 0.2mg/ mL Retinal vs. 4mg/mL  $\beta$ -carotene

After Laser Degradation.

Notes: parent ion masses for peaks labeled are 1)  $M/z$ 174, 2)  $m/z$  192, 3)  $m/z$  180, 4)  $m/z$  286, 5)  $m/z$  218, 6)  $m/z$  288, 7)  $m/z$ 315, 8,9,10)  $m/z$  284 isomers of retinal.

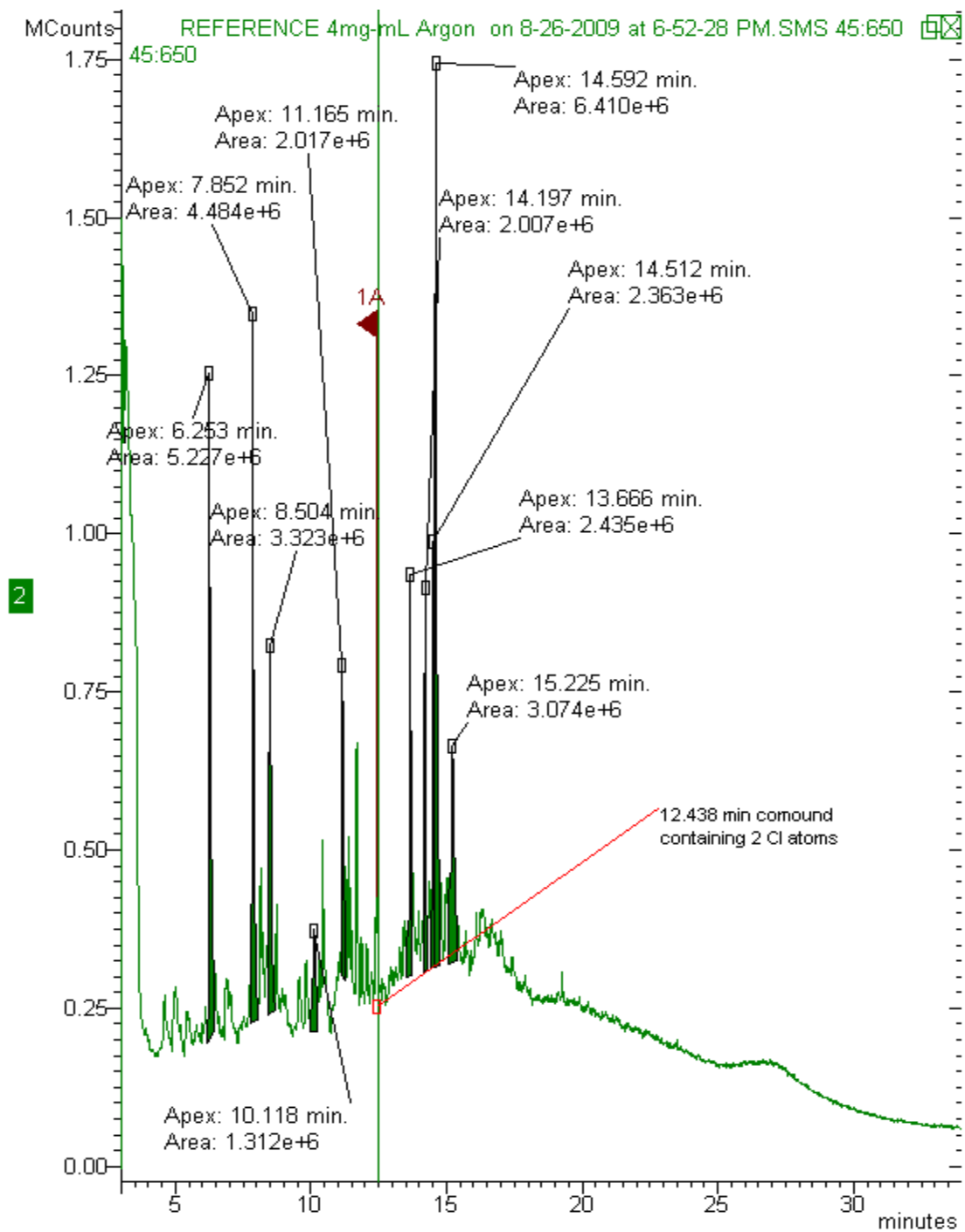


Figure 25 The Main Peaks from TIC of Reaction Products for 4 mg/mL  $\beta$ C  
Induced by 532 nm Laser with Full Intensity

Considering the sensitivity of GC-MS and limited amount of the analyte (4mL of dilute solution maximum each batch), the mixture of intermediates observed complete irradiation by laser allows a number of products to be detected and identified, see Fig 23,24. The mixtures of the “intermediates” chemical structures vary as the exposure time is lengthened. The final visible colorless products in the cuvette are expected to result from a transfer of electrons to chloromethane solvents since they are well known to support the formation of solute radical cations on pulse radiolysis.

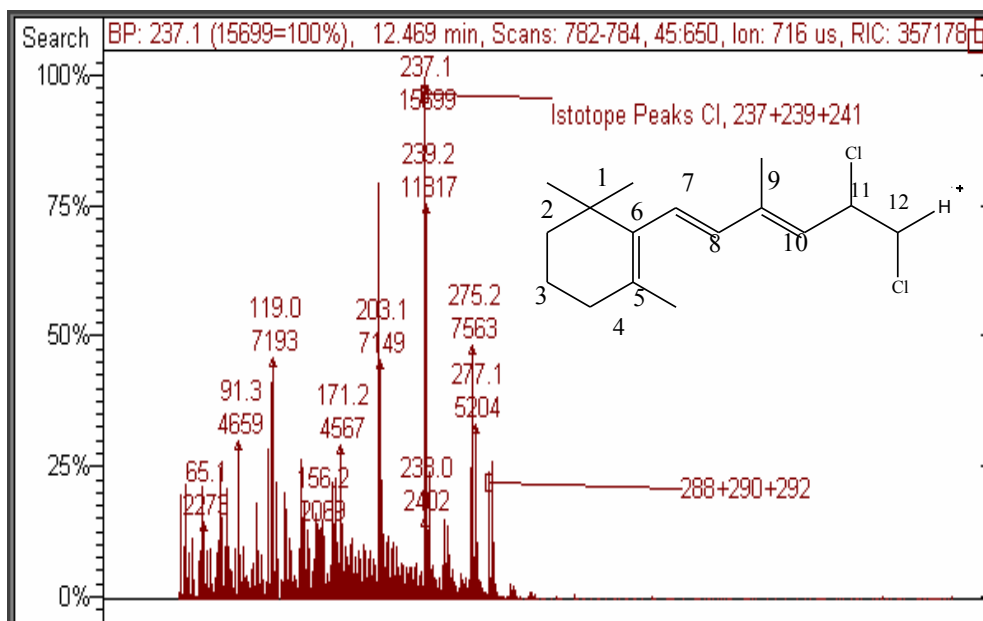


Figure 26 The Extracted Mass Spectra for Retention Time at 12.469min for  $\beta$ C in  $\text{CCl}_4$  Solvent Laser Photo-degradation Products

In order to further substantiate the role of chlorinated solvents, it was hoped that some of the chlorine would be observed within the products of the photo-degradation in carbon tetrachloride. The presence of chlorine in a molecule or ion is easily detected due to the presence of peaks separated by two mass units in the intensity ration of 3:1 consistent with the chlorine isotope distribution. If multiple chlorine atoms are present, a more complex pattern is observed in an ion cluster based on a binomial distribution.

- Ratio ( $a:b$ ) = 3:1
- $(3a + 1b)^n$  for  $Cl_n$
- $(3a + 1b)^1 = 3a + 1b = 3:1$
- $(3a + b)^2 = 9a^2 + 6ab + 1b^2 = 9:6:1$
- $(3a + b)^3 = 27a^3 + 27a^2b + 9ab^2 + 1b^3 = 27:27:9:1$
- $(3a + b)^4 = 81a^4 + 108a^3b + 54a^2b^2 + 12ab^3 + 1b^4 = 81:108:54:12:1$

Examination of the mass spectra of some of the decomposition products show peaks which represent chlorine containing compounds. The peak at a retention time of 12.453 minute represents one of these products. The analysis of the ion clusters presented in Figure 26 shows how a compound with a parent ion cluster of masses 288, 290, 292, 294 fragments first through the loss of a methyl group to give a cluster containing 3 chlorine atoms of masses 273, 275, 277 and 279, and that cluster further fragments through the loss of HCl to form a 2 chlorine cluster with masses 237, 239, 241. There are other peaks in the gas chromatogram that could easily represent other chlorine containing materials.

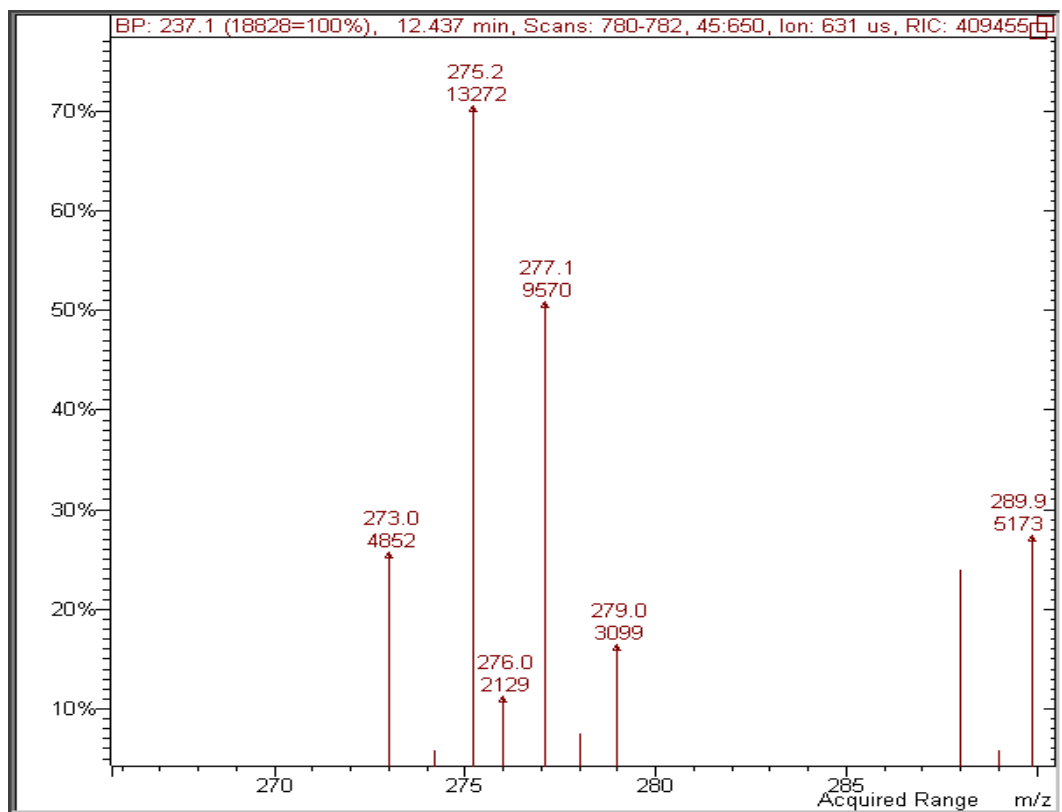
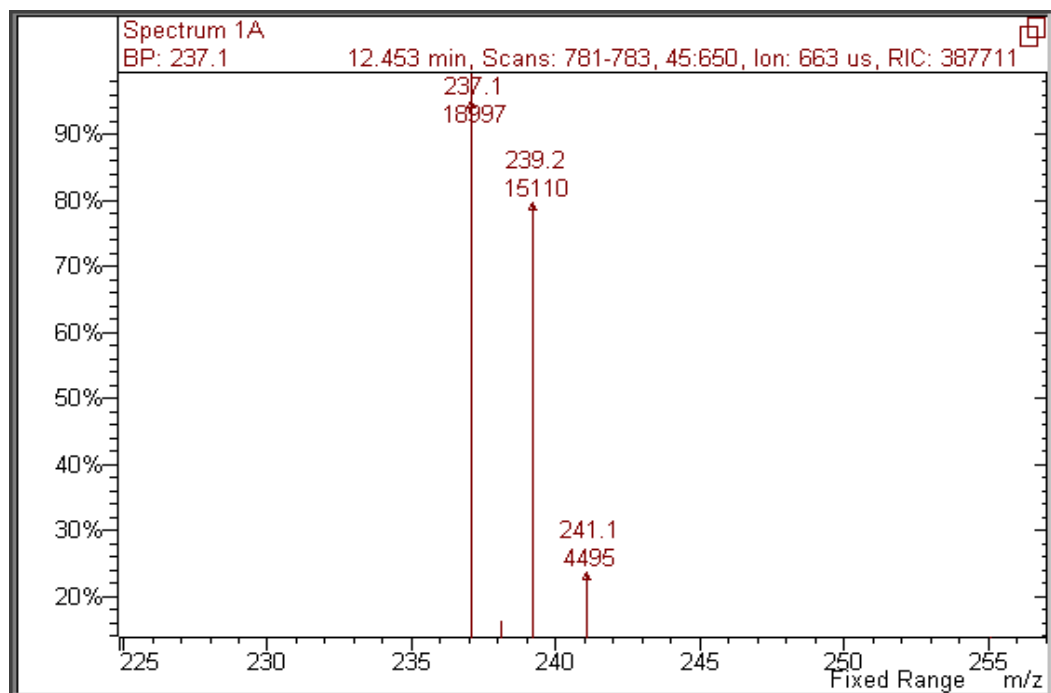


Figure 27 The MS of Peak at m/z 273, 275, 277, 279 and the Possible M+ Peak at m/z 290

The analysis of other peaks in the total ion chromatogram shows products that result from the cleavage of  $\beta$ -carotene. It seems reasonable for  $\beta$ -carotene to heterolytically cleave at the 11-12 position to yield carbon-centered radicals. The reasonable compounds with molecular ions of  $M=286$  and that have two chlorine atoms, one aromatic ring, a neutral loss of  $m/z$  51 are likely to arise from  $\beta$ -carotene are quite limited. Two isomers which vary in substitution position of the carbons of the in-chain methyl groups, which are allylic to in-chain double bonds.

Ion	A Intensity	A % Base ...	B Intensity	B % Base ...
237.1	18828	100.0		
239.2	16271	86.4		
201.2	15065	80.0		
275.2	13272	70.5		
277.1	9570	50.8		
203.1	9017	47.9		
119.0	7246	38.5	53	5.3
202.2	7015	37.3		
117.3	6559	34.8		
171.2	5629	29.9		
115.2	5432	28.9		
289.9	5173	27.5		
241.1	5068	26.9		
141.2	4987	26.5		
204.2	4982	26.5		
273.0	4852	25.8	10	1.0
288.0	4538	24.1	7	0.7
91.3	4532	24.1		
167.3	4470	23.7		
77.1	4105	21.8		
63.2	3950	21.0		
82.0	3829	20.3	46	4.6
50.9	3678	19.5		
165.3	3588	19.1		
128.2	3480	18.5		
121.2	3361	17.9		
238.2	3353	17.8		
143.1	3210	17.0		
152.2	3210	17.0		
279.0	3099	16.5	999	100.0
173.3	3086	16.4		
47.0	3078	16.3	2	0.2
129.2	2996	15.9		
105.2	2982	15.8		
255.1	2942	15.6		
253.3	2815	15.0		
153.3	2786	14.8		
142.3	2750	14.6		
240.1	2720	14.4		
166.3	2529	13.4		
157.3	2472	13.1		

Figure 28 The Abundance of Each Ion with Descending Order of Intensity

On the basis of the abundance of each ion with descending order of intensity, from the above graph for a retention time around 12.469 min, two possible isomers were examined. The base peak are concentrated around 237 mass unit followed by 239 increased by 2 amu  $m/z$  from the molecular ion around 286 with a loss of methyl chloride radicals ( $m/z$  51), and then lose another chloride radicals to form a  $m/z$  at 201 with a abundance of 80.0% as shown below.

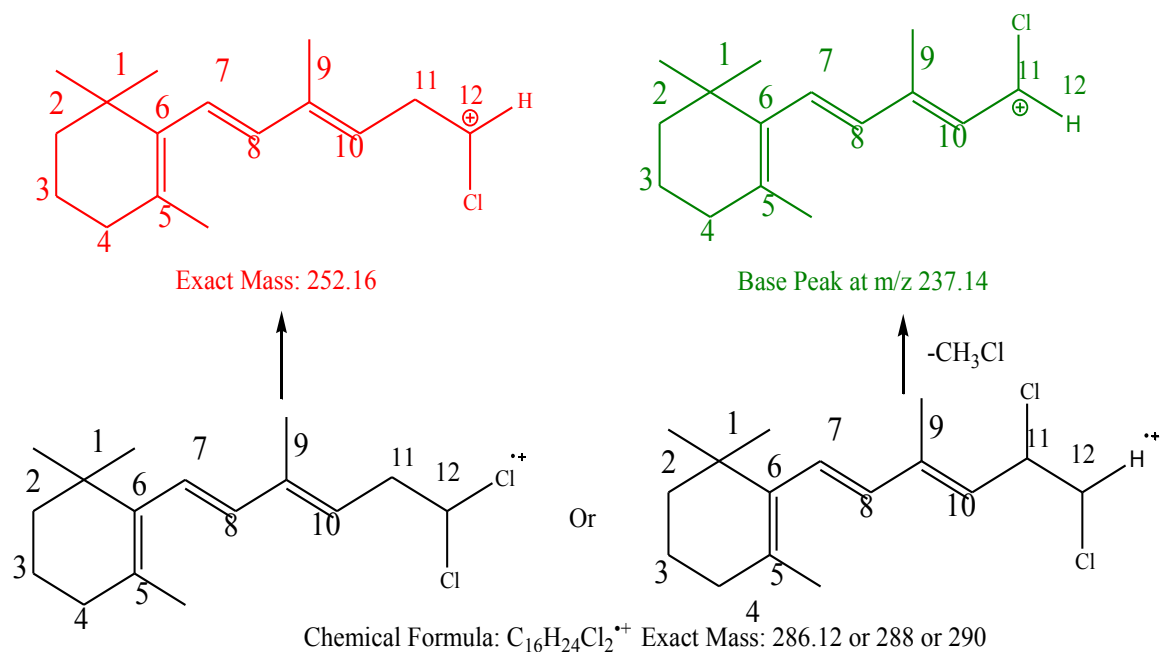


Figure 29 The Possible Isomer Structures Based on MS Cleavage Products

Formed by Addition of Chlorine to Double Bonds in  $\beta$ -carotene

The structures shown in red fonts cannot lose 51 amu, however, the structures in green parts are reasonable to lose a moiety of  $CH_3Cl$  with a  $m/z$  of 51 to generate a base peak at  $m/z$  237 as shown in the Figure 26,27 and 28. This isomer is also prone to subsequent reaction with chlorine radicals lose its double bonds with the prolonged irradiation time.



The tropylium ion in the form of a signal at  $m/z = 91$  fragments. Upon ionization, the benzyl fragment is cleaved off as a cation ( $\text{PhCH}_2^+$ ), which rearranges to the highly stable tropylium cation ( $\text{C}_7\text{H}_7^+$ ). A strong peak appears at  $m/z = 119(91+28)$  might correspond to loss of two methyl groups to form a methyl-substituted tropylium ion which can further fragment to form the aromatic cyclopentadienyl cation ( $m/z 65$ ) which is shown on mass spectrum which in turn might cleave to form another equivalent of ethyne and the aromatic cyclopropenyl cation ( $m/z 39$ ).

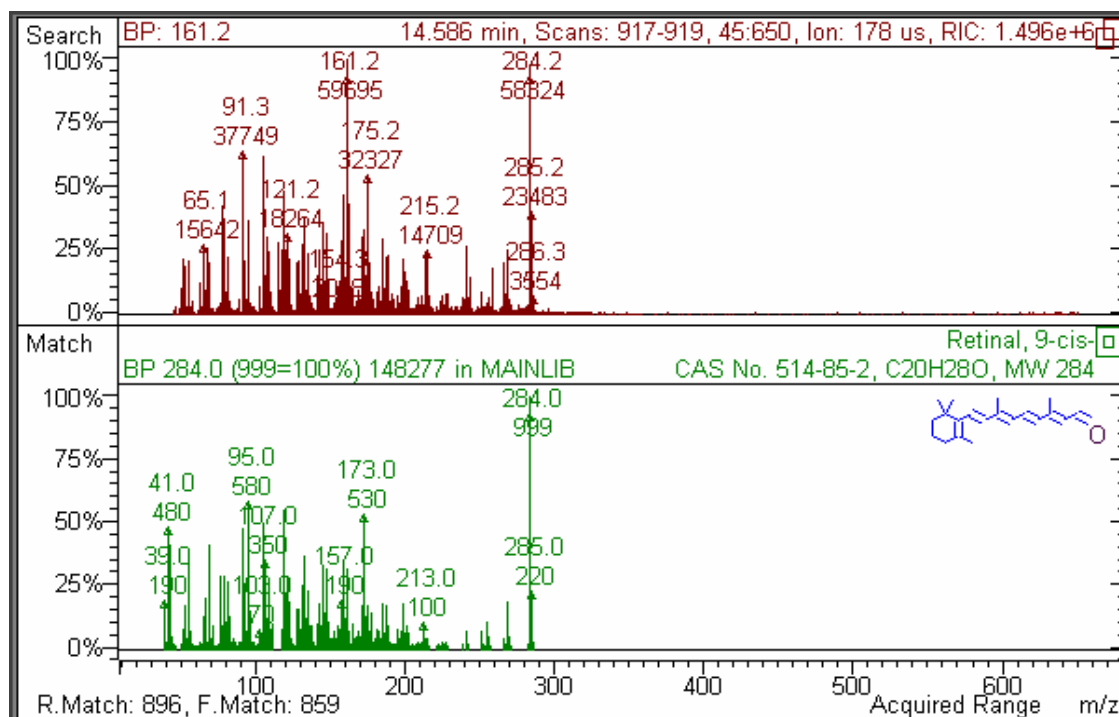
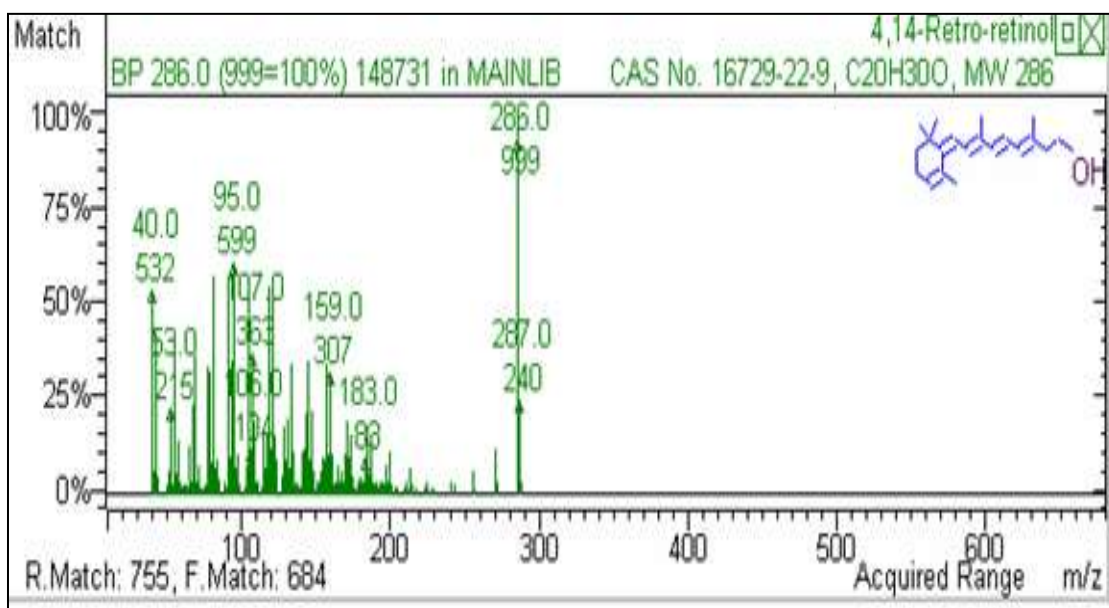


Figure 30 The Mass Spectra and the Proposed Structures by NIST Library  
 between 10.096 and 14.586 min

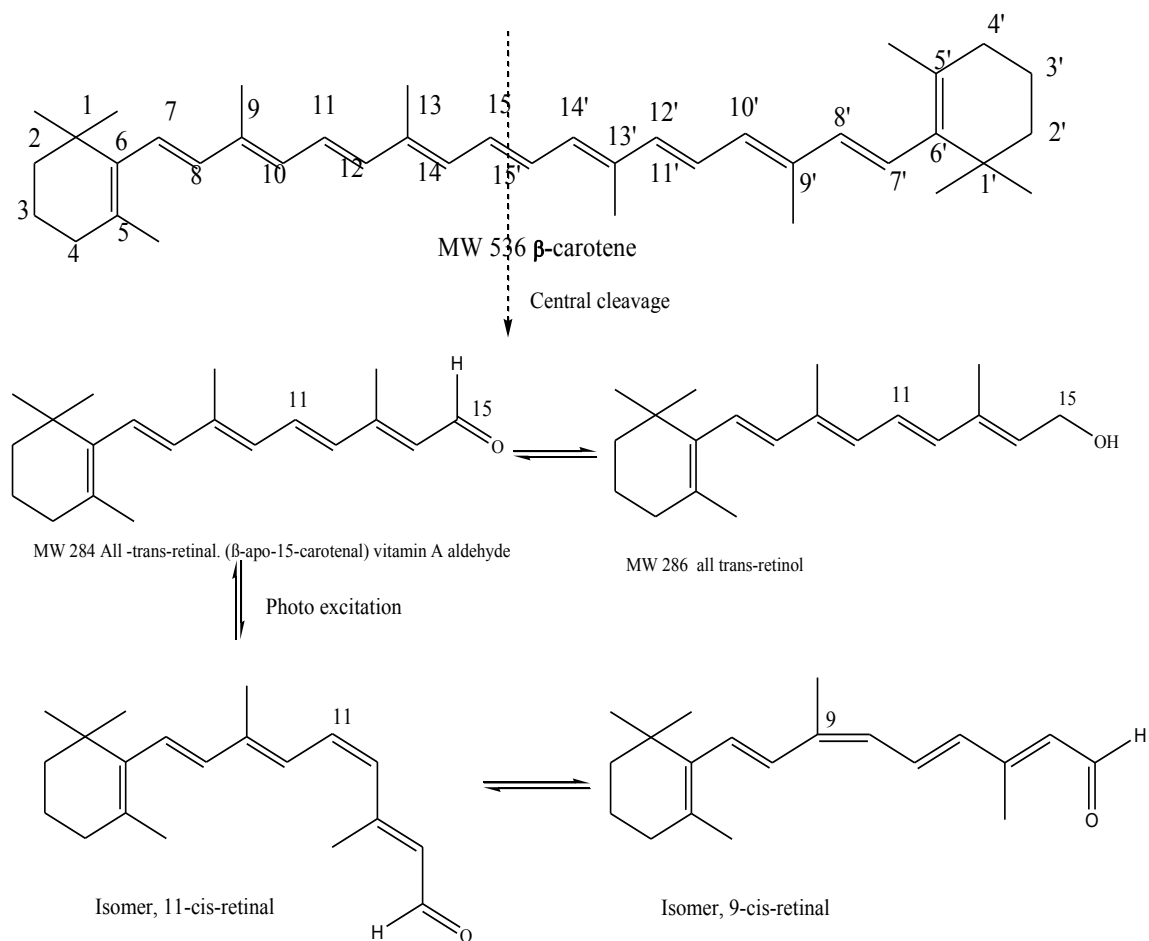


Figure 31 Proposed Pathways of  $\beta$ -carotene into *Trans*, 9-*cis*, and 11-*cis* Retinal Isomers and Retinols.

Another mode of reaction of  $\beta$ -carotene is the photochemical oxidation at the 15-15' position as is shown in Figure 24, 30 and 31. Retinal is known to be essential for vision and possess a skeleton of  $\beta$ -ionone (rose ketones) ring along with polyene side chain terminating as an aldehyde, which can be easily converted to retinol. The *cis* isomers of both retinal and retinol are less stable and are more prone to isomerize to the more stable form, i.e., all-*trans* configuration isomers leading to the activation of the photoreceptor.

There are three unoverlapping peaks around the retention time near 14.5-15.5 min showing the retinal isomers by spiking the 0.2mg/mL standard retinal solution into GC-MS under the same conditions. The likelihood to confirm the three isolated peaks representing the three isomers of retinal, i.e., all trans, 9-cis (positive confirmation by NIST library ) and 11-cis. The  $\beta$ -carotene has also has a potential to be oxidized to retinoic acid.

## E. Generation of the Proposed Thermal and Photo-degradation Intermediate and Final Products

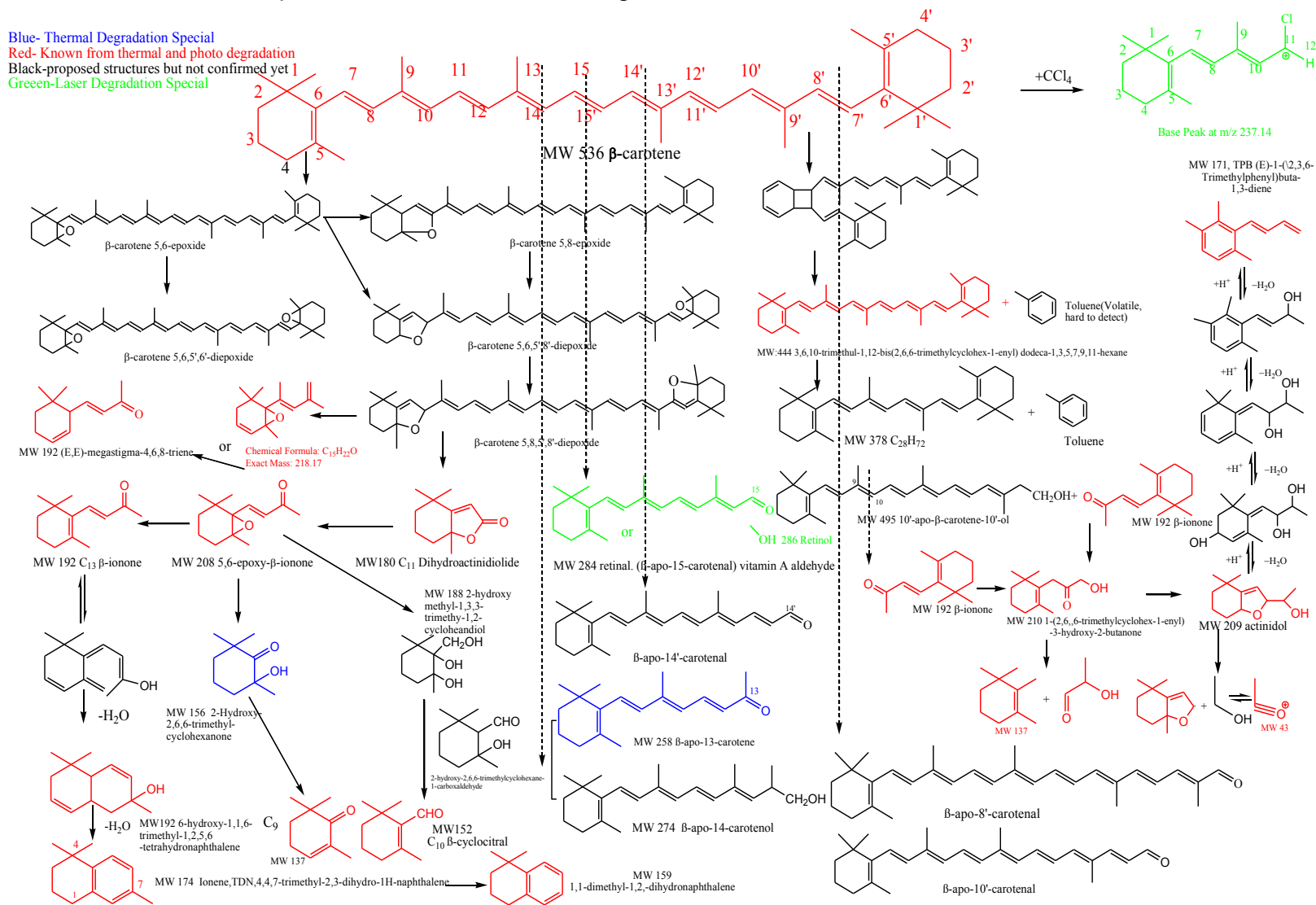


Figure 32 Generation of the Proposed Thermal and Photo-degradation Intermediate and Final Products

A scheme which summarizes the various degradation pathways for  $\beta$ -carotene is shown in Figure 32. It should be understood that the mechanism by which the intermediate and final products are formed from  $\beta$ -carotene and the inability to characterize all the long chain and short chain polyene products of  $\beta$ -carotene are still a subject of ongoing research. Hitherto, we seek to explore the degradation of  $\beta$ -carotene asymmetric cleavage in this study. Vitamin A (retinal) is the initial cleavage products at the central double bond at 15,15'. Oxygenase which has been recognized as the exclusive enzyme is responsible for the cleavage of  $\beta$ -carotene to produce two units of the active form of  $\beta$ -carotene, namely, vitamin A (retinal). In Figure 32, the above possible metabolites are illustrated to assess the impact of heat and photo-excitation pathways on the decomposition of trans- $\beta$ -carotene( 95%).

However, besides the oxidation fission, the conjugated double carbon-carbon bonds from 40 carbon based system are susceptible to cleavage or substitution either chemically or biochemically in vitro or in vivo. Each unique carotenoid and its derivatives with various cyclic end-groups determine their potential biological activities.

The carotenoid polyene system is structured in such a way that epoxides are frequently formed along the polyene skeleton making them vulnerable to heat or light. Many of the proposed intermediates possess an epoxy group, the most stable and the most frequently observed of the monoepoxide are in 5,6- and the diepoxide in 5,6;5',6' positions, shown as  $\beta$ -carotene 5,6-epoxide,  $\beta$ -carotene 5,8-

epoxide,  $\beta$ -carotene 5,6,5',6'-diepoxide,  $\beta$ -carotene 5,6,5',8'-diepoxide. The 5,6-epoxides are readily rearranged into 5,8 and/or 5',8' positions by shortening of the chromophore <sup>48</sup>. There is a wide diversity of structural features and modifications to the basic end-groups, and virtually nothing is known about the biosynthetic reactions that lead to the formation of these structures <sup>49</sup>. The reaction proceeds via planar carbon cation at 5 and 8 position to form C-8 diastereoisomers products, namely, 3S, 5R, 8S isomer and 3S, 5R, 8R isomer as shown in the below scheme (see Figure 33) like an electrophilic attack <sup>50</sup>.

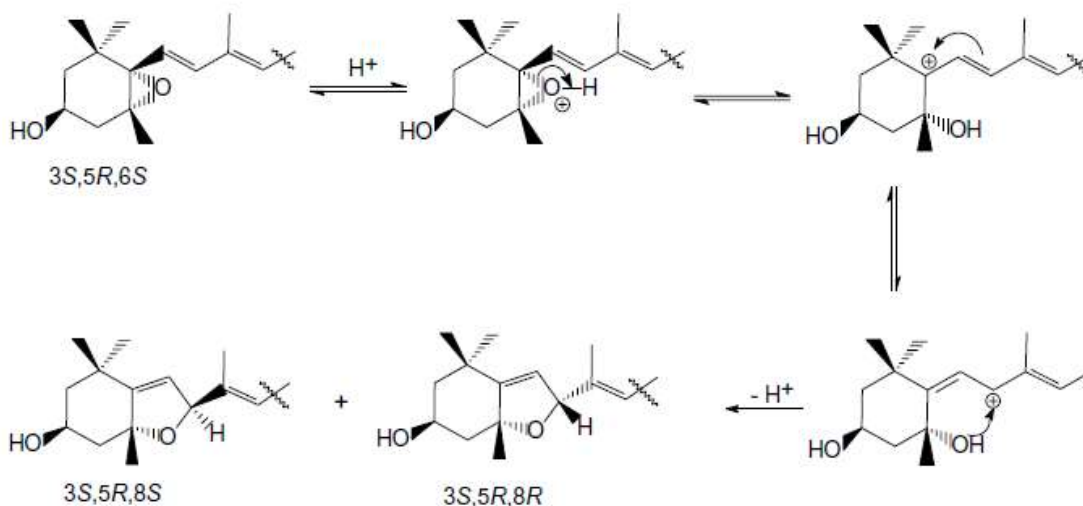


Figure 33 . The Scheme of Planar C<sup>+</sup> at 5 and 8 Position to Form C-8 Diastereoisomers Products <sup>50</sup>

As the degradation progresses, the reaction of photoproducts further complicates the analysis in the later stages of reaction. Most of long chained products of epoxides and apocarotenal were not fully identified by GC-MS, shown as in the black fonts of structures, instead, they are further transformed and cleaved into shorter-chain mono-and di-oxygenated compounds.

Edmunds and Johnstone (1965) proposed a mechanism for  $\beta$ -carotene to react to form an aromatic ring and then to lose a toluene and mass unit of 92 for the formation of an intermediate with a four membered ring, This intermediate rearranges to the final product with a mass unit of 444 to form  $C_{33}H_{48}$ , i.e., 3,6,10-trimethyl-1,12-bis(2,6,6-trimethylcyclohex-1-enyl) dodeca-1,3,5,7,9,11-hexane, which involves the cyclization process to form an eight electrons intermediate with a quaternary member ring<sup>51</sup>.

The intermediate, 5,6-Epoxy-ionone is the precursor of  $\beta$ -ionone by losing an epoxide moiety by opening the closed ring, both of them were found in GC-MS profile with a mass unit of 208 and 192 in the thermal as well as the photo excited reactions. Beta-ionone, the significant contributor of fragrance of roses, is also an intermediate and then might be transformed to its homologous series compounds, 6-hydroxy-1,1,6-trimethyl-1,2,5,6-tetrahydronaphthalene and then further dissociated into ionene, TDN, also called rose ketones, 4,4,7-trimethyl-,3-dihydro-1H-naphthalene with a mass unit of 174 and then finally converted to 1,1-dimethyl-1,2-dihydronaphthalene with a mass unit of 159. All the daughter ions were detected in our GC-MS chromatograms of the pyrolysis products, their mass spectra data were shown on the Appendix III. To be mentioned,  $\beta$ -ionone is easily detected and accounts for more of the products than the other three chemicals mentioned above in that methyl loss lead by allylic bond cleavage to yield a more thermally favorable tertiary allyl ion. All of them shared the same



moiety of dimethyl-dihydro-naphthalene less vulnerable to the environmental resistance. The molecular mass of those mixed compounds were so close, suggesting that they are differing only with respect to the configurations of the side-chain double bonds.

## CHAPTER IV

### CONCLUSIONS

The most important nutritional value is the provitamin A content supplied by  $\beta$ -carotene, which are important to be preserved during processing and storage are gone when heated over 100°C. Loss of both color and nutritional value takes place as a consequence of the heat applied. Other studies using color as an indicator for carotenoids concentration reported lower  $E_a$  values (around 20 kJ mol<sup>-1</sup>) which offers an interesting comparison to as our data of 13.2982KJ/mol ( $R^2=0.9984$ ,  $R=0.9992$ ) between 150 to 350°C. This difference may have been a result of their product matrix such as food, fruits which might be important sources of interference for quantitative detection and influence, which does not permit ready discrimination between carotenoids and other pigments. Such reactions are favored by heat treatment towards  $\beta$ -carotene and required relatively low activation energy, their occurrence might modify the chemical properties, antioxidant capacity, and bioavailability and nutritional value of  $\beta$ -carotene in processed foods.

The real-time monitor on  $\beta$ -carotene photo-degradation rate in solvent systems of mixture of carbon tetrachloride (CCl<sub>4</sub>) and hexane together and hexane alone is

done upon irradiation with the 350nm mercury lamp and 532 nm YAG laser pulses (full and half intensity). The color loss of in chloromethane ( $\text{CH}_x\text{Cl}_{4-x}$ ;  $x=0,1,2$ ) upon exposure to both UV light and 2 photons laser irradiation, while the loss of  $\beta$ -carotene is significantly slowed down in hexane solvent, especially treated with 532nm laser at all intensities .

### UV Photo-degradation

The photo-degradation of  $\beta$ -carotene using a UV-light source, in hexane and hexane with small amounts of added carbon tetrachloride demonstrated that the  $\beta$ -carotene degrades by a first order reaction. The degradation products of  $\beta$ -carotene are less colored because of the resulting shorter chromophore, which stability depending on the media properties, such as solvent polarity, electron-acceptor like  $\text{CCl}_4$ . The activation energy for  $\beta$ -carotene in neat hexane is 7.33147KJ/mol, however, the addition of  $\text{CCl}_4$  into the system has a much lower  $E_a$  value, giving rise to a faster degradation rate than pure hexane.

### Laser Light Irradiation

For laser light source, repeatable experiments on  $\beta$ -carotene in 1%  $\text{CCl}_4$  with the rest of hexane under 25.5°C water circulation temperature control are done with 4 consecutive days , the first 19 data with an increment of 1 min were applied for every 2 mL aliquot in plat face cuvette with full intensity. The ABS value of rate

constants are 0.1129, 0.1126, 0.1126, 0.1113  $\text{min}^{-1}$  with a STDEV of 7.14E-4, averaging value 0.1124  $\text{min}^{-1}$ . The final products are collected and evaporated to dryness with the same method and treated by 1 mL  $\text{CDCl}_3$ . C-13 NMR peak was nowhere to be found indicated that the concentration might not be enough to show structural information. However,  $^1\text{H}$  NMR showed rich peaks (triplet peaks around 4.8-3.7 ppm, integration area is around 1.829; sextet peaks with a total integration area of 95.655, J ranging from 2.3 to 0 ppm). The earlier results for  $E_a$  determination of  $\beta\text{C}$  in pure  $\text{CCl}_4$  suggested the 1<sup>st</sup> order,  $E_a$  value is found to be 9.2424 KJ/mol with a correlation of 0.9596 (temperature dependence varying from 20 to 60 °C with an increment of 10°C).

## CHAPTER V

### FUTURE RESEARCH

This study has successfully examined the kinetics and identified some of the products of the thermal and photochemical degradation of  $\beta$ -carotene. There are, however some areas for further research on this system. A few of these are listed below.

- Buildup a rapid and easy methods for Liquid chromatography–mass spectrometry (LC-MS) oriented towards the specific detection and potential identification of chemicals to obtain the maximum performance and detection sensitivity.
- Change GC-MS conditions, finding an optimal column optimize injector and column programming temperatures to have better peak shapes and resolutions.
- Applying tandem mass spectrometry technology, also known as MS/MS or MS<sup>2</sup> to even better understanding the degradation pathways between parent and fragment ions under different CID conditions.
- Investigate the role of carbon tetrachloride in accelerating the degradation rate of  $\beta$ -carotene.
- Identification of the impact of dissolved oxygen on the degradation rate of  $\beta$ -carotene

- Elucidate the relationship between activation energy and bond energy for  $\beta$ -carotene.
- Build MS library to identify the possible intermediate formed and final degradation products, discover the possible relationships between them.

## BIBLIOGRAPHY

1. Andreas Schiebe, M. M. (2002). Simultaneous determination of carotenes and tocopherols in ATBC drinks by high-performance liquid chromatography . Analytical, Nutritional and Clinical Methods Section , 76 (3), 357-362.Çinar, I. (2004).  
Carotenoid pigment loss of freeze-dried plant samples. Electron. J. Environ. Agric. Food Chem. , 363-367.
2. Jeevan Kumar Prasain, R. M. (2005). Electrospray tandem mass spectrometric analysis of zeaxanthin and its oxidation products. Journal of Mass Spectrometry , 40 (7), 916–923.
3. Claus Rentel, S. S. (1998). Silver-Plated Vitamins: A Method of Detecting Tocopherols and Carotenoids in LC/ESI-MS Coupling. Anal. Chem , 70 (20), 4394–4400.
4. Krinsky NI, Y. K. (2003). Carotenoid-radical interactions. Biochem Biophys Res Commun , 305 (3), 754-760.
5. Wikipedia. (2008). [http://en.wikipedia.org/wiki/Radical\\_%28chemistry%29](http://en.wikipedia.org/wiki/Radical_%28chemistry%29)
6. MOORE, J. P. (2003 University of Florida Master Thesis). Carotenoid Synthesis and Retention in Mango (Mangifera indica).
7. De Mann, J. M. (1999). Principles of Food Chemistry' 3rd Ed. .Aspen Publishers, Inc.: Gaithersburg, Maryland, USA.
- 8.

9. RODRIGUEZ-AMAYA, J. F. (2008). Degradation of Lycopene and  $\beta$ -carotene in Model Systems and in Lyophilized Guava. *JOURNAL OF FOOD SCIENCE* , 78 (8), 589-594.
10. Philip N. Onyewu, H. D. (1982). Formation of two thermal-degradation products of  $\beta$ -carotene. *J. Agric. Food Chem* , 30 (6), 1147–1151.
11. Godoy, H. T., & Rodriguez-Amaya, D. B. (1987). Changes in individual carotenoids on processing and storage of mango (*mangifer indica*) slices and puree. *Int. J. Food Sci.*, 22, 451-460.
12. Antonio Pérez-Gálvez, J. J.-M. (2005). Thermal-degradation Products Formed from Carotenoids during a Heat-Induced Degradation Process of Paprika Oleoresins (*Capsicum annum* L.). *J. Agric. Food Chem* , 53, 4820-4826.
13. Wikipedia. [http://en.wikipedia.org/wiki/Cis%E2%80%93trans\\_isomerism](http://en.wikipedia.org/wiki/Cis%E2%80%93trans_isomerism)
14. Joanna, F., Leszek, F., Rainer, H., & Hugo, S. (2005). Cyclic endoperoxides of beta-carotene, potential pro-oxidants, as products of chemical quenching of singlet oxygen. *Biochimica et biophysica acta* , 1709 (1), 1-4.
15. Britton, G. (1995). Carotenoids. Volume 1B:Isolation and Analysis
16. Chen, M. T. (2002). Stability of lycopene during heating and illumination in a model system . *Food Chemistry* , 78 (4), 425-432.
17. Zechmeister, L. a. (1944). Cis-trans isomerization and cis-peak effect in the alpha-carotene set and in some other stereoisomeric sets. *J. Am. Chem. Soc.* , 66, 137-144.
18. I., M. (1964). BETA-CAROTENE: THERMAL-DEGRADATION. *Science* , 44, 533-534.
19. OUYANG, J. M.-T. (1980). FORMATION OF CARBONYL COMPOUNDS FROM P-CAROTENE DURING PALM OIL DEODORIZATION. *Journal of Food Science* , 45 (5), 1214–1217.



20. Philip N. Onyewu, C.-T. H. (1986). Characterization of beta-carotene thermal-degradation products in a model food system. *Journal of the American Oil Chemists' Society* , 63 (1), 1437-1441.
21. Evelyn B. Rodriguez and Delia B. Rodriguez-Amaya. (2007). Formation of apocarotenals and epoxy-carotenoids from  $\beta$ -carotene by chemical reactions and by autoxidation in model systems and processed foods. *Food Chemistry* , 101 (2), 563-572 .
22. Begum, F. (2006). Photo-degradation of  $\beta$ -carotene in chloromethane solvents: effects of molecular oxygen and nature of the photoproducts. Pg. 5 Murray State University Master Thesis .
23. Rezanka, T., Olsovska, J., Sobotka, M., & Sigler, K. (2009). The Use of APCI-MS with HPLC and Other Separation Techniques for Identification of Carotenoids and Related Compounds . *Current Analytical Chemistry* , 5 (1), 1-25.
24. Michel Carail and Catherine Caris-Veyrat. Carotenoid oxidation products: From villain to saviour? *Pure Appl. Chem.*, Vol. 78, No. 8, pp. 1493–1503, 2006.
25. Martin, H. D. (1999). Chemistry of carotenoid oxidation and free radical reactions. *Pure Appl. Chem* , 71 (12), 2253-2262.
26. Kispert, A. S. (1996). Role of Excited Singlet State in the Photooxidation of Carotenoids: A Time-Resolved. *J. Phys. Chem* , 100, 669-671.
27. Ali El-Agamey, M. B. (2005). Photolysis of carotenoids in chloroform: enhanced yields of carotenoid radical cations in the presence of a tryptophan ester. *Radiation Physics and Chemistry* , 72, 341-345.
28. S Adhikaria, S. K. (2000). Pulse radiolytic oxidation of  $\beta$ -carotene with halogenated alkylperoxyl radicals in a quaternary microemulsion: formation of retinol. *Biophysical Chemistry* , 88, 111-117.

29. Breemen, R. B. (1995). Electrospray Liquid Chromatography-Mass Spectrometry of Carotenoids. *Anal. Chem* , 67 (13), 2004–2009.
30. Richard B. Van Breemen, H. H. (1993). Continuous-flow fast-atom-bombardment liquid chromatography/mass spectrometry of carotenoids. *Anal. Chem* , 65 (8), 965–969.
31. Mercadante, C. D. (2009). Chapter 12 Thermal and Photochemical Degradation of Carotenoids. In J. T. Landrum, *Carotenoids: physical, chemical, and biological functions and properties* (p. 229). CRC Press.
32. T. Lackera, S. S. (1999). Separation and identification of various carotenoids by C30 reversed-phase high-performance liquid chromatography coupled to UV and atmospheric pressure chemical ionization mass spectrometric detection. *Journal of Chromatography A* , 854, 37-44.
33. Dan Qiu, Z.-R. C.-R. (2009). Effect of heating on solid  $\beta$ -carotene. 112, 344-349.
34. Shuji Nakamura, S. F. Introduction to nitride semiconductor blue lasers and light emitting diode. 2000.
35. <http://www.rayonet.org/graphscharts.html>, <http://www.rayonet.org/reactors.html> .
36. John Thomas Landrum *Carotenoids: physical, chemical, and biological functions and properties*, page 241.
37. Jeevarajan, J. A.; Kispert, L. D "Electrochemical oxidation of carotenoids containing donor/acceptor substituents.". *J. Electroanal. Chem.* 411, 57-66 (1996).
38. Introduction to spectroscopy / Donald L. Pavia et al. PUBLISHER Belmont, CA : Br/Cole, Cengage Learning, c2009.
39. József Deli\* and Erzsébet Ósz. Carotenoid 5,6-, 5,8- and 3,6-epoxides ARKIVOC 2004 (vii) 150-168.
40. Maria Manuela Mendes-Pinto. Carotenoid breakdown products the— norisoprenoids—in wine aroma. *Archives of Biochemistry and Biophysics* ,Recent

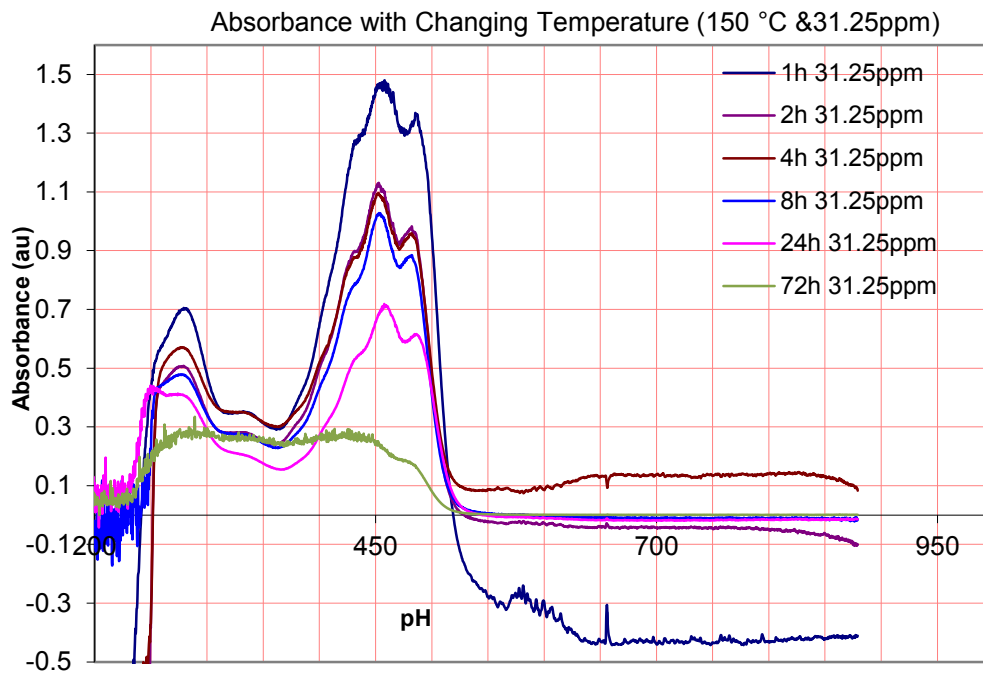
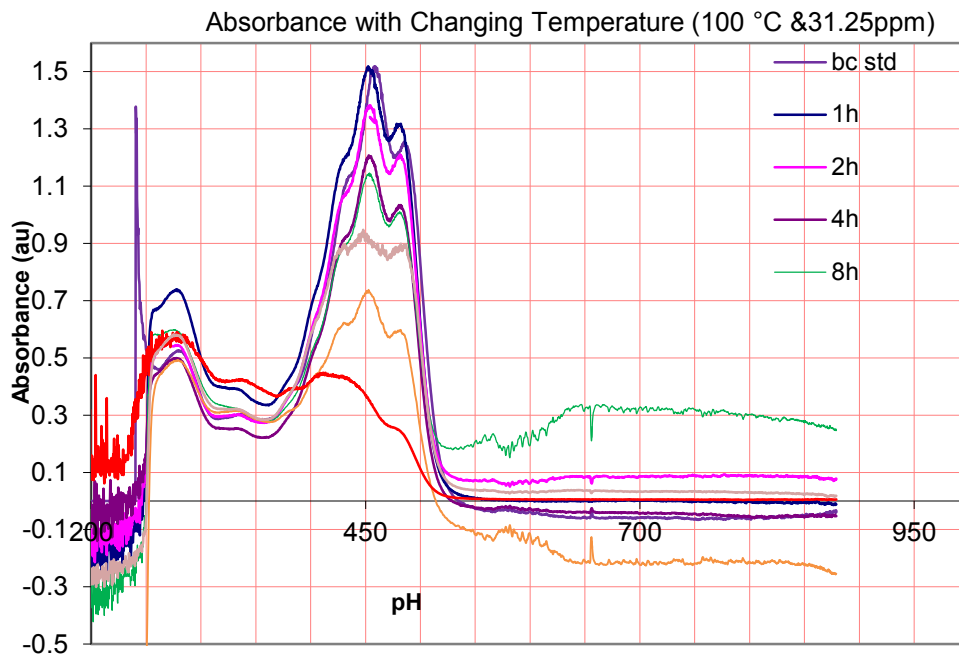
- Achievements of Carotenoid Science and Technology. Volume 483, Issue 2, 15  
2009, 236-245.
41. Michel Carail and Catherine Caris-Veyrat. Pure Appl. Chem. Carotenoid oxidation products: From villain to saviour? Vol. 78, No. 8, pp. 1493-1503, 2006.
  42. Marie-Françoise Nonier, Nathalie Vivas De Gaulejac, Nicolas Vivas, Christiane Vitry. Characterization of carotenoids and their degradation products in oak wood. Incidence on the flavor of wood. Comptes Rendus Chimie Volume 7, Issues 6-7, 2004, 689-698.
  43. Pawinee Kanasawud, Jean C. Crouzet. Mechanism of formation of volatile compounds by thermal-degradation of carotenoids in aqueous medium. 2. Lycopene degradation. J. Agric. Food Chem., 1990, 38 (5), 1238–1242.
  44. Pasquale Crupi. Analysis of Carotenoids in Grapes To Predict Norisoprenoid Varietal Aroma of Wines from Apulia. J. Agric. Food Chem., 2010, 58 (17), pp 9647-9656.
  45. ANTONIO PEÑA REZ-GAÑALVEZ, Thermal-degradation products formed from carotenoids during a heat-induced degradation process of Paprika Oleoresins.(*Capsicum annum* L.) J. Agric. Food Chem. (2005) 53, 4820-4826.
  46. Ganie *et al.*, Carbon tetrachloride induced kidney and lung tissue damages and antioxidant activities of the aqueous rhizome extract of *Podophyllum hexandrum*. BMC Complementary and Alternative Medicine 2011, 11-17.
  47. Lena Jonsson. Thermal-degradation of carotenes and influence on their physiological functions. Nutritional and Toxicological Consequences of Food Processing. Plenum Press, New York 1991.
  48. Philip N. Onyewu, Henryk Daun, and Chi-Tang Ho. Formation of Two Thermal-degradation Products of  $\beta$ -Carotene. J. Agric. Food Chem. 1982, 30, 1147-1151.

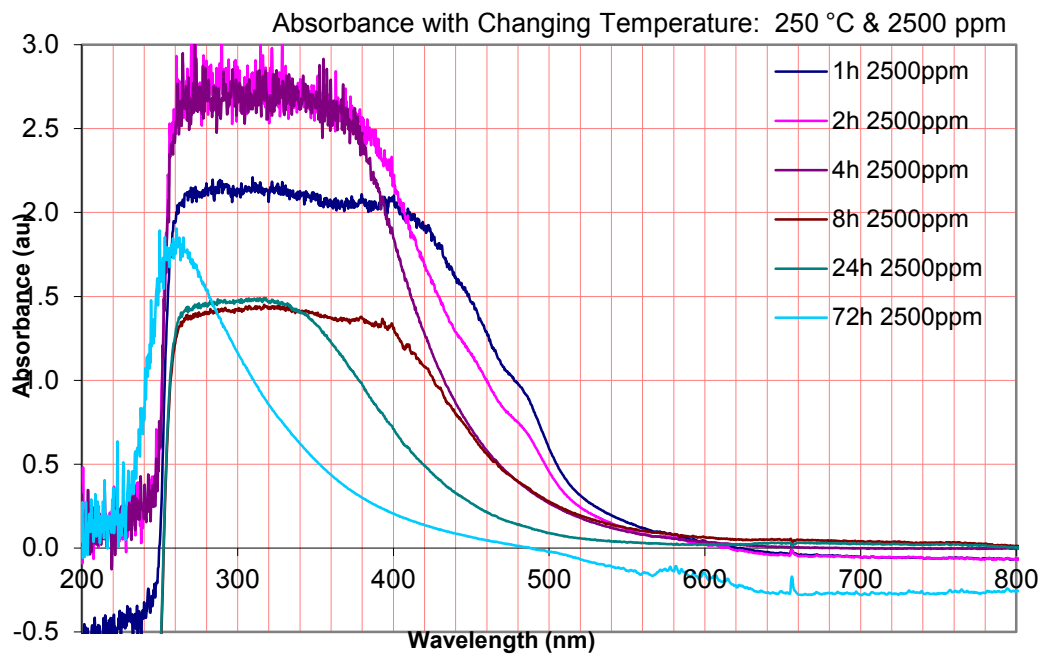
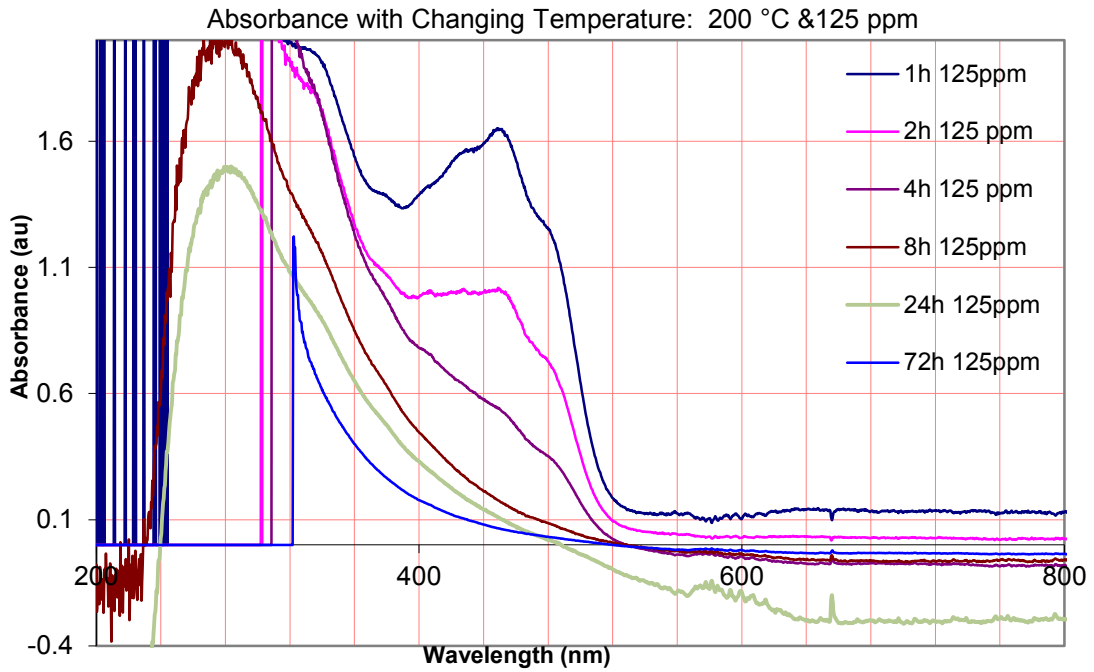
49. Norman I. Krinsky, Susan T. Mayne, Helmut Sies. Carotenoids in Health and Disease.
50. Bonnie TY P, Choo Y M. Oxidation and thermal-degradation of caortenoids. Journal of Oil Palm research. Vol. II, No 1, 62-78, 1999.
51. J. Marais. 1,1,6-Trimethyl-1,2-dihydronaphthalene(TDN): A possible degradation product of lutein and beta-carotene. Research Note. S. Afr. J. Enol. Vitic, 1992, 13(1): 52-55.

## APPENDIX

In Appendix, we provide a full table of thermal and photo-degradation for  $\beta$ -carotene products by UV-Vis spectrophotometer and GC-MS.

## APPENDIX I THERMAL-DEGRADATION OF CRYSTALLINE $\beta$ C RESULTS





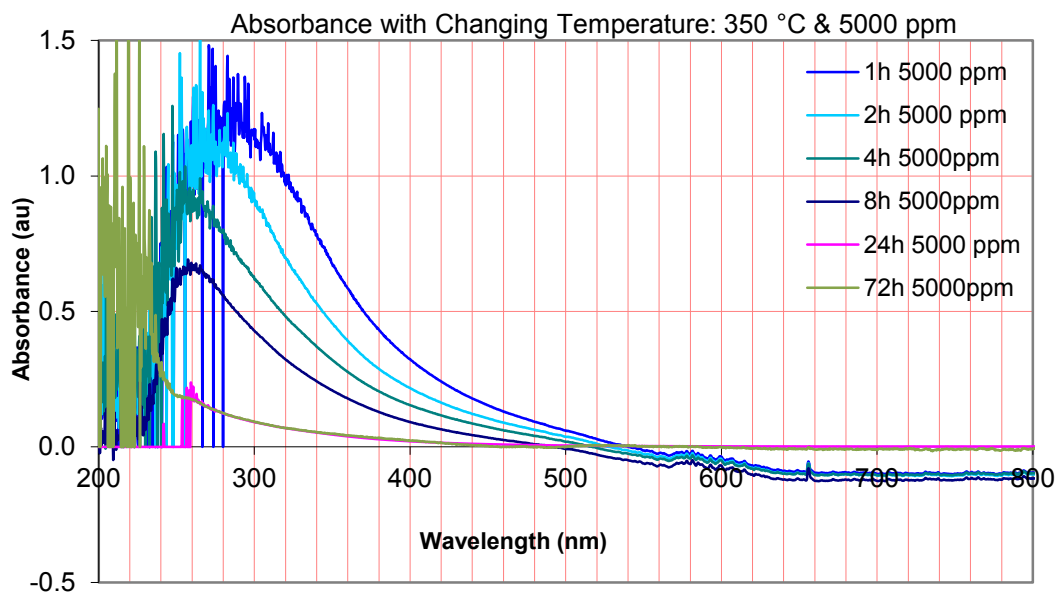
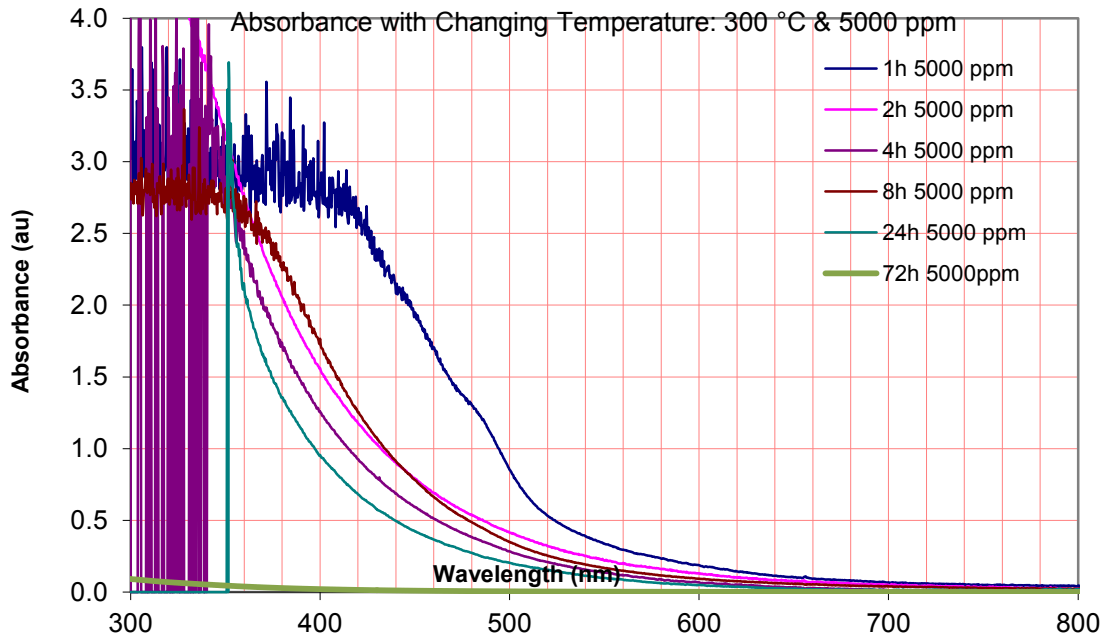




Table UV-Vis Spectrometry Results on  $\beta$ -carotene Thermal-degradation at 100 °C &  $\lambda_{\max}$  (31.25 $\mu$ g/mL solution)

Time(h)	1		2		4		8		24		72		8 (after 5 days)	
100 °C	$\lambda$ (nm)	Abs	$\lambda$ (nm)	Abs	$\lambda$ (nm)	Abs	$\lambda$ (nm)	Abs	$\lambda$ (nm)	Abs	$\lambda$ (nm)	Abs	$\lambda$ (nm)	Abs
31.25 $\mu$ g/mL	451.04	1.505	451.75	1.374	451.75	1.200	451.39	1.139	451.04	1.123	451.39	0.361	451.04	0.734
31.25 $\mu$ g/mL	451.39	1.514	452.10	1.371	452.10	1.198	451.75	1.141	451.39	1.122	451.75	0.362	451.39	0.73
31.25 $\mu$ g/mL	451.75	1.514	452.45	1.378	452.45	1.196	452.10	1.139	451.75	1.128	452.10	0.362	451.75	0.734
31.25 $\mu$ g/mL	452.10	1.509	452.80	1.380	452.80	1.207	452.45	1.138	452.10	1.118	452.45	0.357	452.1	0.727
31.25 $\mu$ g/mL	452.45	1.519	453.15	1.371	453.15	1.207	452.80	1.144	452.45	1.122	452.80	0.356	452.45	0.731
31.25 $\mu$ g/mL	452.80	1.505	453.50	1.382	453.50	1.200	453.15	1.136	452.80	1.131	453.15	0.351	452.8	0.738
31.25 $\mu$ g/mL	453.15	1.509	453.86	1.380	453.86	1.202	453.50	1.146	453.15	1.126	453.50	0.351	453.15	0.729
31.25 $\mu$ g/mL	453.50	1.513	454.21	1.378	454.21	1.200	453.86	1.144	453.50	1.123	453.86	0.350	453.5	0.731
31.25 $\mu$ g/mL	453.86	1.509	454.56	1.382	454.56	1.202	454.21	1.134	453.86	1.117	454.21	0.348	453.86	0.729
31.25 $\mu$ g/mL	454.21	1.507	454.91	1.373	454.91	1.205	454.56	1.142	454.21	1.120	454.56	0.343	454.21	0.728
31.25 $\mu$ g/mL	454.56	1.506	455.26	1.376	455.26	1.200	454.91	1.142	454.56	1.118	454.91	0.341	454.56	0.725
Avg	452.80	1.510	453.50	1.377	453.50	1.202	453.15	1.140	452.80	1.123	453.15	0.353	452.80	0.7305
5000 $\mu$ g/mL	452.80	241.60	453.50	220.29	453.50	192.25	453.15	182.47	452.80	179.61	453.15	56.45	452.80	116.89
STDEV	1.0656	0.004502	1.0641	0.004306	1.0641	0.003683	1.0652	0.003802	1.0656	0.004346	1.0652	0.006433	1.0656	0.003348
loss(100%)		91.72242		92.4525		93.41332		93.74821		93.84638		98.06591		95.99527

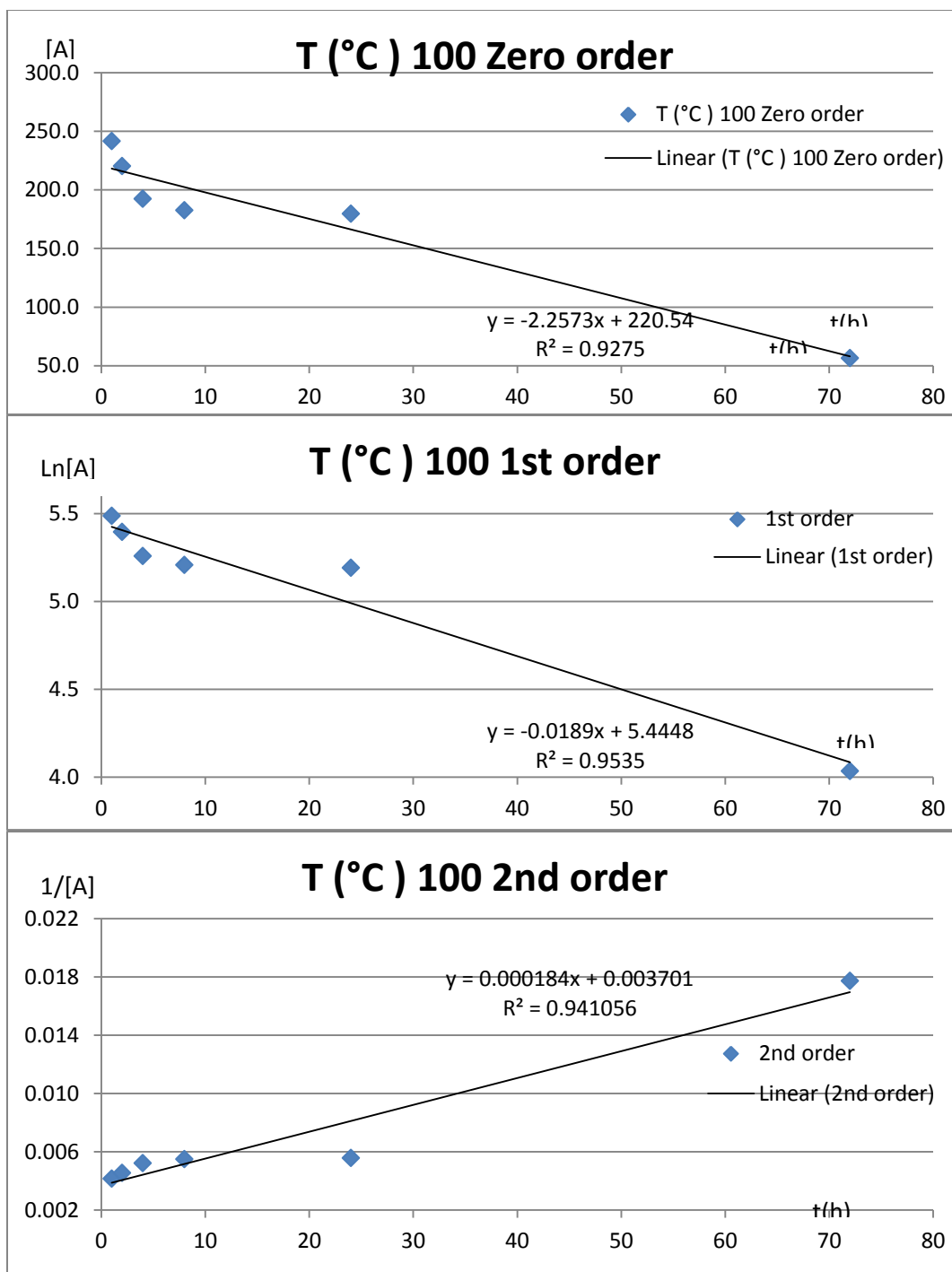


Figure. Rate Constant for  $\beta$ -carotene Thermal-degradation at 100 °C for Three Orders of Reaction

Table UV-Vis Spectrometry Results on  $\beta$ -carotene Thermal-degradation at 150 °C &  $\lambda_{max}$  (31.25  $\mu\text{g}/\text{mL}$  Solution)

Time(h)	1		2		4		8		24		72	
150 °C	$\lambda(\text{nm})$	Abs	$\lambda(\text{nm})$	Abs	$\lambda(\text{nm})$	Abs	$\lambda(\text{nm})$	Abs	$\lambda(\text{nm})$	Abs	$\lambda(\text{nm})$	Abs
31.25 $\mu\text{g}/\text{mL}$	451.75	1.466	451.04	1.123	450.69	1.088	451.39	1.022	452.1	0.694	444	0.242
31.25 $\mu\text{g}/\text{mL}$	452.10	1.453	451.39	1.122	451.04	1.091	451.75	1.022	452.45	0.706	444.35	0.237
31.25 $\mu\text{g}/\text{mL}$	452.45	1.459	451.75	1.128	451.39	1.09	452.1	1.02	452.8	0.71	444.7	0.251
31.25 $\mu\text{g}/\text{mL}$	452.80	1.460	452.10	1.118	451.75	1.094	452.45	1.02	453.15	0.699	445.06	0.244
31.25 $\mu\text{g}/\text{mL}$	453.15	1.469	452.45	1.122	452.10	1.091	452.8	1.027	453.5	0.708	445.41	0.250
31.25 $\mu\text{g}/\text{mL}$	453.50	1.467	452.80	1.131	452.45	1.094	453.15	1.028	453.86	0.7085	445.76	0.237
31.25 $\mu\text{g}/\text{mL}$	453.86	1.455	453.15	1.126	452.80	1.096	453.5	1.026	454.21	0.7095	446.11	0.236
31.25 $\mu\text{g}/\text{mL}$	454.21	1.453	453.50	1.123	453.15	1.089	453.86	1.027	454.56	0.7185	446.47	0.241
31.25 $\mu\text{g}/\text{mL}$	454.56	1.471	453.86	1.117	453.50	1.089	454.21	1.027	454.91	0.707	446.82	0.239
31.25 $\mu\text{g}/\text{mL}$	454.91	1.463	454.21	1.120	453.86	1.089	454.56	1.024	455.26	0.7105	447.17	0.232
Avg	453.33	1.462	454.56	1.118	452.27	1.091	452.98	1.024	453.68	0.707	445.59	0.229
5000 $\mu\text{g}/\text{mL}$	453.33	224.86	454.56	172.00	452.27	167.86	452.98	157.58	453.68	108.78	445.59	35.20
STDEV	1.0641	0.006620	1.0656	0.004346	1.0652	0.002685	1.0652	0.003093	1.0643	0.006641	1.0674	0.006091
5000 $\mu\text{g}/\text{mL}$	Loss(100%)	92.2959		94.10702		94.24881		94.60091		96.27313		98.7940

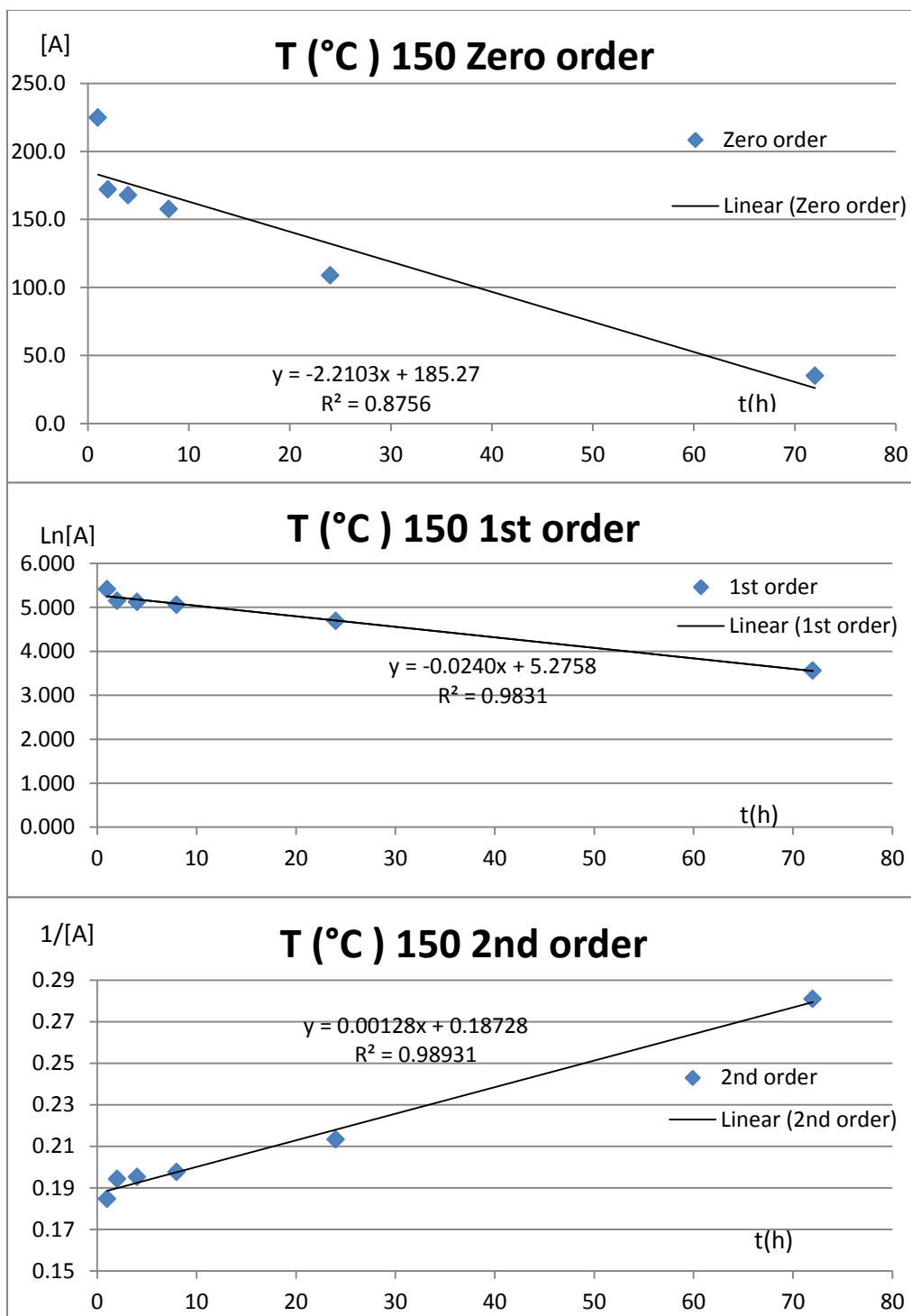


Figure. Rate Constant for  $\beta$ -carotene Thermal-degradation at 150 °C for Three Orders of Reaction

Table 2 UV-Vis Spectrometry Results on  $\beta$ -carotene thermal-degradation at 200 °C &  $\lambda$  max (125  $\mu$ g/mL solution)

Time(h)	1		2		4		8		24		72	
	$\lambda$ (nm)	Abs	$\lambda$ (nm)	Abs	$\lambda$ (nm)	Abs	$\lambda$ (nm)	Abs	$\lambda$ (nm)	Abs	$\lambda$ (nm)	Abs
125 $\mu$ g/mL	447.52	1.007	448.23	0.825	447.52	0.549	447.52	0.549	447.52	0.345	447.52	0.0684
125 $\mu$ g/mL	447.87	1.011	448.58	0.825	447.87	0.546	447.87	0.543	447.87	0.342	447.87	0.0676
125 $\mu$ g/mL	448.23	1.007	448.93	0.822	448.23	0.542	448.23	0.54	448.23	0.339	448.23	0.0664
125 $\mu$ g/mL	448.58	1.007	449.28	0.825	448.58	0.543	448.58	0.534	448.58	0.336	448.58	0.0660
125 $\mu$ g/mL	448.93	1.019	449.64	0.822	448.93	0.544	448.93	0.531	448.93	0.327	448.93	0.0664
125 $\mu$ g/mL	449.28	1.015	449.99	0.823	449.28	0.540	449.28	0.528	449.28	0.321	449.28	0.0656
125 $\mu$ g/mL	449.64	1.013	450.34	0.823	449.64	0.542	449.64	0.525	449.64	0.324	449.64	0.0652
125 $\mu$ g/mL	449.99	1.015	450.69	0.824	449.99	0.538	449.99	0.519	449.99	0.318	449.99	0.0648
125 $\mu$ g/mL	450.34	1.01	451.04	0.823	450.34	0.536	450.34	0.513	450.34	0.312	450.34	0.0636
125 $\mu$ g/mL	450.69	1.009	451.39	0.824	450.69	0.534	450.69	0.507	450.69	0.309	450.69	0.0640
Avg	449.11	1.011	449.81	0.824	449.11	0.541	449.11	0.529	449.11	0.327	449.11	0.0658
5000 $\mu$ g/mL	449.11	40.452	449.81	32.944	449.11	21.656	449.11	21.156	449.11	13.092	449.11	2.632
STDEV	1.0670	0.004111	1.0641	0.001174	1.0670	0.004551	1.0670	0.013345	1.0670	0.012685	1.0670	0.001500
5000 $\mu$ g/mL	Loss(100%)	98.61405		98.87129		99.25803		99.27516		99.55145		99.90982

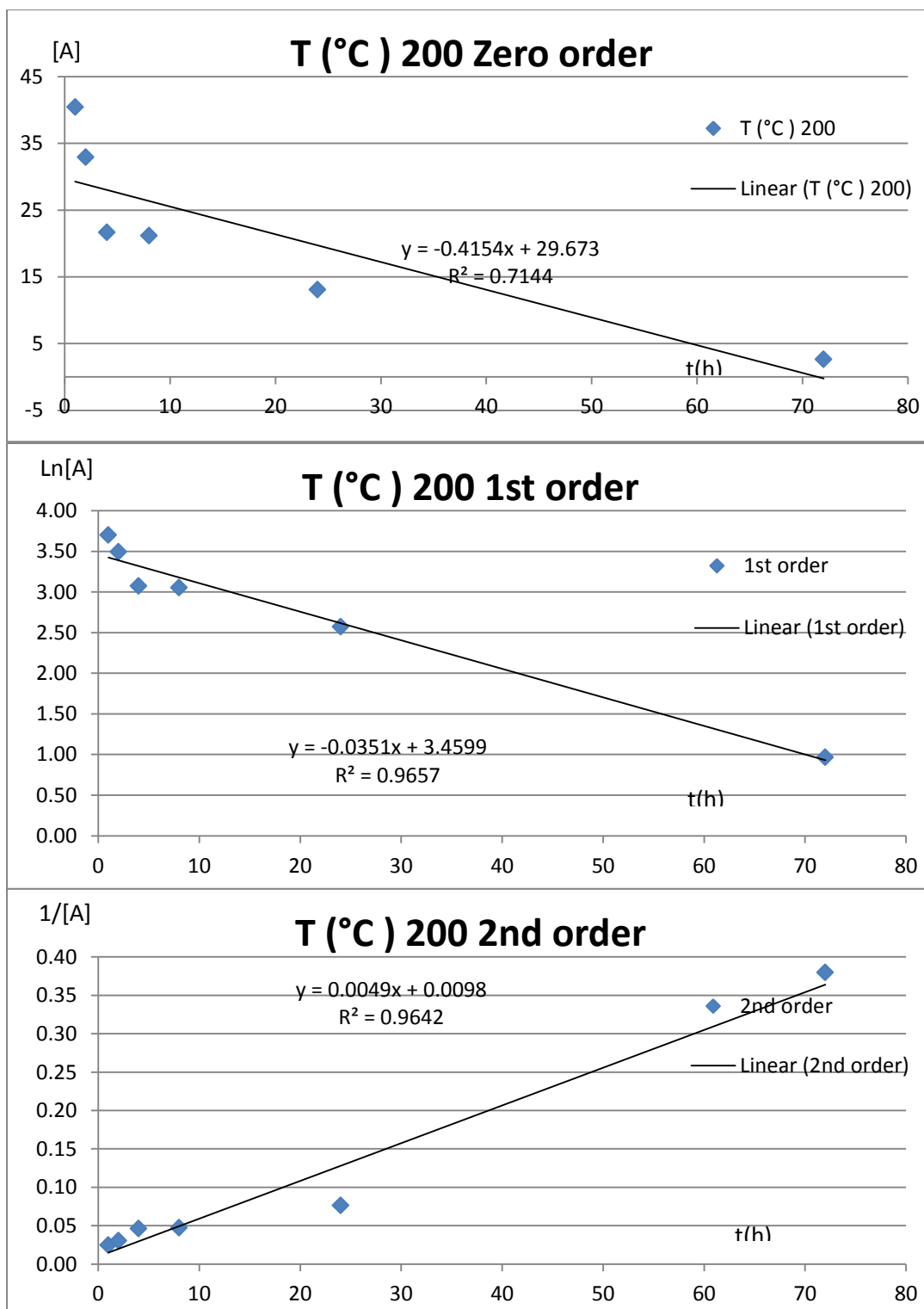


Figure. Rate Constant for  $\beta$ -carotene Thermal-degradation at 200 °C for Three Orders of Reaction

Table UV-Vis Spectrometry Results on  $\beta$ -carotene Thermal-degradation at 250 °C &  $\lambda_{\max}$  (2500  $\mu\text{g/mL}$  solution)

Time(h)	1		2		4		8		24		72	
	$\lambda(\text{nm})$	Abs	$\lambda(\text{nm})$	Abs	$\lambda(\text{nm})$	Abs	$\lambda(\text{nm})$	Abs	$\lambda(\text{nm})$	Abs	$\lambda(\text{nm})$	Abs
2500 $\mu\text{g/mL}$	447.52	1.512	447.52	1.192	447.52	0.745	447.52	0.713	447.52	0.283	447.52	0.072
2500 $\mu\text{g/mL}$	447.87	1.500	447.87	1.175	447.87	0.741	447.87	0.709	447.87	0.282	447.87	0.069
2500 $\mu\text{g/mL}$	448.23	1.514	448.23	1.181	448.23	0.736	448.23	0.709	448.23	0.28	448.23	0.068
2500 $\mu\text{g/mL}$	448.58	1.503	448.58	1.174	448.58	0.73	448.58	0.697	448.58	0.277	448.58	0.069
2500 $\mu\text{g/mL}$	448.93	1.486	448.93	1.169	448.93	0.724	448.93	0.691	448.93	0.274	448.93	0.067
2500 $\mu\text{g/mL}$	449.28	1.475	449.28	1.164	449.28	0.720	449.28	0.685	449.28	0.271	449.28	0.067
2500 $\mu\text{g/mL}$	449.64	1.467	449.64	1.158	449.64	0.717	449.64	0.683	449.64	0.268	449.64	0.067
2500 $\mu\text{g/mL}$	449.99	1.466	449.99	1.151	449.99	0.709	449.99	0.677	449.99	0.267	449.99	0.065
2500 $\mu\text{g/mL}$	450.34	1.466	450.34	1.158	450.34	0.707	450.34	0.675	450.34	0.265	450.34	0.065
2500 $\mu\text{g/mL}$	450.69	1.455	450.69	1.144	450.69	0.701	450.69	0.67	450.69	0.263	450.69	0.064
Avg	449.11	1.484	449.11	1.167	449.11	0.723	449.11	0.691	449.11	0.273	449.11	0.067
5000 $\mu\text{g/mL}$		2.969		2.333		1.446		1.382		0.546		0.067
STDEV	1.0670	0.02151	1.0670	0.01450	1.0670	0.01494	1.0670	0.01550	1.0670	0.007272	1.0670	0.002359
5000 $\mu\text{g/mL}$	Loss(%)	99.89828		99.92006		99.95046		99.95266		99.98129		99.99769

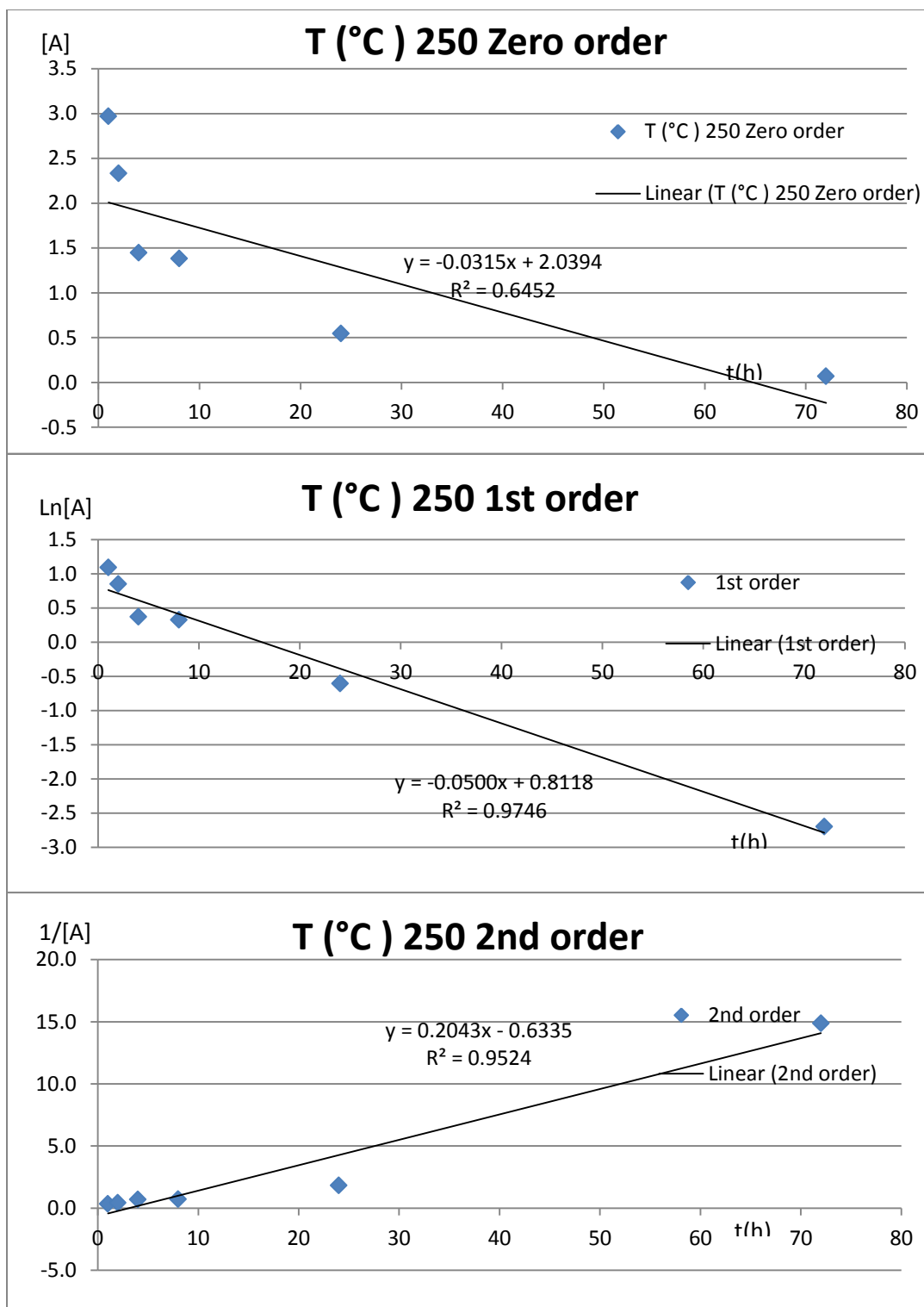


Figure. Rate Constant for  $\beta$ -carotene Thermal-degradation at 250 °C for Three Orders of Reaction



Table UV-Vis Spectrometry Results on  $\beta$ -carotene Thermal-degradation at 300 °C &  $\lambda_{\max}$ (5000  $\mu\text{g/mL}$  solution)

time(h)	1		2		4		8		24		72	
300 °C	$\lambda(\text{nm})$	Abs	$\lambda(\text{nm})$	Abs	$\lambda(\text{nm})$	Abs	$\lambda(\text{nm})$	Abs	$\lambda(\text{nm})$	Abs	$\lambda(\text{nm})$	Abs
5000 $\mu\text{g/mL}$	447.52	1.041	447.52	0.818	447.52	0.615	447.52	0.439	447.52	0.166	447.52	0.010313
5000 $\mu\text{g/mL}$	447.87	1.038	447.87	0.812	447.87	0.611	447.87	0.437	447.87	0.164	447.87	0.010250
5000 $\mu\text{g/mL}$	448.23	1.028	448.23	0.812	448.23	0.609	448.23	0.435	448.23	0.164	448.23	0.010188
5000 $\mu\text{g/mL}$	448.58	1.027	448.58	0.804	448.58	0.607	448.58	0.431	448.58	0.163	448.58	0.010125
5000 $\mu\text{g/mL}$	448.93	1.020	448.93	0.800	448.93	0.602	448.93	0.432	448.93	0.162	448.93	0.010125
5000 $\mu\text{g/mL}$	449.28	1.019	449.28	0.796	449.28	0.600	449.28	0.429	449.28	0.161	449.28	0.010063
5000 $\mu\text{g/mL}$	449.64	1.012	449.64	0.796	449.64	0.595	449.64	0.428	449.64	0.160	449.64	0.010000
5000 $\mu\text{g/mL}$	449.99	1.012	449.99	0.792	449.99	0.593	449.99	0.424	449.99	0.160	449.99	0.009938
5000 $\mu\text{g/mL}$	450.34	1.009	450.34	0.790	450.34	0.593	450.34	0.421	450.34	0.160	450.34	0.009938
5000 $\mu\text{g/mL}$	450.69	1.003	450.69	0.786	450.69	0.588	450.69	0.422	450.69	0.158	450.69	0.009813
Avg	449.11	1.021	449.11	0.801	449.11	0.601	449.11	0.430	449.11	0.162	449.11	0.010075
STDEV	1.0670	0.01251	1.0670	0.01063	1.0670	0.009007	1.0670	0.006197	1.0670	0.002633	1.0670	0.0001553
5000 $\mu\text{g/mL}$	Loss(100%)	99.96502		99.97257		99.97940		99.98527		99.99446		99.99445

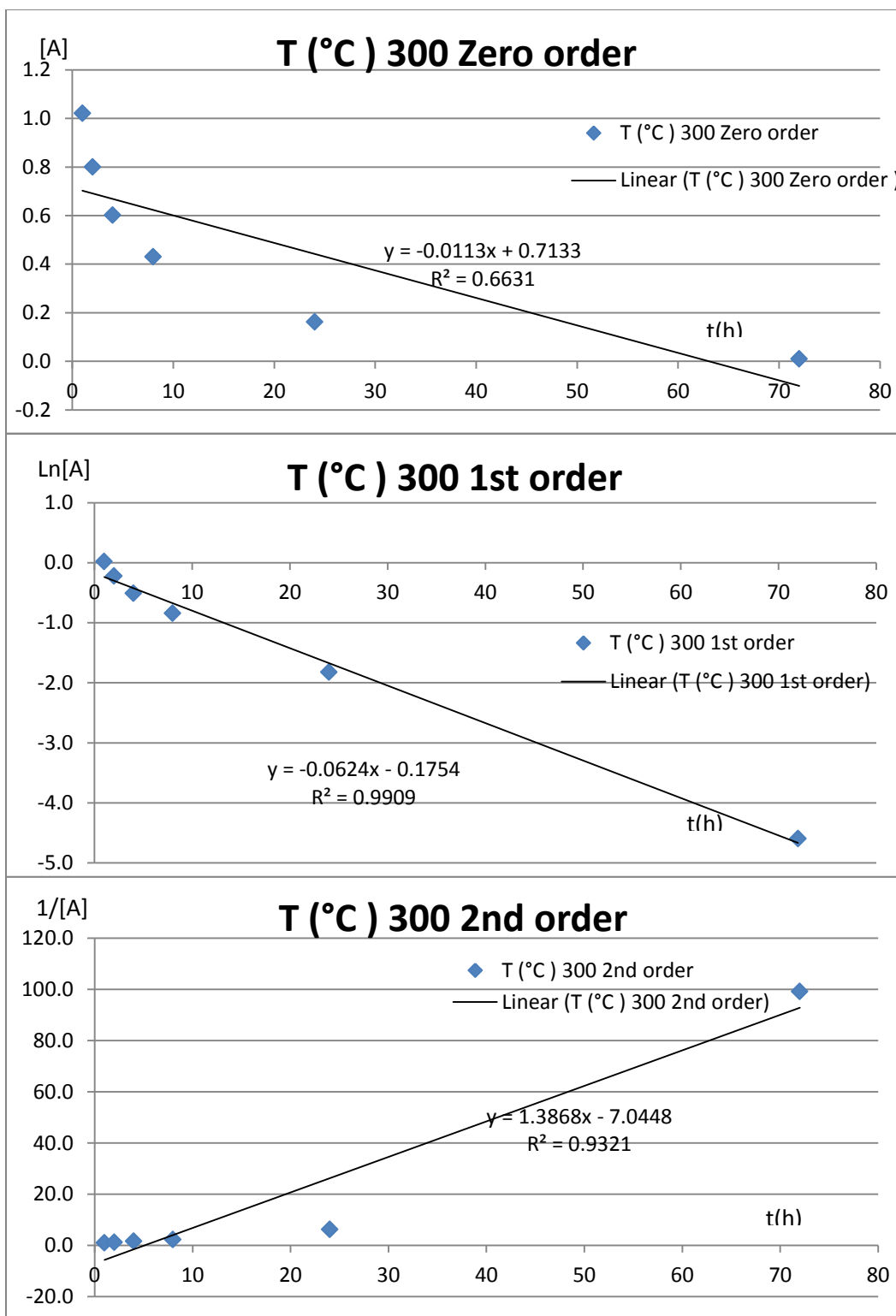


Figure. Rate Constant for  $\beta$ -carotene Thermal-degradation at 150 °C for Three Orders of Reaction

Table UV-Vis Spectrometry Results on  $\beta$ -carotene Thermal-degradation at 350 °C &  $\lambda_{\max}$  (5000  $\mu\text{g/mL}$  solution)

Time(h)		1		2		4		8		24		72	
350 °C	$\lambda(\text{nm})$	Abs	$\lambda(\text{nm})$	Abs	$\lambda(\text{nm})$	Abs	$\lambda(\text{nm})$	Abs	$\lambda(\text{nm})$	Abs	$\lambda(\text{nm})$	Abs	
5000 $\mu\text{g/mL}$	447.52	0.16	447.52	0.110	447.52	0.0768	447.52	0.0368	447.52	0.0103	447.52	0.00500	
5000 $\mu\text{g/mL}$	447.87	0.158	447.87	0.108	447.87	0.0760	447.87	0.0360	447.87	0.0103	447.87	0.00300	
5000 $\mu\text{g/mL}$	448.23	0.158	448.23	0.108	448.23	0.0756	448.23	0.0360	448.23	0.0102	448.23	0.00300	
5000 $\mu\text{g/mL}$	448.58	0.1576	448.58	0.108	448.58	0.0756	448.58	0.0356	448.58	0.0101	448.58	0.00500	
5000 $\mu\text{g/mL}$	448.93	0.156	448.93	0.107	448.93	0.0748	448.93	0.0352	448.93	0.0101	448.93	0.00300	
5000 $\mu\text{g/mL}$	449.28	0.1548	449.28	0.107	449.28	0.0744	449.28	0.0352	449.28	0.0101	449.28	0.00400	
5000 $\mu\text{g/mL}$	449.64	0.1548	449.64	0.106	449.64	0.0740	449.64	0.0348	449.64	0.0100	449.64	0.00300	
5000 $\mu\text{g/mL}$	449.99	0.1536	449.99	0.106	449.99	0.0736	449.99	0.0344	449.99	0.0099	449.99	0.00300	
5000 $\mu\text{g/mL}$	450.34	0.1528	450.34	0.105	450.34	0.0728	450.34	0.0336	450.34	0.0099	450.34	0.00300	
5000 $\mu\text{g/mL}$	450.69	0.152	450.69	0.104	450.69	0.0732	450.69	0.0332	450.69	0.0098	450.69	0.00300	
5000 $\mu\text{g/mL}$	449.11	0.156	449.11	0.107	449.11	0.0747	449.11	0.0351	449.11	0.0101	449.11	0.00350	
STDEV	1.0670	0.00260	1.0670	0.00175	1.0670	0.00131	1.0670	0.00112	1.0670	0.000155	1.0670	0.000850	
5000 $\mu\text{g/mL}$	Loss(100%)	99.99466		99.99634		99.99744		99.99880		99.99966		99.99988	

## APPENDIX II PHOTO-DEGRADATION OF $\beta$ -CAROTENE

Table Photo-degradation Rate for  $\beta$ -carotene in Hexane at 15°C

Time	$\lambda$ (nm)										STDEV	Avg	Ln(Abs)
(min)	444.35	444.70	445.06	445.41	445.76	446.11	446.47	446.82	447.17	447.52	1.0670	445.94	
0	2.254	2.269	2.281	2.287	2.247	2.250	2.250	2.247	2.239	2.271	0.0163	2.260	0.8151
5	2.038	2.050	2.063	2.070	2.049	2.054	2.060	2.061	2.059	2.080	0.0117	2.058	0.7219
10	1.819	1.828	1.838	1.844	1.834	1.840	1.846	1.847	1.848	1.863	0.0121	1.841	0.6101
15	1.658	1.667	1.675	1.682	1.677	1.682	1.687	1.690	1.692	1.703	0.0129	1.681	0.5196
20	1.422	1.428	1.435	1.440	1.439	1.444	1.449	1.451	1.453	1.461	0.0119	1.442	0.3662
25	1.322	1.328	1.335	1.340	1.340	1.345	1.349	1.352	1.354	1.360	0.0119	1.343	0.2945
30	1.197	1.202	1.207	1.211	1.211	1.215	1.218	1.220	1.221	1.225	0.0089	1.213	0.1928
35	1.062	1.065	1.070	1.074	1.075	1.078	1.080	1.082	1.084	1.087	0.0082	1.076	0.0730
40	0.949	0.952	0.956	0.959	0.960	0.963	0.965	0.967	0.968	0.971	0.0071	0.961	-0.0398
45	0.841	0.844	0.847	0.850	0.851	0.854	0.856	0.857	0.858	0.861	0.0065	0.852	-0.1603
50	0.744	0.746	0.749	0.751	0.752	0.754	0.756	0.757	0.758	0.759	0.0051	0.753	-0.2842
55	0.558	0.560	0.562	0.563	0.565	0.567	0.569	0.570	0.570	0.569	0.0044	0.565	-0.5704
60	0.496	0.498	0.499	0.500	0.502	0.504	0.506	0.507	0.507	0.507	0.0042	0.503	-0.6880
65	0.418	0.420	0.421	0.422	0.424	0.425	0.427	0.427	0.427	0.427	0.0034	0.424	-0.8585
70	0.360	0.361	0.363	0.363	0.364	0.366	0.367	0.367	0.367	0.367	0.0027	0.365	-1.0092
75	0.296	0.297	0.298	0.298	0.299	0.300	0.301	0.302	0.301	0.301	0.0023	0.299	-1.2063
80	0.236	0.237	0.238	0.238	0.239	0.240	0.240	0.240	0.240	0.239	0.0017	0.238	-1.4325
85	0.185	0.186	0.186	0.186	0.187	0.187	0.188	0.188	0.187	0.187	0.0012	0.187	-1.6783
90	0.150	0.150	0.151	0.150	0.151	0.152	0.152	0.152	0.151	0.150	0.0010	0.151	-1.8911
95	0.121	0.121	0.122	0.121	0.122	0.122	0.123	0.123	0.122	0.121	0.0008	0.122	-2.1054
100	0.094	0.094	0.094	0.094	0.095	0.095	0.095	0.095	0.094	0.094	0.0005	0.094	-2.3602
105	0.020	0.020	0.020	0.020	0.021	0.021	0.022	0.021	0.021	0.020	0.0007	0.021	-3.8825
110	0.037	0.037	0.037	0.037	0.037	0.038	0.038	0.038	0.037	0.037	0.0005	0.037	-3.2888
120	0.032	0.032	0.032	0.032	0.032	0.033	0.033	0.033	0.032	0.031	0.0007	0.032	-3.4358
130	0.018	0.018	0.018	0.017	0.018	0.018	0.018	0.018	0.018	0.017	0.0005	0.018	-4.0286

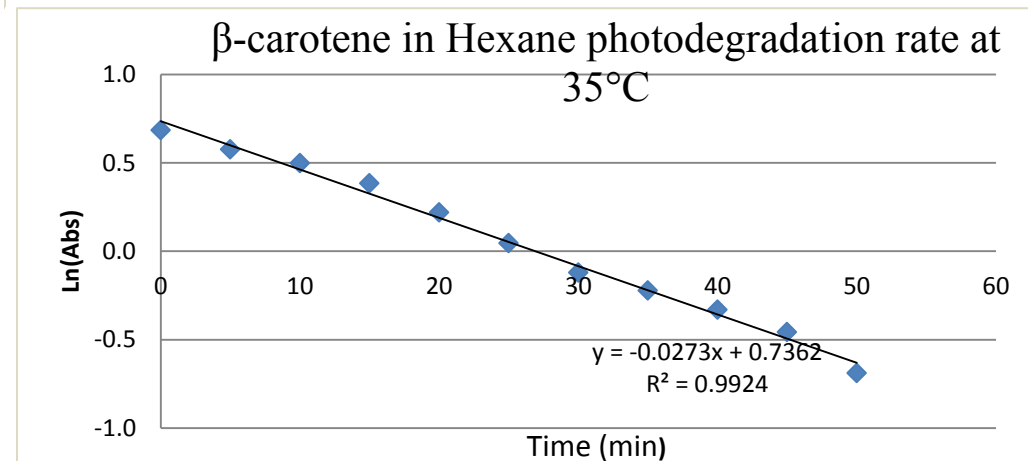
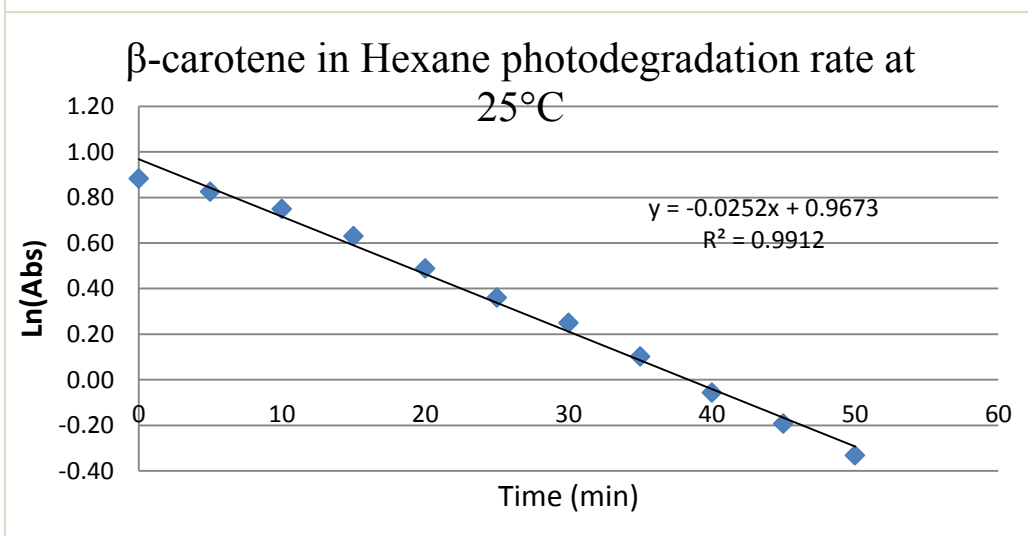
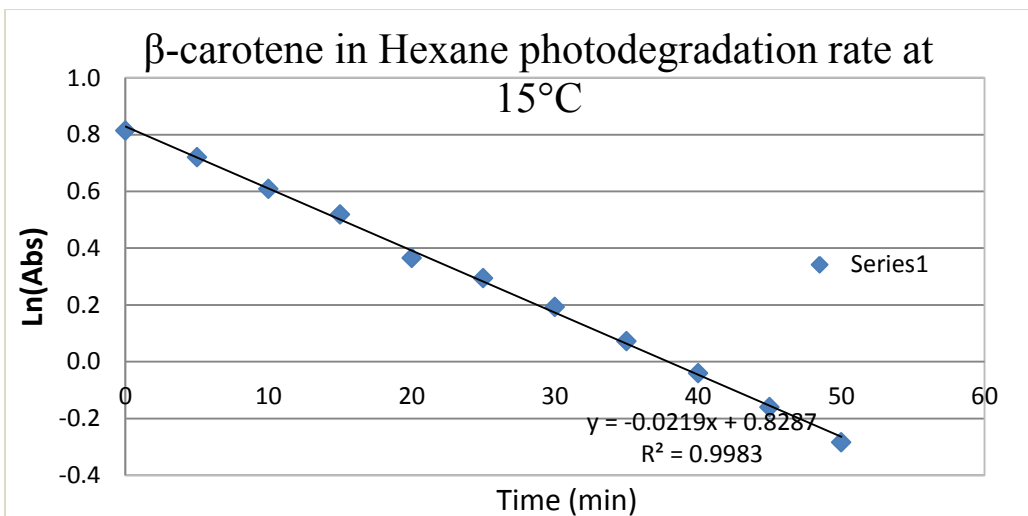


Figure. Rate Constant for  $\beta$ -carotene Photo-degradation in Hexane at 15,25,35 °C (First Order)

Table The Photo-degradation Rate for  $\beta$ -carotene in Hexane at 25°C

Time	$\lambda$ (nm)												STDEV	Avg	
(min)	444.4	444.7	445.1	445.4	445.8	446.1	446.5	446.8	447.2	447.5	447.9	448.2	1.25842	446.3	Ln(Abs)
0	2.384	2.368	2.346	2.337	2.369	2.384	2.427	2.467	2.466	2.463	2.506	2.508	0.06150	2.419	0.8833
5	2.248	2.236	2.228	2.223	2.247	2.257	2.289	2.323	2.326	2.321	2.350	2.358	0.04960	2.284	0.8259
10	2.077	2.074	2.069	2.068	2.086	2.097	2.123	2.147	2.150	2.150	2.174	2.178	0.04220	2.116	0.7496
15	1.841	1.842	1.842	1.845	1.859	1.870	1.884	1.901	1.906	1.908	1.921	1.924	0.03259	1.879	0.6305
20	1.598	1.601	1.602	1.605	1.616	1.623	1.635	1.645	1.649	1.651	1.660	1.663	0.02440	1.629	0.4880
25	1.410	1.413	1.415	1.418	1.426	1.431	1.439	1.446	1.449	1.451	1.456	1.457	0.01759	1.434	0.3606
30	1.270	1.271	1.266	1.252	1.295	1.276	1.294	1.291	1.301	1.305	1.307	1.277	0.01746	1.284	0.2498
35	1.091	1.094	1.096	1.098	1.103	1.107	1.112	1.116	1.118	1.119	1.121	1.122	0.01137	1.108	0.1026
40	0.934	0.936	0.937	0.939	0.943	0.945	0.948	0.951	0.952	0.952	0.953	0.953	0.00724	0.945	-0.0563
45	0.814	0.816	0.818	0.819	0.822	0.825	0.828	0.830	0.831	0.831	0.832	0.832	0.00674	0.825	-0.1926
50	0.709	0.711	0.712	0.713	0.716	0.718	0.720	0.721	0.722	0.722	0.723	0.723	0.00511	0.718	-0.3320
55	0.607	0.609	0.609	0.610	0.612	0.614	0.615	0.617	0.617	0.617	0.617	0.617	0.00382	0.613	-0.4887
60	0.510	0.511	0.511	0.512	0.514	0.515	0.516	0.517	0.517	0.517	0.517	0.517	0.00278	0.515	-0.6646
65	0.418	0.419	0.419	0.419	0.421	0.421	0.422	0.423	0.423	0.423	0.423	0.423	0.00195	0.421	-0.8647
70	0.345	0.345	0.345	0.345	0.346	0.347	0.348	0.348	0.348	0.348	0.347	0.347	0.00131	0.347	-1.0596
75	0.238	0.238	0.238	0.238	0.238	0.239	0.239	0.240	0.240	0.239	0.239	0.238	0.00078	0.239	-1.4327
80	0.196	0.197	0.196	0.196	0.197	0.197	0.197	0.198	0.198	0.197	0.196	0.196	0.00075	0.197	-1.6258
85	0.159	0.159	0.158	0.158	0.159	0.159	0.159	0.159	0.159	0.159	0.158	0.158	0.00049	0.159	-1.8409
90	0.128	0.129	0.128	0.128	0.128	0.129	0.129	0.129	0.129	0.129	0.128	0.128	0.00052	0.129	-2.0518
95	0.100	0.100	0.100	0.099	0.100	0.100	0.100	0.100	0.101	0.100	0.100	0.1	0.00043	0.100	-2.3026
100	0.090	0.090	0.090	0.089	0.090	0.090	0.090	0.090	0.091	0.090	0.090	0.09	0.00043	0.090	-2.4079
105	0.071	0.071	0.071	0.070	0.071	0.071	0.072	0.072	0.072	0.071	0.071	0.071	0.00058	0.071	-2.6427
110	0.062	0.062	0.061	0.061	0.061	0.062	0.062	0.062	0.062	0.062	0.061	0.061	0.00051	0.062	-2.7874
115	0.057	0.058	0.057	0.057	0.057	0.058	0.058	0.058	0.058	0.058	0.058	0.058	0.00049	0.058	-2.8531

(To be Continued)

Table The Photo-degradation Rate for  $\beta$ -carotene in Hexane at 25°C

Time	$\lambda$ (nm)												STDEV	Avg	
(min)	444.4	444.7	445.1	445.4	445.8	446.1	446.5	446.8	447.2	447.5	447.9	448.2	1.25842	446.3	Ln(Abs)
120	0.047	0.048	0.047	0.047	0.047	0.048	0.048	0.048	0.048	0.048	0.048	0.048	0.00049	0.048	-3.0435
125	0.039	0.040	0.039	0.039	0.039	0.040	0.040	0.040	0.041	0.040	0.040	0.04	0.00062	0.040	-3.2251
130	0.039	0.040	0.039	0.039	0.039	0.040	0.040	0.040	0.041	0.040	0.040	0.04	0.00062	0.040	-3.2251
135	0.033	0.033	0.033	0.033	0.033	0.033	0.034	0.034	0.034	0.034	0.033	0.034	0.00051	0.033	-3.3987
140	0.031	0.031	0.031	0.030	0.031	0.031	0.032	0.032	0.032	0.032	0.032	0.032	0.00067	0.031	-3.4604
145	0.035	0.036	0.035	0.035	0.035	0.036	0.036	0.036	0.037	0.036	0.036	0.036	0.00062	0.036	-3.3312
150	0.035	0.036	0.035	0.035	0.035	0.036	0.036	0.036	0.037	0.036	0.036	0.036	0.00062	0.036	-3.3312
155	0.025	0.025	0.025	0.025	0.025	0.026	0.026	0.026	0.027	0.026	0.026	0.026	0.00065	0.026	-3.6626
160	0.022	0.023	0.022	0.022	0.022	0.023	0.023	0.023	0.024	0.024	0.023	0.023	0.00072	0.023	-3.7795
165	0.025	0.025	0.025	0.025	0.025	0.026	0.026	0.026	0.027	0.027	0.026	0.026	0.00075	0.026	-3.6593
170	0.021	0.021	0.021	0.021	0.021	0.022	0.022	0.023	0.023	0.023	0.022	0.023	0.00090	0.022	-3.8205
175	0.025	0.025	0.025	0.025	0.025	0.026	0.026	0.027	0.027	0.027	0.026	0.027	0.00090	0.026	-3.6529

Table The Photo-degradation Rate for  $\beta$ -carotene in Hexane at 45°C

Time	$\lambda$ (nm)								STDEV	Avg	
(min)	445.41	445.76	446.11	446.47	446.82	447.17	447.52	447.87	0.86170	446.64	Ln(Abs)
0	1.988	2.001	1.982	2.009	2.002	2.006	1.990	1.996	0.009423	1.9968	0.6915
5	1.854	1.867	1.852	1.873	1.867	1.869	1.858	1.862	0.007517	1.8628	0.6221
10	1.626	1.627	1.629	1.636	1.644	1.649	1.656	1.663	0.013997	1.6413	0.4955
15	1.489	1.488	1.492	1.497	1.506	1.509	1.516	1.521	0.012601	1.5023	0.4070
20	1.300	1.300	1.303	1.306	1.312	1.314	1.317	1.321	0.008008	1.3091	0.2694
25	1.158	1.159	1.162	1.164	1.169	1.171	1.174	1.176	0.006844	1.1666	0.1541
30	0.995	0.995	0.997	1.000	1.004	1.005	1.007	1.009	0.005503	1.0015	0.0015
35	0.862	0.863	0.864	0.866	0.868	0.869	0.871	0.871	0.003536	0.8668	-0.1430
40	0.724	0.724	0.726	0.727	0.729	0.729	0.730	0.730	0.002504	0.7274	-0.3183
45	0.595	0.595	0.595	0.596	0.597	0.597	0.598	0.597	0.001165	0.5963	-0.5171
50	0.487	0.487	0.487	0.488	0.489	0.489	0.489	0.488	0.000926	0.4880	-0.7174
55	0.390	0.389	0.389	0.390	0.391	0.391	0.391	0.390	0.000835	0.3901	-0.9413



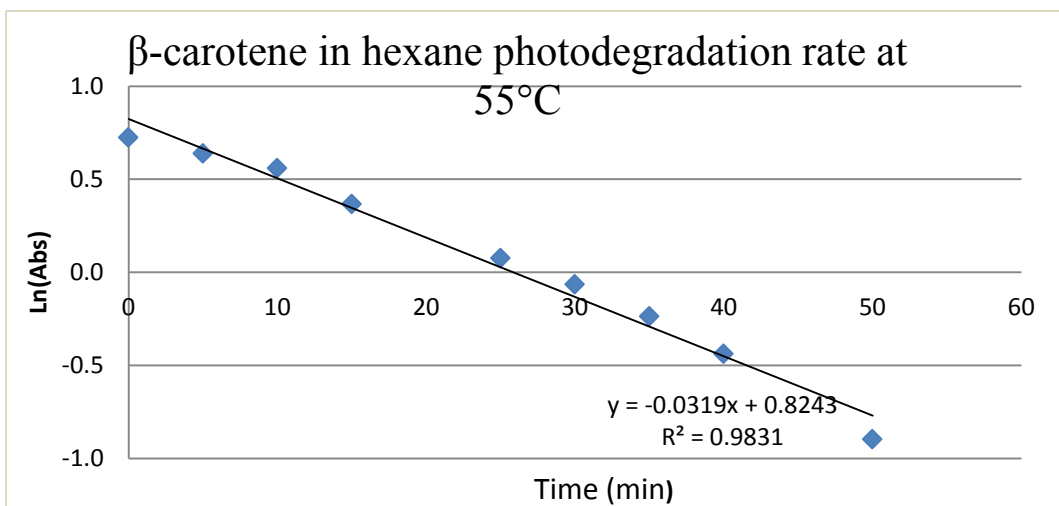
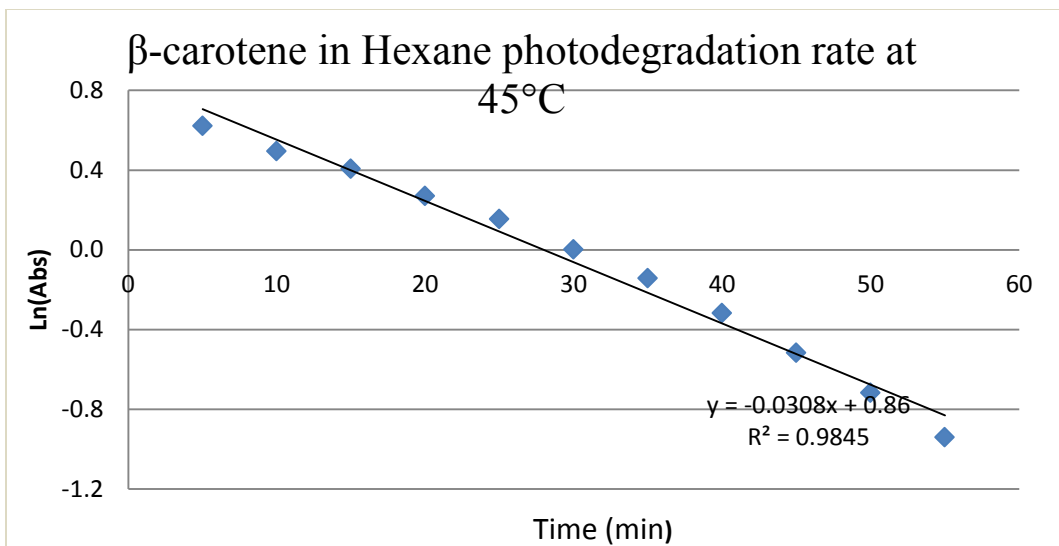
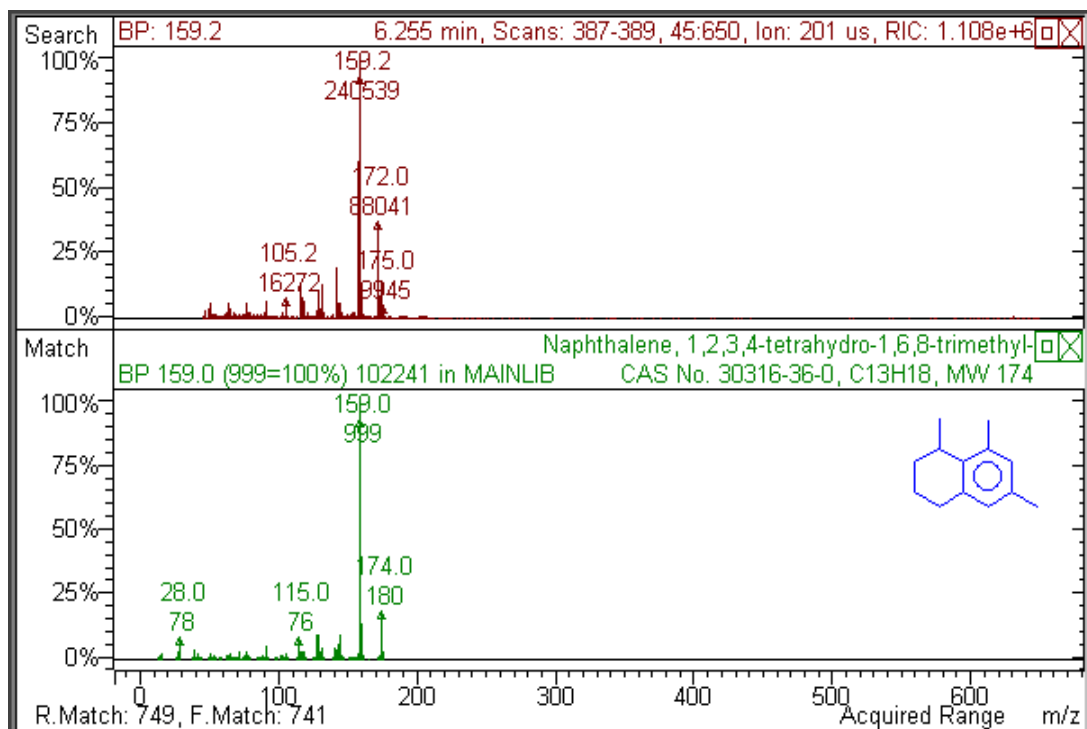


Figure. Rate Constant for  $\beta$ -carotene Photo-degradation in Hexane at 45 and 55°C (First Order)

Table The Photo-degradation Rate for  $\beta$ -carotene in Hexane at 55°C

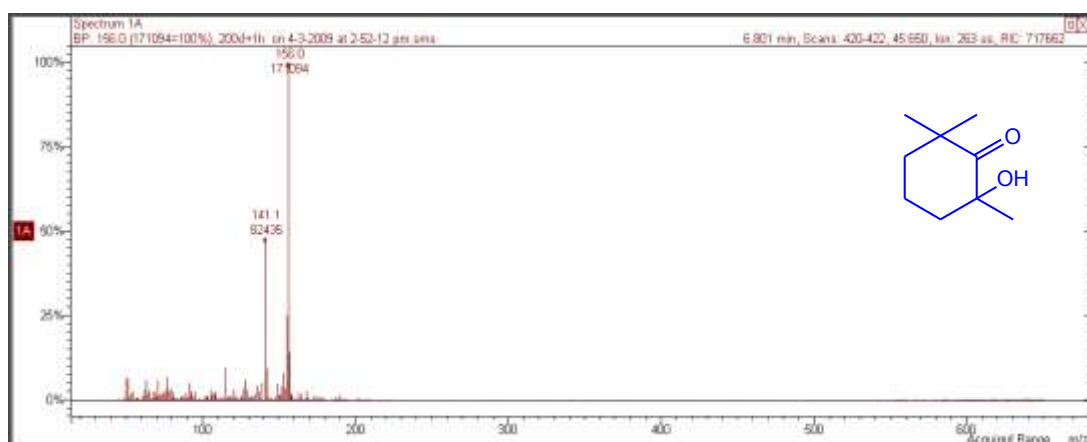
Time	$\lambda$ (nm)											STDEV	Avg	
(min)	446.11	446.47	446.82	447.17	447.52	447.87	448.23	448.58	448.93	449.28	449.64	1.1684	447.8745	ln(Abs)
0	2.057	2.060	2.063	2.058	2.058	2.064	2.054	2.066	2.066	2.061	2.056	0.0041	2.0603	0.7228
5	1.890	1.890	1.892	1.890	1.891	1.898	1.891	1.896	1.897	1.891	1.889	0.0032	1.8923	0.6378
10	1.740	1.744	1.746	1.746	1.747	1.751	1.746	1.752	1.750	1.745	1.741	0.0038	1.7462	0.5574
15	1.444	1.445	1.446	1.444	1.444	1.445	1.442	1.443	1.441	1.438	1.435	0.0033	1.4425	0.3663
25	1.084	1.083	1.083	1.083	1.081	1.079	1.078	1.076	1.074	1.074	1.070	0.0047	1.0786	0.0757
30	0.941	0.939	0.940	0.940	0.938	0.937	0.936	0.934	0.932	0.930	0.927	0.0046	0.9358	-0.0663
35	0.794	0.793	0.793	0.792	0.791	0.789	0.788	0.787	0.785	0.783	0.780	0.0045	0.7886	-0.2374
40	0.650	0.649	0.649	0.648	0.647	0.646	0.645	0.643	0.642	0.640	0.638	0.0040	0.6452	-0.4382
50	0.412	0.411	0.411	0.410	0.409	0.408	0.407	0.406	0.405	0.404	0.402	0.0032	0.4077	-0.8972

## APPENDIX III THE MASS SPECTRAL DATA OF SOME FRAGMENT IONS

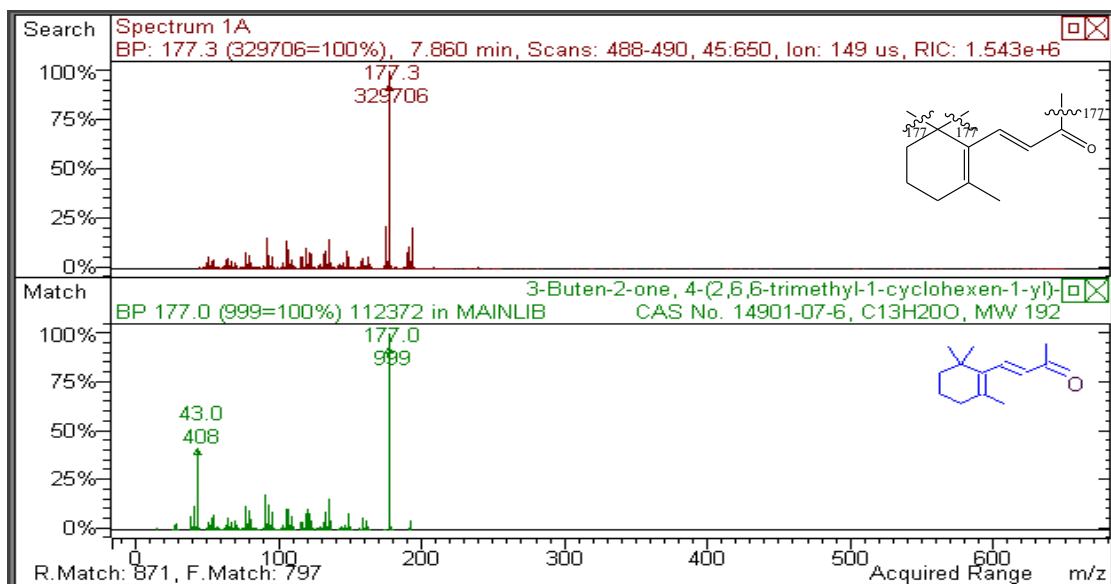


Fragment ions 1: MS at m/z 174

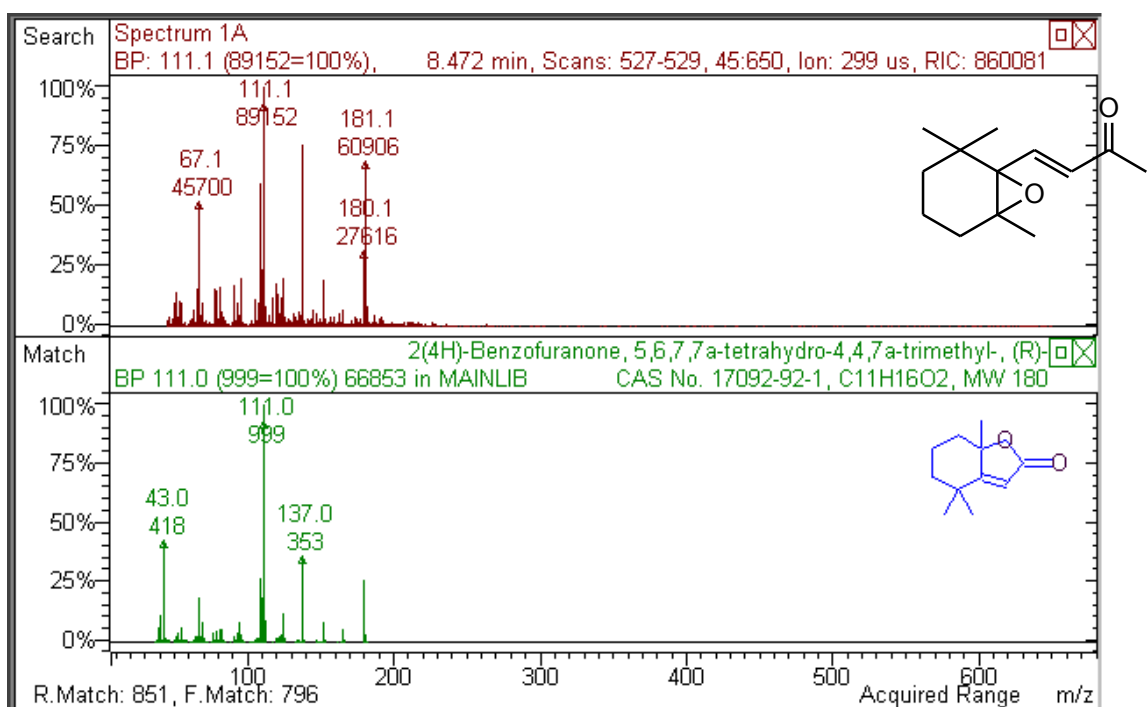
MS of m/z 174 extracted from TIC of standard  $\beta$ -carotene solution and thermal reaction products solution Ionene, TDN, 4,4,7-trimethyl-2,3-dihydro-1H-naphthalene)



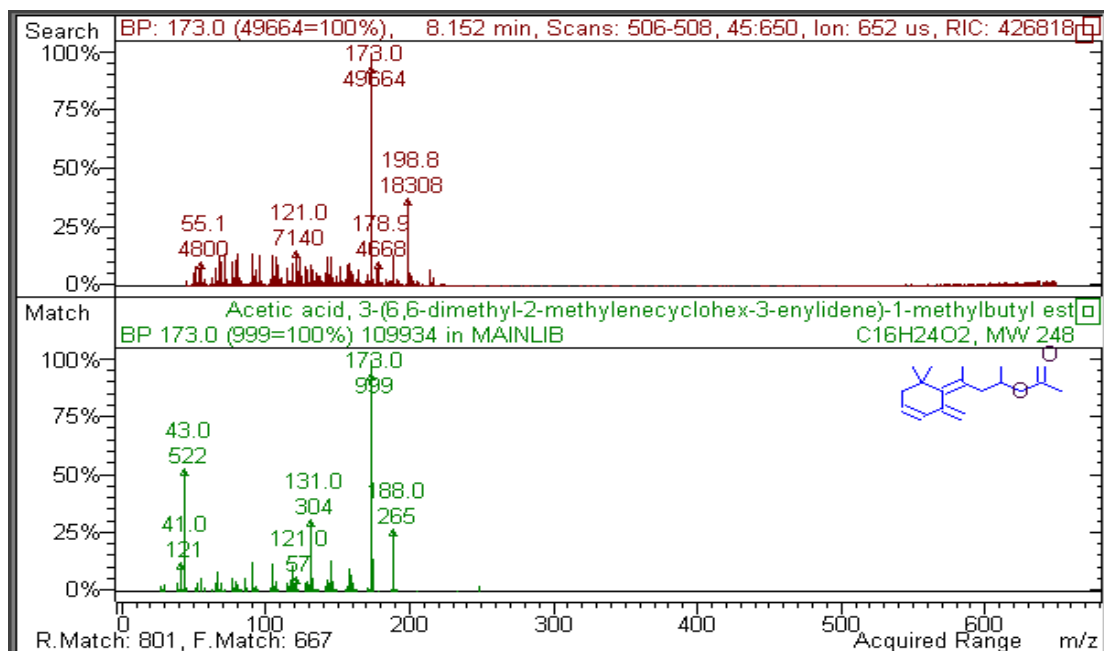
Fragment ions 2: MS at m/z 156 The Extracted MS at m/z 156 Thermal-degradation 200°C 1h (2-hydroxy-2,6,6-trimethyl-cyclohexanone)



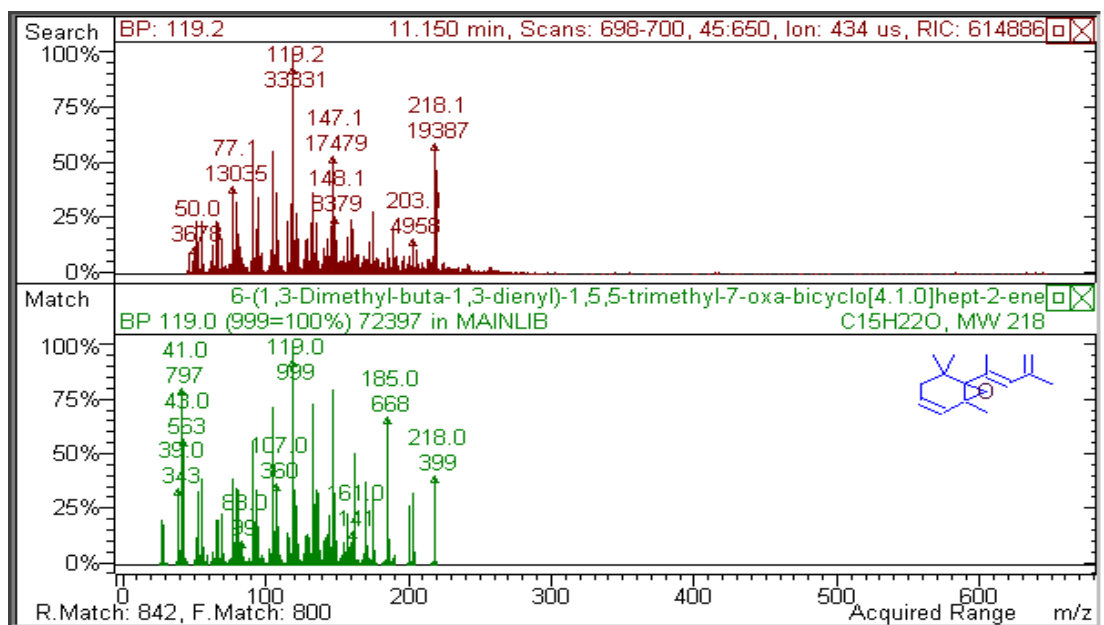
Fragment Ions 3: MS at m/z 192



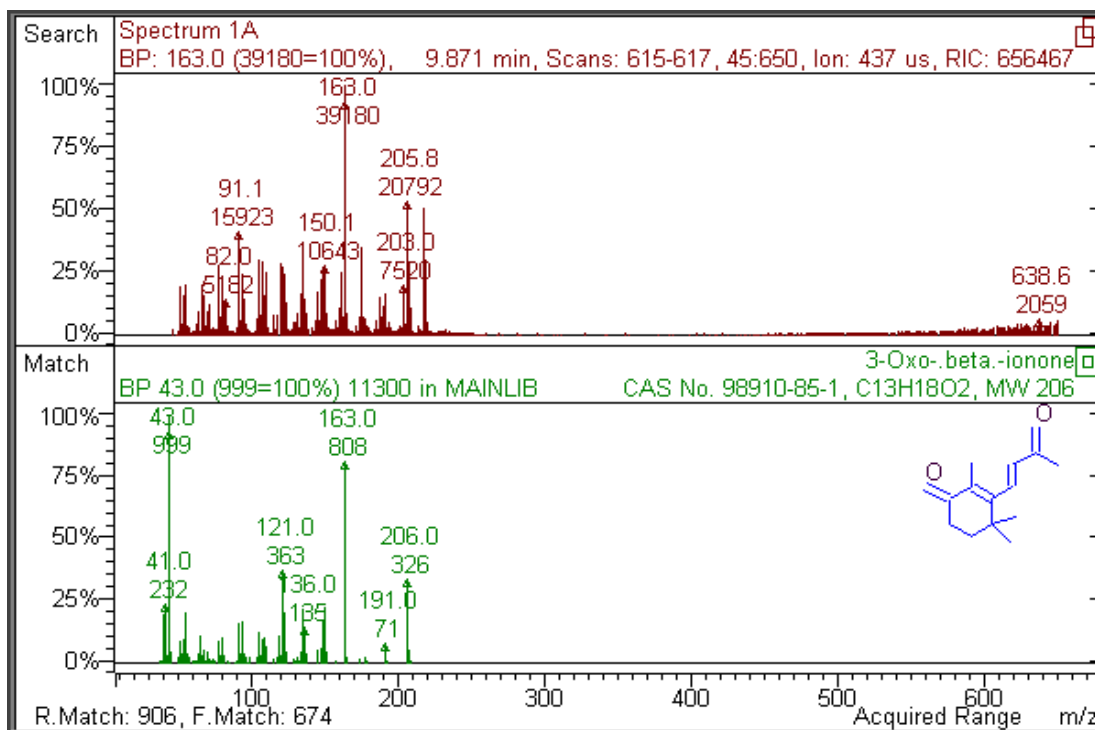
Fragment Ions 4: MS at m/z 180



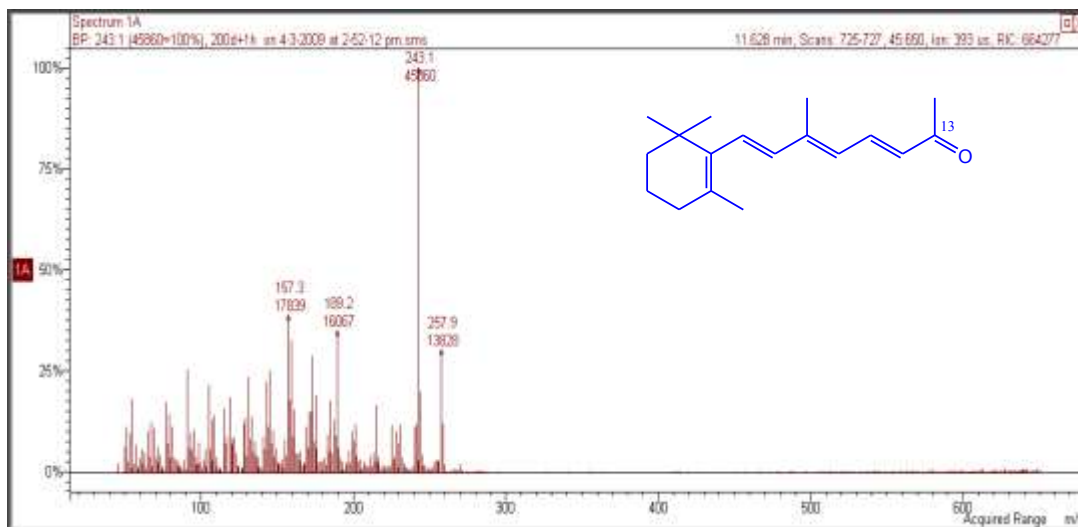
Fragment Ions 5: MS at m/z 248



Fragment Ions 6: MS at m/z 218



Fragment Ions 7: MS at m/z 206



Fragment Ions 8: MS at m/z 258